NASA CONTRACTOR REPORT 166380

Development of a Rotorcraft/Propulsion Dynamics Interface Analysis: Volume I

Russell Hull

CONTRACT NAS2–10765
August 1982

NASA

NASA CONTRACTOR REPORT 166380

Development of a Rotorcraft/Propulsion Dynamics Interface Analysis: Volume I

Russell Hull
Systems Control Technology
Palo Alto, California

Prepared for
Ames Research Center
under Contract NAS2-10765

National Aeronautics and
Space Administration

Ames Research Center
Moffett Field, California 94035

This Page Intentionally Left Blank

FOREWORD

The work described in this report was performed under Contract No. NAS2-10765 for the National Aeronautics and Space Administration, Ames Research Center. The technical monitor for NASA-Ames was Dr. William Warmbrodt. The principle author from Systems Control Technology, Inc. was Mr. Russell L. Hull. Mr. James H. Vincent was program manager. Technical support was provided by Mr. James W. Fuller. Programming support was provided by Mr. Bob Bullock. Report preparation efforts were directed by Ms. Clare Walker.

This Page Intentionally Left Blank

TABLE OF CONTENTS

TABLE OF CONTENTS (Continued)

NOTATION

a_{11}, a_{12}, a_{21}, a_{22} = components of the A dynamics matrix

A = coefficient matrix in state equation $\dot{\bar{x}} = A\bar{x} + B\bar{u}$

AEE = engine state coefficient matrix in engine state equation

A_{RFU} = fuselage state coefficient matrix in rotor state equation

A_{RR} = rotor state coefficient matrix in rotor state equation

A_{RT} = drive train state coefficient matrix in rotor state equation

ATE1, ATE2 = engine 1 and 2 state coefficient matrix in drive train state equation

ATT = drive train state coefficient matrix in drive train state equation

A_{1S} = main rotor lateral cyclic control input

$A(\psi)$ = coefficient matrix in rotating frame blade flapping equation

$A'(\psi)$ = coefficient matrix in rotating frame blade lagging equation

b_1, b_2 = components of the B input matrix

B = coefficient matrix in state equation $\dot{\bar{x}} = A\bar{x} + b\bar{u}$

BEF = fuel control output coefficient matrix in engine state equation

BET = drive train output coefficient matrix in engine state equation

BETA = collective setting

B_{RC} = rotor control coefficient matrix in rotor state equation

B_{RFU} = fuselage output coefficient matrix in rotor state equation

B_{RL} = lag damper coefficient matrix in rotor state equation

B_{RT} = drive train output coefficient matrix in rotor state equation

BTL = lag damper output coefficient matrix in drive train state equation

BTR = rotor output coefficient matrix in drive train state equation

B_{1S} = main rotor longitudinal cyclic control input

$B(\psi)$ = coefficient matrix in rotating frame blade flapping equation

$B'(\psi)$ = coefficient matrix in rotating frame blade lagging equation

c/c_c = damping ratio

c_1, c_2, c_3 = coefficients

C = coefficient matrix in output equation $\bar{y} = C\bar{x} + D\bar{u}$

C_{AFU} = fuselage state coefficient matrix in fuselage aero output equation

C_{AR} = rotor state coefficient matrix in fuselage aero output equation

C_{EE} = engine state coefficient matrix in engine output equation

C_{FG} = parameter, fuel flow to gas generator dynamics

C_{GP} = parameter, gas generator to power turbine dynamics

C_{RFU} = fuselage state coefficient matrix in rotor output equation

C_{RR} = rotor state coefficient matrix in rotor output equation

C_{RT}	=	drive train state coefficient matrix in rotor output equation
CTE1, CTE2	=	engine state coefficient matrix in drive train output equation
C_{TT}	=	drive train state coefficient matrix in drive train output equation
C_1	=	speed ratio, tail rotor/main rotor
d_e	=	equivalent viscous damping between engine and fuselage
d_H	=	equivalent viscous damping between rotor hub and fuselage
d_{HE}	=	equivalent viscous damping due to shaft rate of deflection between engine and hub
D	=	coefficient matrix in output equation $\bar{y} = C\bar{x} + D\bar{u}$
D_{AC}	=	rotor control coefficient matrix in fuselage aero output equation
D_{AFU}	=	fuselage output coefficient matrix in fuselage aero output equation
D_{AR1}	=	rotor accelerations coefficient matrix in fuselage aero output equation
D_{AT}	=	drive train output coefficient matrix in fuselage aero output equation
D_{EF}	=	fuel control output coefficient matrix in engine output equation
D_{RC}	=	rotor control coefficient matrix in rotor output equation
D_{RFU}	=	fuselage output coefficient matrix in rotor output equation
D_{RR1}	=	rotor acceleration output coefficient matrix in rotor output equation

D_{RT} = drive train output coefficient matrix in rotor output equation

ECU = electronic control unit

f_o, f_{1c}, f_{1s}, f_{2c}, f_{2s} = components of $F(\psi)$ matrix expanded in a truncated series

F_i = i^{th} force component

$F(\psi)$ = coefficient matrix in rotating frame blade flapping equation

$F'(\psi)$ = coefficient matrix in rotating frame blade lagging equation

$G(\psi)$ = coefficient matrix in rotating frame blade flapping equation

$G'(\psi)$ = coefficient matrix in rotating frame blade lagging equation

H = rotor forward force

H = transpose of transformation matrix from rotating blade coordinates to multi-blade coordinates

HMU = hydromechanical unit

I_g = inertia of gas generator turbine and compressor

I_h = inertia of rotor hub

I_p = inertia of power turbine and output shaft

J = matrix

J = rotor lateral force

k_{H1}, k_{H2} = equivalent torsional stiffness between the rotor hub and engine 1 and 2

LDS = load demand spindle

L_F = fuselage roll aerodynamic torque

L_H = rotor roll torque

m	=	mass
M_F	=	fuselage pitch aerodynamic torque
M_H	=	rotor pitch torque
NG	=	gas generator turbine speed
NP	=	power turbine speed
N_F	=	fuselage yaw aerodynamic torque
N_g	=	gas generator turbine speed (rpm)
N_p	=	power turbine speed (rpm)
N_{P1}, N_{P2}	=	shaft speed of power turbines 1 and 2
p	=	roll rate, fuselage
PAS	=	power available spindle
PO	=	ambient pressure (altitude)
P_R	=	compression ratio
P_{S3}	=	compressor output static pressure (psi)
P_{41}	=	gas generator turbine inlet pressure (psi)
P_{45}	=	power turbine inlet pressure (psi)
q	=	pitch rate, fuselage
Q_{COMP}	=	compressor load torque
Q_E	=	engine output torque (ft lb)
Q_{GTURB}	=	gas generator turbine output torque
Q_H	=	rotor yaw torque
Q_{LD}	=	sum of lag damper torques
Q_{MR}	=	main rotor torque

Q_{PTURB}	=	power turbine output torque
Q_{P1}, Q_{P2}	=	torque transferred by drive train to power turbines 1 and 2 (ft lb)
Q_{ROTOR}	=	helicopter load torque on engine
Q_1, Q_2	=	torque, engines 1 and 2
r	=	yaw rate, fuselage
r_{H1}, r_{H2}	=	gear ratio between the main rotor hub and engines 1 and 2 (rotor speed/engine speed)
R_L	=	variable rate limit
s	=	Laplacian operator
SHP	=	shaft horse power
t_f	=	final time
T	=	rotor axial force
T_{IN}	=	temperature in
T_r	=	engine thrust before rate limiting
T_2	=	temperature, ambient
T_{45}	=	power turbine inlet temperature
u	=	axial velocity, fuselage
u	=	input
v	=	lateral velocity, fuselage
VG	=	variable guide vane setting
w	=	vertical velocity, fuselage
W_{45R}	=	engine mass flow condition
W_F	=	fuel flow rate (pps)

$\bar{x}$ = vector of states

x_E = vector of engine states

x_1, x_2 = states 1 and 2

X_{E1}, X_{E2} = vector of states for engine 1 and engine 2

X_F = fuselage forward aerodynamic force

X_T = vector of drive train states

$\bar{y}$ = vector of outputs

y_E = vector of engine outputs

y_F = vector of fuel control outputs

y_L = vector of lag damper outputs

y_R = vector of rotor outputs

y_T = vector of drive train outputs

Y_F = fuselage lateral aerodynamic force

Z_F = fuselage downward aerodynamic force

GREEK, ETC.

α = linear parameter

β = vector of multi-blade flapping coordinates

β_r = vector of rotating frame flapping coordinates

β_o, β_{1c}, β_{1s}, β_{2c}, β_{2s} = multi-blade flapping coordinates for a five-bladed rotor

β_1, β_2, β_3, β_4, β_5 = rotating frame flapping coordinates for a five-bladed rotor

γ = ratio of specific heats

δ_T = power lever angle

ϵ_1, ϵ_2 = deflections in the drive train between engine 1 and the rotor hub, and engine 2 and the rotor hub (referenced to the hub frame)

ξ = vector of multi-blade lagging coordinates

ξ_r = vector of rotating frame lagging coordinates

ξ_o, ξ_{1c}, ξ_{1s}, ξ_{2c}, ξ_{2s} = multi-blade flapping coordinates for a five-bladed rotor

ξ_1, ξ_2, ξ_3, ξ_4, ξ_5 = rotating frame flapping coordinates for a five-bladed rotor

η_c = compressor efficiency

θ = roll attitude, fuselage

θ_c = main rotor collective control input

θ_{TR} = tail rotor collective control input

μ = rotor advance ratio

Σ = summation signal

τ = time constant

τ_g = gas generator turbine dynamic time constant

τ_p = power turbine dynamics time constant

ϕ = roll attitude, fuselage

ψ = yaw attitude, fuselage

ψ_i = azimuth angle of i^{th} blade

Ω_p = power turbine rotation rate

Ω_{MR} = main rotor rotation rate

Ω_{TR} = tail rotor rotation rate

SUBSCRIPTS, SUPERSCRIPTS, ETC.

$( )_{IC}$	=	( ) at initial condition
$( )_N$	=	new ( ), refers to condition at current time step
$( )_O$	=	old ( ), refers to condition at previous time step
$( )_o$	=	trim or initial value of ( )
$( )_{TRIM}$	=	trim condition of ( )
$\Delta( )$	=	perturbation of ( ) from trim
$\delta( )$	=	perturbation of ( )
$*( )$	=	the axis transformation components have been deleted from ( )
$/( )/$	=	absolute value of ( )
$( )^T$	=	transpose of ( )
$( )^{-1}$	=	inverse of ( )
$(\bar{})$	=	vector ( )
$(\dot{})$	=	$\frac{d}{dt}( )$

I. INTRODUCTION AND SUMMARY

1.1 INTRODUCTION

It is important to be able to predict coupled propulsion system and rotor system dynamic responses for rotorcraft. The capability is needed for assessing the effects of varied fuel control design, rotor lag damper characteristics, and drive system equivalent flexibility, among other possible improvements. Specific occurrences of coupled propulsion system/rotor system dynamic problems have been observed in current rotorcraft, such as the CH-47C. The potential exists for stability problems in new vehicles, such as the UTTAS, AAH, and XV-15, and in prototype vehicles designed for enhanced performance, such as the X-Wing or HH-20 (CCR). Experimental and operational data from rotorcraft indicate that improper matching of rotor dynamic characteristics with drive system and engine response modes is a fundamental source of undesirable vehicle stability and vibration characteristics. The technology applies to a wide range of rotor system types and propulsion/fuel control configurations.

Development of the capability to predict coupled propulsion/rotor dynamic responses for a range of rotorcraft designs has not been systematically initiated. The basic reason is that the development of a comprehensive analysis approach using a generic methodology, is a highly multidisciplinary objective. The objective is broader than the specific product development and manufacturing objectives of many helicopter or engine companies.

1.2 SUMMARY

Systems Control Technology, Inc. (SCT) undertook a program to establish a generic methodology and model structure for performing coupled propulsion/rotor response analysis that would be applicable to a variety of rotorcraft types. In this program, SCT performed the following tasks:

(1) Developed a model structure, adaptable to a wide range of rotorcraft configurations, for simulating coupled rotor/propulsion dynamics.

(2) Defined a methodology for parameterizing the model structure to represent a particular rotorcraft.

(3) Constructed a nonlinear coupled rotor/propulsion model for a particular (though not existing) rotorcraft as a test case to use in analyzing coupled system dynamics. The model included a propulsion system and a rotor/fuselage system as follows:

> (a) The propulsion system was constructed from an existing engine/fuel control model and a drive train model derived by the author.
>
> (b) An existing helicopter rotor and airframe handling qualities simulation was used for the rotor fuselage system.

(4) Constructed a partially linear coupled rotor/propulsion model by applying perturbation and subset regression techniques to linearize the engine and rotor components of the nonlinear model. This step was not completed due to difficulties associated with the periodic dynamic effects in the rotor dynamics at the rotorcraft speed chosen for linearization.

1.3 ORGANIZATION OF REPORT

This report is divided into two volumes. Volume I contains the body of the report and the analytical part of the appendix. Volume II contains documentation on the computer models that were developed.

In Volume I, Chapter II gives a problem overview and discusses the background of the problem. Chapter III describes the generic modeling methodology. Chapters IV and V document the development of the propulsion system and the rotor/fuselage models, respectively. Chapter VI describes the formulation of the resulting coupled rotor/propulsion system model and describes a test case that was developed. Finally, Chapter VII summarizes the project and makes recommendations for further model development.

This Page Intentionally Left Blank

II. BACKGROUND AND PROBLEM OVERVIEW

This section reviews the background of the program and details the issues associated with development of a coupled rotor and propulsion system analysis.

2.1 BACKGROUND AND PROBLEM OVERVIEW

2.1.1 Background

The basic dynamic elements of a typical helicopter propulsion drive system are shown in Figure 2.1. One or more engines drive a system of shafts, gear reductions, the main rotor(s) and the tail rotor. The main and tail rotor are the primary force and moment producers. While many elements of this sytem have been designed to minimize coupling between the elements, recent experience has demonstrated the need for a more systematic treatment of rotor/propulsion system interaction.

In older helicopters, the flight and propulsion system dynamics of the rotorcraft were not closely coupled because there was a separation between the speeds of response of these subsystem dynamics. Propulsion system dynamics were much faster than the flight dynamics, and thus handling qualities designers could assume the rotor had a constant rate as far as handling qualities were concerned. In recent helicopter designs, however, demands for higher flight performance have led to designs in which there is significant and even destabilizing coupling between subsystems.

One dramatic example of this involved the CH-47C helicopter with a Lycoming T-53 engine [1]. During testing of this vehicle, severe rotor oscillations were encountered, leading to pronounced fuselage vibration. Time histories of the responses of several of the variables that were involved are shown in Figure 2.2a

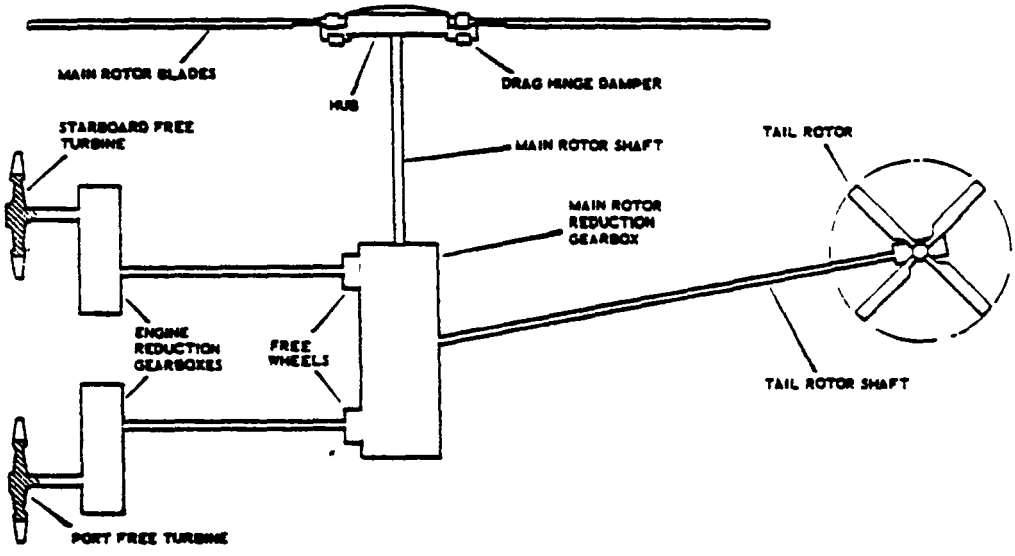

Figure 2.1 Typical Helicopter Rotor and Transmission System

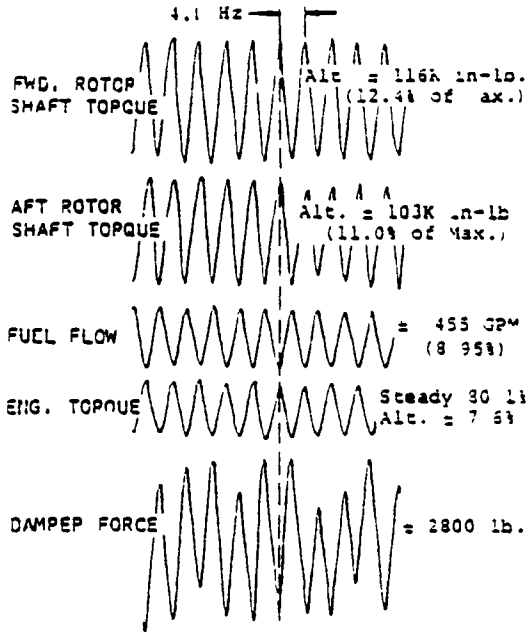

Original Fuel Controls
Standard Lag Dampers

Figure 2.2a Torque Oscillation Flight Test Data [1]

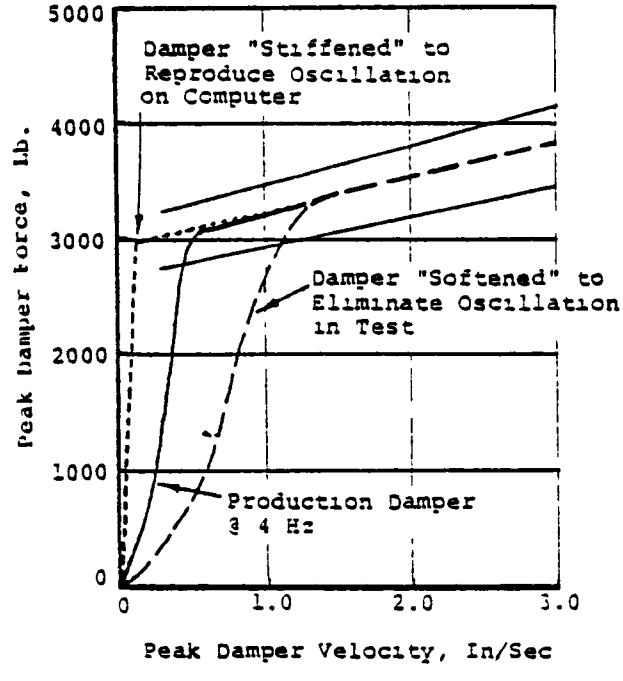

Figure 2.2b Lag Damper Force-Velocity Curves [1]

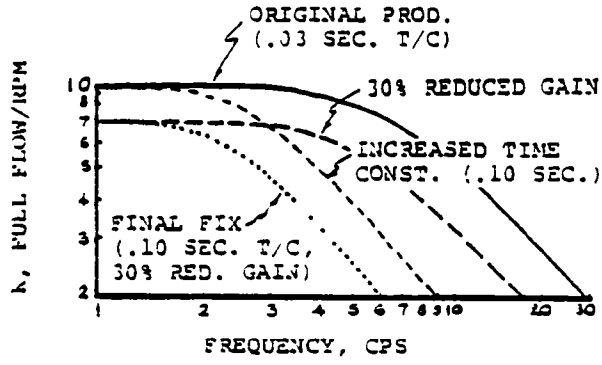

Figure 2.2c Fuel Control Frequency Response [1]

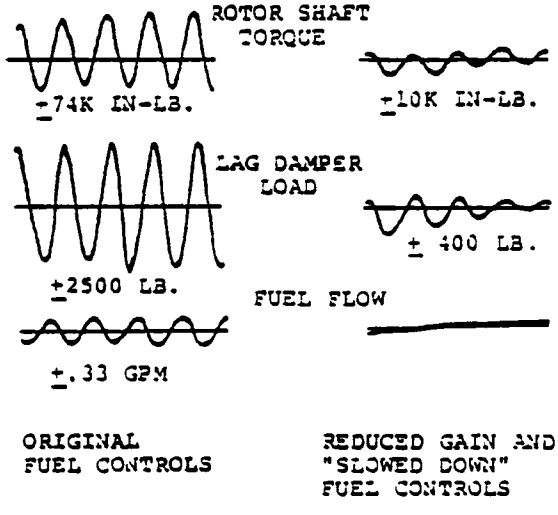

Figure 2.2d Final Torque Oscillation Simulation [1]

[1]. Two parameters were varied in the test program to reduce the oscillation shown. First, the blade lag damper was "tuned down" which reduced that particular problem (Figure 2.2b), and then the fuel control time constant was increased and the gain reduced (Figure 2.2c). The result was the acceptable response of Figure 2.2d.

In response to the CH-47C problem, and related experiences, a series of studies was sponsored by the Army at Ft. Eustis. Results of these studies are detailed in Ref. 2. Table 2.1 lists some of the relevant interface problems that are discussed in the volumes describing these studies.

The background for the current program was the recognized need for a systematic approach to analyze and avoid such problems in design and test programs.

2.1.2 Problem Overview

The principal elements which must be considered in a systematic rotor/propulsion system response analysis are:

- engine models;
- fuel control models;
- rotor model; and
- drive train models.

The frequency range of interest initially is a range of approximately 0-5 Hz (or zero to approximately once per rotor revolution). A model valid over a larger frequency range would be desirable. However, this would require more detailed representations of the rotor system, drive train, and aircraft. This effort is beyond the scope of the present analysis and consequently application of the model is restricted to this frequency range. Still, a significant number of previous engine/airframe/drive train dynamic interface development problems [2] have occurred within this frequency range, including

Table 2.1

Interface Problem History

- TORSIONAL MODE OSCILLATION - COLLECTIVE LAG
  - SIKORSKY CH-53E/T64
  - BELL OH-4A/DDA 250 SERIES
  - BOEING CH-47C/LYCOMING T55-L-11
- EXCESSIVE ROTOR DROOP & OTHER RPM CONTROL PROBLEMS
  - SIKORSKY/BLACKHAWK
  - BELL YAH-63/GE T700
  - BOEING YUH-61A/GE T700
- ENGINE HUNTING
  - SIKORSKY XH-59A/PT6T-6
- ENGINE LOAD SHARING OSCILLATION - 2 ENGINES
  - SIKORSKY SH-34H/GE T5
  - TILT ROTOR
- EXCESSIVE TRANSIENT LOADING (HIGHER FREQUENCY)
  - BELL YAH-63/GE T700 - OVERSPEED TRIP
  - BOEING CH-47/LYCOMING T55 - ROTOR START UP

engine torque oscillations, engine load-sharing problems, and excessive transient RPM droop.

Modern rotorcraft utilize free-turbine engines where the second or power turbine section is connected to the output shaft (Figure 2.3 [3]). Because the load on this output shaft varies with collective control and flight speed, modern turbines, in particular, require multiple sensing feedback paths and multivariable controls to sustain design RPM. The control system of the current GE/T700 engine, for example, is illustrated in Figure 2.4 [3].

The propulsion system dynamics are especially important to flight control in the vertical mode because the propulsion system is then the only source of power. To change the amount of lift over even a few seconds, the fuel flow must be changed. In forward flight, kinetic energy can be exchanged for lift. In the vertical mode there is no mechanism of energy storage that is large enough to provide a sustained engine output variation. Because of the close relationship between flight and engine performance, overall performance can be enhanced by jointly controlling these modes.

In current practice, the engine and flight control system are designed separately. Handling quality analyses and automatic flight control design analyses do not typically consider the main rotor RPM a degree of freedom. In addition, specific goals for engine transient response are not well defined. Instead, the engine is specified to respond to a step input as quickly as possible without overly degrading stability margins. This approach has its limits, especially when the engine/fuel controller response is not fast enough for good handling, but is so fast that it interacts with some torsional/flexural modes and causes vibrational oscillations. This situation can often occur in rotorcraft design because of the relatively low-frequency torsional bending mode of the rotor. Figure 2.5 [4] shows some of the torsional modes for the XV-15. The first mode is shown to

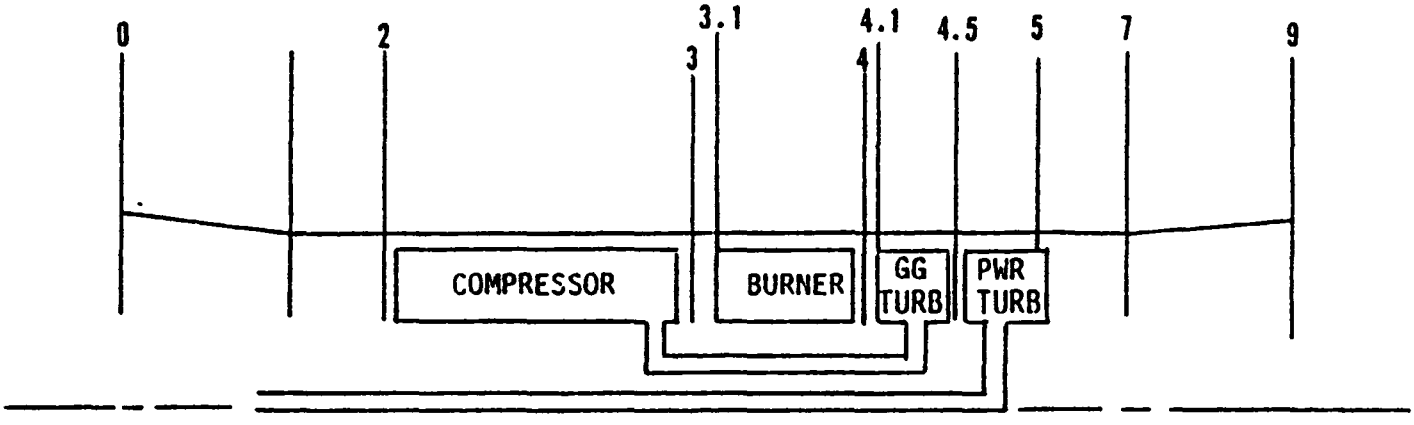

0. FREE STREAM AIR CONDITIONS
1. INDUCTION SYSTEM OUTLET/ENGINE INLET INTERFACE
2. COMPRESSOR INLET
3. COMPRESSOR OUTLET
3.1 BURNER INLET
4. BURNER OUTLET/FIRST TURBINE STAGE INLET INTERFACE
4.1 FIRST TURBINE ROTOR STAGE INLET
4.5 GAS GENERATOR TURBINE OUTLET/POWER TURBINE INLET INTERFACE (INLET TO POWER TURBINE NOZZLE)
5. LAST TURBINE STAGE OUTLET
7. ENGINE OUTLET/EXHAUST DUCT INLET INTERFACE
9. EXHAUST DUCT OUTLET

Figure 2.3 Elements of Current Rotorcraft Engines [3]

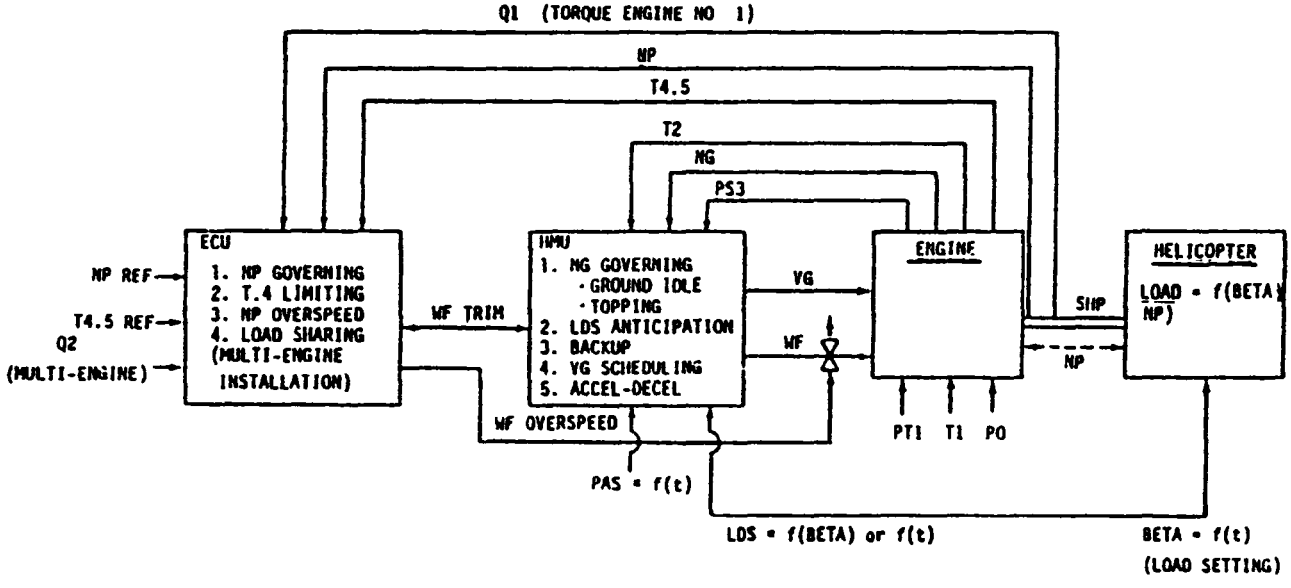

Figure 2.4 T700 Control System [3]

Torsional modes	Frequency (per rev)		Mode shapes
	565 rpm	458 rpm	Pylon
1st asymmetric flexible mode (interconnect shaft mode)	39	48	Engine Rotor Interconnect See Note
1st symmetric flexible mode (symmetric power turbine mode)	1 26	1 55	
2nd asymmetric flexible mode (asymmetric power turbine mode)	1 43	1 76	
2nd symmetric flexible mode (symmetric pylon roll mode)	3 42	4 22	
3rd asymmetric mode (asymmetric pylon roll)	3 49	4 30	

Note Engine rotations referred to tilt rotor
Positive engine rotation same as corresponding tilt rotor

Figure 2.5 Torsional Rotor/Drive Train/Engine Bending Modes for XV-15 [4]

be at 3.67 Hz. In addition, many conventional articulated helicopters need to incorporate a lag damper to prevent ground resonance. This adds another set of torsional modes, the first of which involve rigid blade collective lag about the lag hinge, at approximately 3 Hz. The demand for more responsive helicopters in recent years has been met by using more responsive engines. However, due to torsional mode interaction, the limitation of this approach has been reached, and manufacturers have started to use combined automatic flight/propulsion control systems.

In conventional helicopters, the propulsion system dynamics can cause handling problems and reduced responsiveness. A common mode of flight/propulsion interaction is known as rotor droop. Conventional rotorcraft regulate the rotor RPM to be near a design value which is limited in part by consideration of various rotor blade bending modes. When there is an external disturbance or a step-collective input, the increased drag on the rotor makes it slow down or droop. The increased torque demand is apparent to a separately designed fuel controller only through RPM droop, and therefore the engine response is delayed. This droop is caused by the transfer of rotor kinetic energy into lift. However, as the RPM decreases so does the lift and the effectiveness of the collective input. This degrades the handling quality of the vehicle. Also, when the rotor torque increases due to fuel controller action, the yaw reaction torque on the fuselage increases. This causes a perturbation in yaw that is further compounded when the main and tail rotor RPMs droop causing a reduction in tail rotor effectiveness. Pilots often compensate for droop by applying some pedal input along with collective stick input. The cross-coupling between the propulsion system and the yaw mode can also act in reverse. A change in yaw moment causes a change in the reaction torque on the rotor, which will cause an RPM variation. A fast fuel controller can detect this and cause the engine to change its

torque output. However, due to dynamic phase lag, this torque change acts not so much to regulate RPM, but rather to reduce the stability in the dutch roll mode. These fuselage/engine cross-coupling phenomena are discussed for the Blackhawk helicopter in Ref. 5.

The XV-15 has some additional engine/airframe interactions that have caused trouble [6]. The aerodynamic damping of the RPM governing system decreases with decreasing power required. This has caused the governor to oscillate in high-speed flight. The current solution is to lower the governing gain for good operation with worst-case damping.

The state of the art solution to engine/airframe interaction is to keep the fuel flow controller slow enough to eliminate unfavorable coupling and to use a rudimentary form of combined control. The combined control involves using the collective stick input to bias the RPM error signal. In this way the engine is made aware of the changed torque requirement when the pilot commands it. This was used in the Blackhawk and, to a much greater degree, in the tilt rotor. When the rotor inertia is small, the link between the collective input and throttle control needs to be more pronounced. In the XV-15 tilt rotor, for example, the lever in what is normally the collective stick position is the power lever which is the engine throttle control. The collective rotor blade pitch control levers are cam-linked to the power lever. Also, the RPM is not regulated using fuel flow, but rather by adjusting the collective pitch of the rotors. This method of regulation prevents the exchange of rotor kinetic energy for lift. It is necessary because the rotors have relatively low moments of inertia and therefore do not store much energy. Exchange of energy causes larger RPM variations in smaller rotors.

The helicopter or XV-15 response could be further improved if a controller were designed based on the combined coupled airframe/propulsion system characteristics.

Another important engine control problem occurs with multiple engines. This problem is load-sharing oscillations, as demonstrated in Figure 2.6 [7]. An initial load-sharing problem (now solved) occurred in the Sikorsky SH-34H/T-58 helicopter.

The major tool required for combined propulsion/flight control is a suitable dynamic model.

2.2 METHODS OF ANALYSIS

In the past, the procedure for designing for adequate combined system (engine, rotor, fuel control, etc.) performance has been to:

(1) design the engine control for optimal response to step-load change;

(2) design the rotor system assuming it will be driven by the engine at constant RPM;

(3) use currently known rules of thumb to account in the design for interactions between system elements (e.g. rotor, fuel control, engine).

More recently, at Sikorsky for example [5], high-fidelity nonlinear models have been used to analyze the interactions of rotorcraft system components and to design to prevent or to correct interaction problems. Other approaches have involved ad hoc modifications to nonlinear models to allow consideration of specific interaction problems.

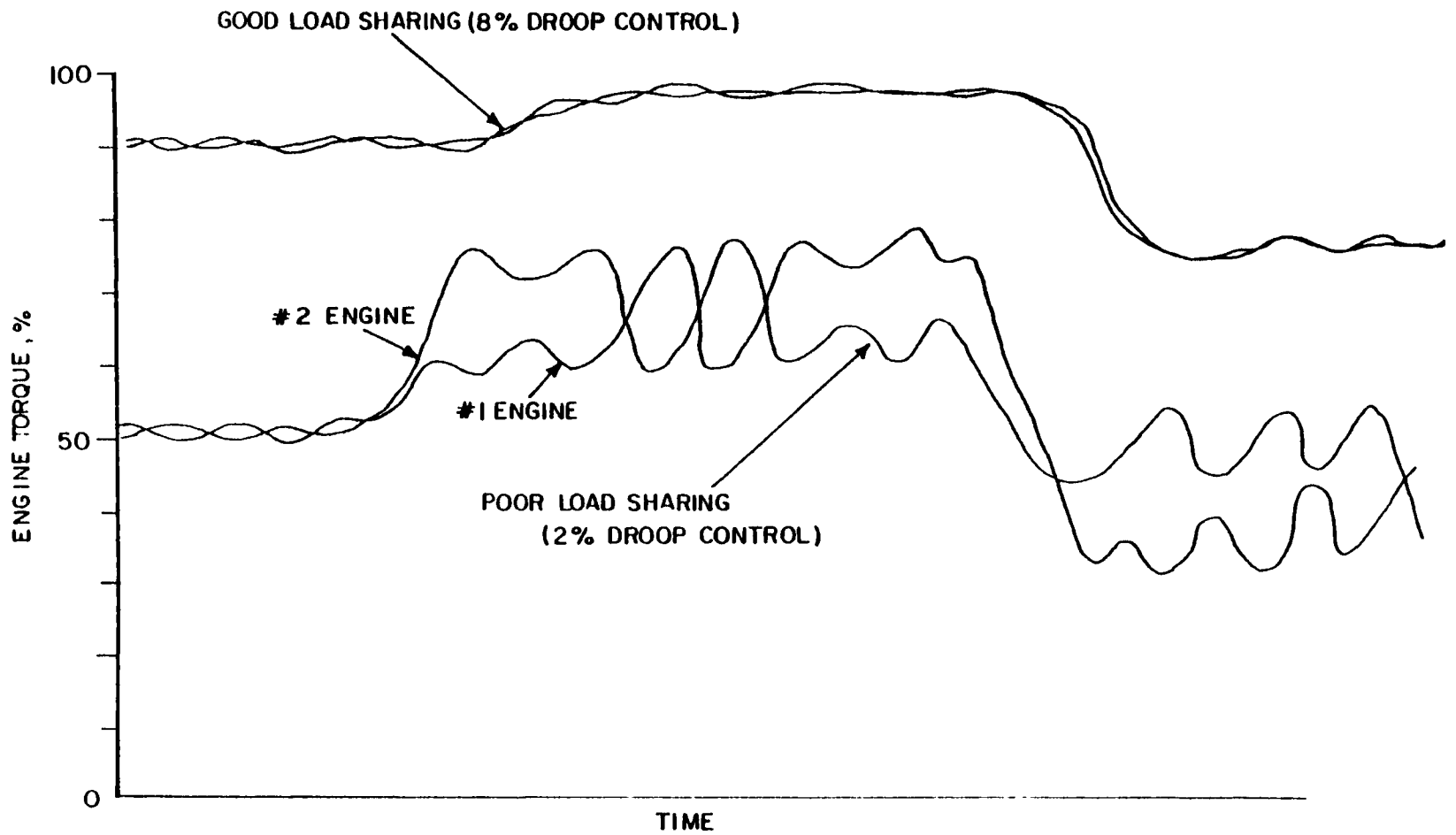

Figure 2.6 Engine Load Sharing Oscillations [7]

III. GENERIC MATH MODELING

The purpose of this project was to develop a generic methodology and a model structure for performing coupled rotor/propulsion response analysis. The methodology was desired to allow accurate consideration of the interactions of rotorcraft system components, in a specific frequency range, without the complexity of high-fidelity nonlinear models. This chapter describes the method of approach that was developed. The sections of this chapter that follow identify the requirements on the model structure and the approach developed to meet these requirements.

3.1 PURPOSE

A rotorcraft/propulsion dynamics model would be used in applications like the following:

- flight/rotor/propulsion control system research and development
- trade studies for defining specification requirements, e.g. ensuring acceptable coupling of rotor and propulsion dynamics
- predicting flight characteristics for flight test planning and flight safety analysis
- support of development flight testing in areas such as troubleshooting, control system revision, and data analysis

These applications require an accurate model, but do not require the high complexity of some nonlinear engine and rotor component models that are available, but not coupled together.

3.2 MODEL STRUCTURE REQUIREMENTS AND SCOPE

The intended uses of the model require that it accurately predict rotorcraft handling qualities, instabilities, oscillations, and transient performance within a specified frequency range. The intended uses also require that the model structure and variables relate directly to physical explanations so the results of an application of the model can be easily interpreted in terms of the structure.

Certain effects should be considered in the model. These include torsional mode stability, engine load-sharing problems, RPM droop and effects on handling quality.

Only a limited frequency range is required for the model. Figure 3.1, compiled by Sikorsky Aircraft [5], shows frequencies, representative of a medium-sized helicopter, from which it is apparent that the dynamic modes of interest in this project occur at frequencies between zero and the shaft speed, Ω_{MR}. This frequency range includes the first torsional modes of the rotor/drive system and rotor/airframe, the drive system/fuel control "hunting" frequency, fuselage instabilities, and the rigid flap and lag motions of the rotor blades.

3.3 GENERIC MODELING APPROACH

The sections that follow give a general picture of a generic modeling approach that was developed that can be used to construct a coupled rotor/propulsion dynamic response model for investigating performance in the zero to once per rotor revolution frequency range.

3.3.1 Model Structure

The generic modeling approach entails construction of a total system model from linear or nonlinear state models of each

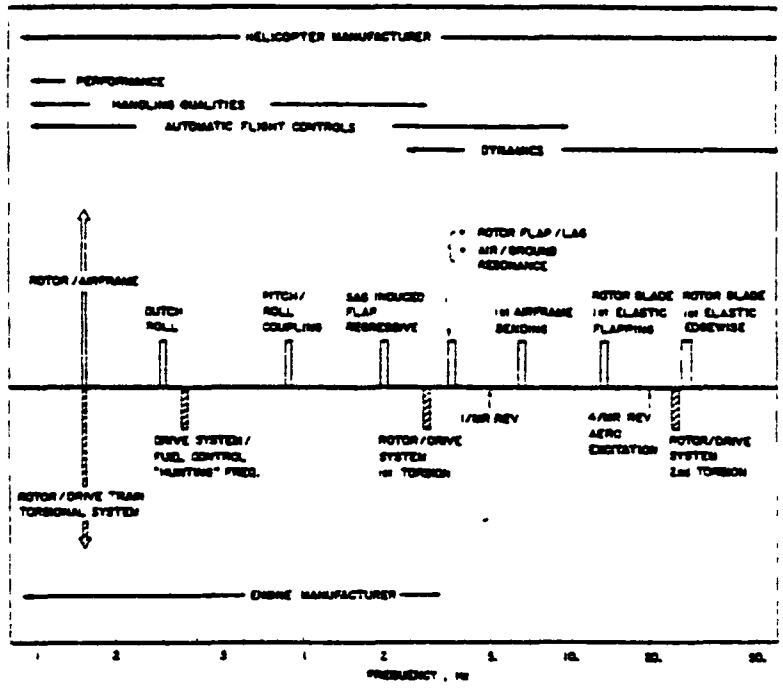

Figure 3.1 Modal Frequencies of Interest In Engine/Fuel Control Design [5]

subsystem component (e.g. fuselage, rotor, engine). This approach provides a flexible, adaptive model structure that can be used to simulate a variety of rotorcraft designs. The structure allows subsystem models to be added, deleted, replaced, or modified to meet a particular application.

Figure 3.2 shows the generic structure chosen for the rotor/propulsion dynamics model. The figure shown is for the dynamics of a twin engine, single main rotor helicopter in hover or forward flight. This figure contains a block for each subsystem model. Connecting lines show the paths of interaction between subsystems. The subsystems are linked along these paths by physical principles.

The structure used for each component in the coupled system rotorcraft model is shown in Figure 3.3. This input/output form is general, and allows independent subsystem components to be easily connected together into a system.

The subsystem model components are derived from detailed nonlinear simulations of each component. These detailed simulations can be obtained from the component manufacturers (e.g. for engines and fuel controls) or currently available simulations (e.g. the GENHEL rotor, airframe, control system simulation).

The control system components of the model can be allowed to contain important nonlinearities. The control systems are the lag damper, fuel control, and flight control. Nonlinear effects are important in the control models because of their effects on the dynamic response. Also the model may be used in the design and analysis of control systems and thus may require high-fidelity nonlinear control models.

3.3.2 Linear Model Formulation Methodology

Models for the linear components of the combined system model are formulated using perturbation techniques. With these

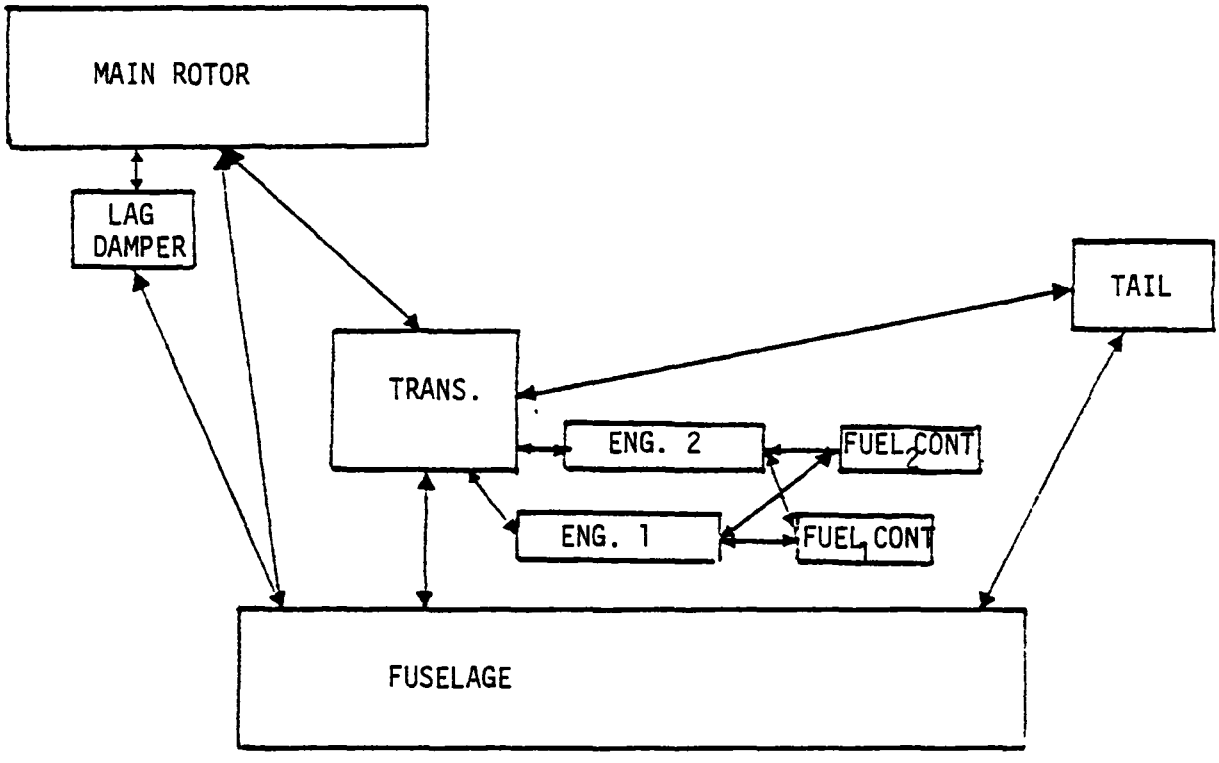

Figure 3.2 Components of Coupled Generic Rotorcraft Model

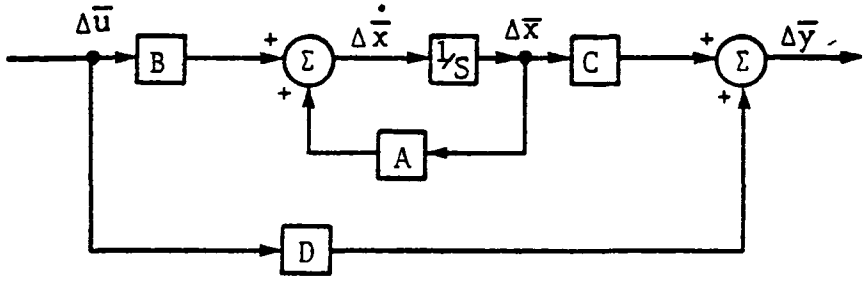

Figure 3.3 Input/Output Form Used For Modeling Subsystems

techniques, equations are constructed using perturbation values about trim (or nominal) operating conditions of the rotorcraft. The trim values can be added back onto the predicted response perturbations to yield the "total" response values.

Several techniques are available for extracting these linear, simplified models from complex nonlinear simulations. These include:

- state and derivative perturbation techniques;
- subset regression techniques;
- system identification techniques with time histories generated from a nonlinear simulation model.

Additionally, equations can be derived or extracted analytically.

3.3.3 Subsystems

The subsystems of the generic model shown in Figure 3.2 include the following:

- rotor
- fuselage
- engines (2)
- fuel controls (2)
- drive train
- lag damper
- tail rotor

Some of the details and assumptions which were used in developing the generic form for modeling each of these subsystems are described below.

Fuselage

The fuselage was assumed to be rigid. It was modeled by nine states. These included axial, lateral, and vertical velocities (u, v, w); roll, pitch, and yaw rate (p, q, r); and roll, pitch and yaw attitude (ϕ, θ, ψ).

Rotor

The rotor was modeled using multi-blade coordinates.

Any of three approaches could have been used. These included rotating frame coordinates, multi-blade coordinates, and tip-path-plane coordinates.

In rotating frame coordinates, each blade is modeled separately. This representation makes intersystem (e.g. between rotor and fuselage) dynamic coupling analysis more complex and results in a loss in engineering insight. A fixed-frame representation is more amenable to intersystem dynamic coupling analysis. A fixed-frame representation, such as in multi-blade or tip-path-plane coordinates, using constant coefficient values is adequate for many rotor/drive train/engine coupling modes.

Because the fixed frame representation offers better insight into what is happening and is less complex, it was used in the generic model structure. A multi-blade rather than tip-path-plane representation was used with the number of main rotor flapping states and lagging states each to be equal to the number of blades. This number of states could later be reduced if it were found to represent higher frequencies than required in the model.

Lag Damper

Helicopter lag dampers are very nonlinear, as shown by the typical response plotted in Figure 3.4 [7]. Because the lag

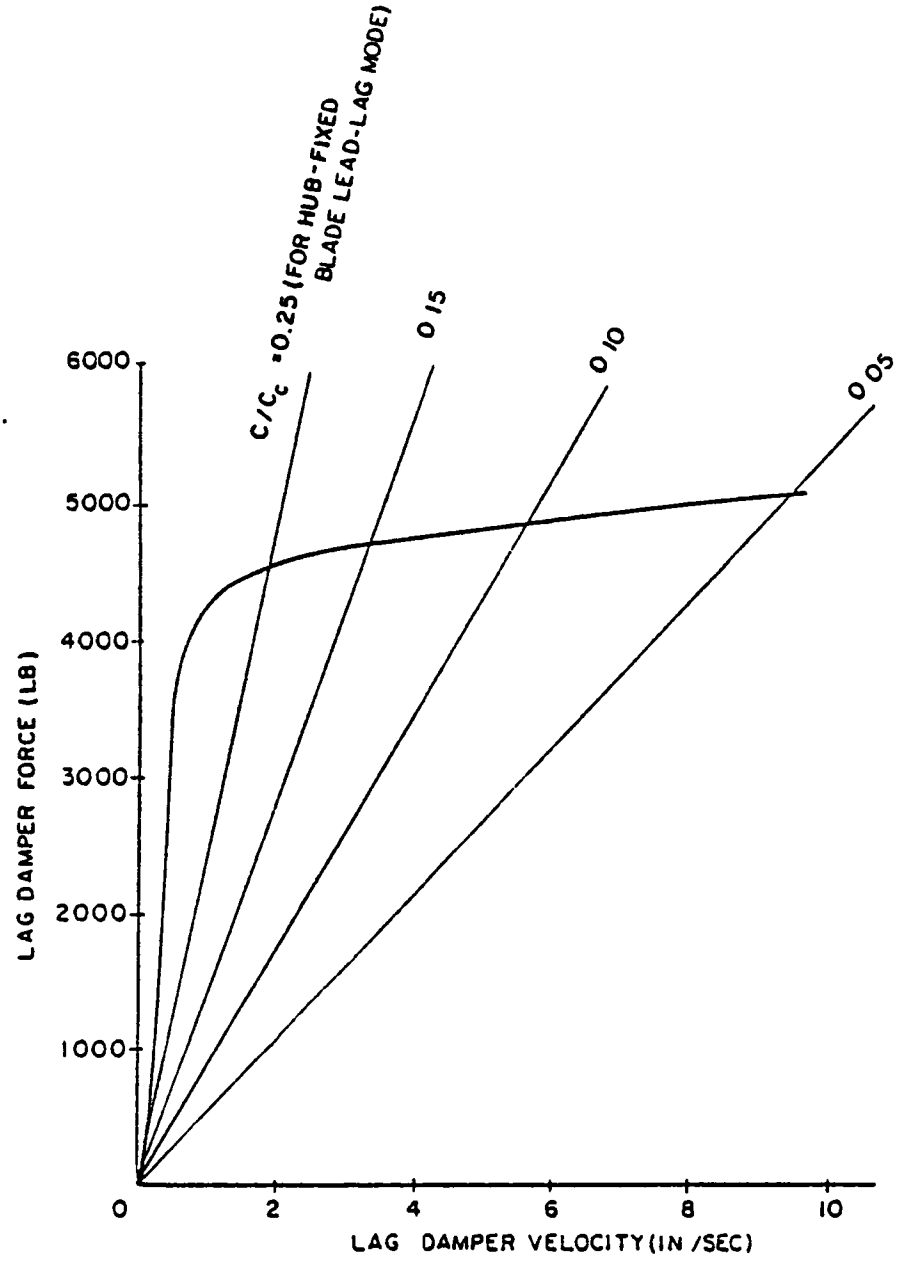

Figure 3.4 Lag Damper Instantaneous Force-Velocity Relationship [7]

damper has an important effect on the rotor dynamics, it should be modeled as a separate, nonlinear element in the model. This approach was taken. It allows straightforward analysis of the sensitivity of rotorcraft performance to variations in the lag damper design.

Drive Train

Drive trains are normally modeled as systems of torsional springs, dampers, and inertias. Gearing ratios add some complexity to this, but standard models [1,5,12,13] are still linear. Nonlinear backlash effects were not considered.

Engine and Fuel Control

The engine and engine control system models were required to describe the dynamics and coupling to the rotor and airframe up to the rotor RPM frequency (3 to 5 Hz). A perturbational model was used for the engine model while a nonlinear simulation was used for the fuel control. The perturbational engine model was extracted from a nonlinear engine simulation.

Tail Rotor

Tail rotor dynamics could either be modeled explicitly, as a separate part of the model, or as a control acting directly on the dynamics of the fuselage, without separate tail rotor dynamics. Because this was the first construction of the model the simpler approach was taken. At a later date, the structure could be extended to allow explicit modeling of the tail rotor.

Control Systems

A flight control system model was necessary in order to test "fly" the model. A control system in an existing helicopter simulation was used.

The pilot controls included in the model were:

- main rotor - collective pitch, longitudinal and lateral cyclic pitch
- tail rotor - collective pitch

3.4 MODEL ORGANIZATION

The generic model structure was constructed in a modular fashion with modules as were shown in Figure 3.2. In this manner, the modules could be developed independently. This formulation gave the generic model structure flexibility because any module could be independently modified or replaced by a new module or one parameterized for a different helicopter. The detailed development of each of the modules of the model that was developed to test and demonstrate the structure are discussed in the chapters that follow.

This Page Intentionally Left Blank

IV. PROPULSION SYSTEM MODELING

A propulsion system model of a particular engine, fuel control and drive train combination was constructed n the format of the generic model structure. The model was constructed n order to test and demonstrate the methodology being developed. The development of this propulsion system model is described in this chapter.

The elements which make up the propulsion system are:

- engine models
- fuel control models
- drive train models.

This chapter describes the development of this propulsion system model. The results of the chapter are a fully parameterized computer simulation modeling a specific helicopter engine/fuel control/drive train combination.

4.1 DEVELOPMENT OF ENGINE AND FUEL CONTROL MODELS

4.1.1 Problem Overview

The propulsion system can be described in mathematical terms in several ways. The choice of model form has an important impact on the usefulness of the resulting model. A consideration in developing the model is the interface between the engine and the input/output boundaries. Models that describe the throttle linkage and fuel control as well as the engine may be significantly different from "open-loop" models of the engine.

An engine model for the propulsion system is desired which describes the engine torque response to fuel inputs from the fuel control and to drive train and rotor dynamic loadings (within excitable bandwidths). Dynamics in the engine or fuel control

which are not excited during this operation are not considered important to the modeling task. The sophistication of the engine model should be consistent with that of the other elements of the coupled rotor/propulsion system model. The coupled model is intended to reproduce dynamic phenomena in the zero to once-per-rotor-revolution frequency range.

The value of the engine model will be in its description of important aspects of performance. Steady-state values of torque and shaft speed should be predicted accurately. Dynamic response to small perturbations should accurately reflect engine behavior. Match of intermediate variables such as internal temperatures and pressures describing engine operation is not critical to predicting interaction problems between the rotor and propulsion system.

Models used to describe typical engine behavior vary widely in complexity and accuracy [8]. The simplest description of engine response is a plot of corrected engine thrust versus power lever angle. A typical characteristic is shown in Figure 4.1. This plot can be used as a dynamic model if an appropriate time lag is associated between the actual throttle position and a lagged or virtual position. The engine is observed to accelerate and decelerate at rates dependent on the power level. This effect can be represented in the model as a variable rate limit. The experimental model thus generated is shown in Figure 4.2. No attempt is made at a phenomenological explanation of the behavior. Parameters are adjusted from observations. Since this model does not reflect the internal cause of the torque response, the match between the system behavior for various size inputs and for different starting and ending values of torque will be poor. A more significant drawback of these models is the poor closed-loop description of the behavior. This mismatch is typically manifested by an incorrect prediction of the closed-loop stability of the system. This is due primarily to matching the step response in estimating parameters rather than

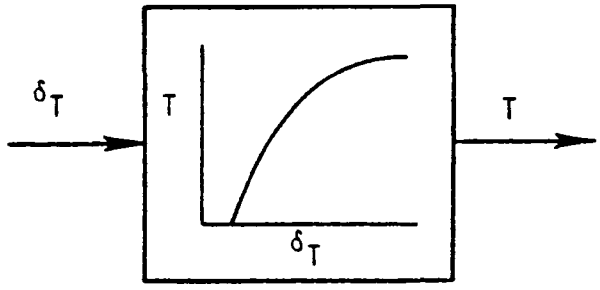

Figure 4.1 Thrust Response to Throttle Input

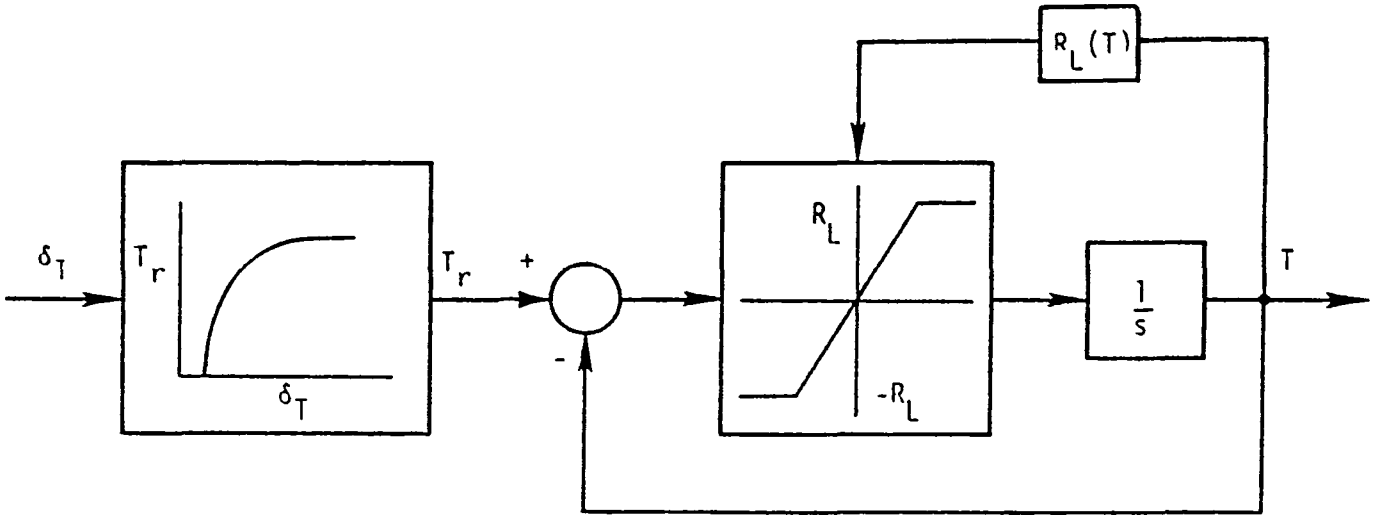

Figure 4.2 Experimental Model of Engine Dynamics

matching frequency response over a suitable bandwidth. Generally, frequency matching requires more complex model forms. In order to accommodate this lack of precision, simple models tend to be "improved" by ad hoc additions which attempt to correct the fundamental non-phenomenological characteristics of the formulation.

Far more complex digital simulations can be generated which model component characteristics measured from rig tests and aerothermodynamic phenomena occurring in the gas path. Such a simulation is shown schematically in Figure 4.3. These simulations include basic physical laws relating energy, work, mass flow, and acceleration as they dynamically interact in the engine. Various "adjustable" parameters such as lumped isentropic efficiencies and areas are adjusted to match the observed steady-state relationships between input and output variables. A detailed representation of the governor is included, and the overall response can be tuned to match observed dynamics. While the type of simulation recreates steady-state performance accurately, the match of transient response is poorer due to modeling uncertainties in the complex equations. Predicted stability characteristics for closed-loop control are quite good, however.

The drawbacks of detailed analytical simulations are that:

(1) a large computer capability is necessary;

(2) detailed internal engine and control information is required which is often not available; and

(3) the added complexity cannot be justified or validated from input/output performance observed in operation.

Clearly, a middle ground must exist.

An experimentally validated analytical description of the propulsion system is ideally suited to an analysis of an integrated rotorcraft system. It can be developed by considering the available measurement data and the type of inputs provided.

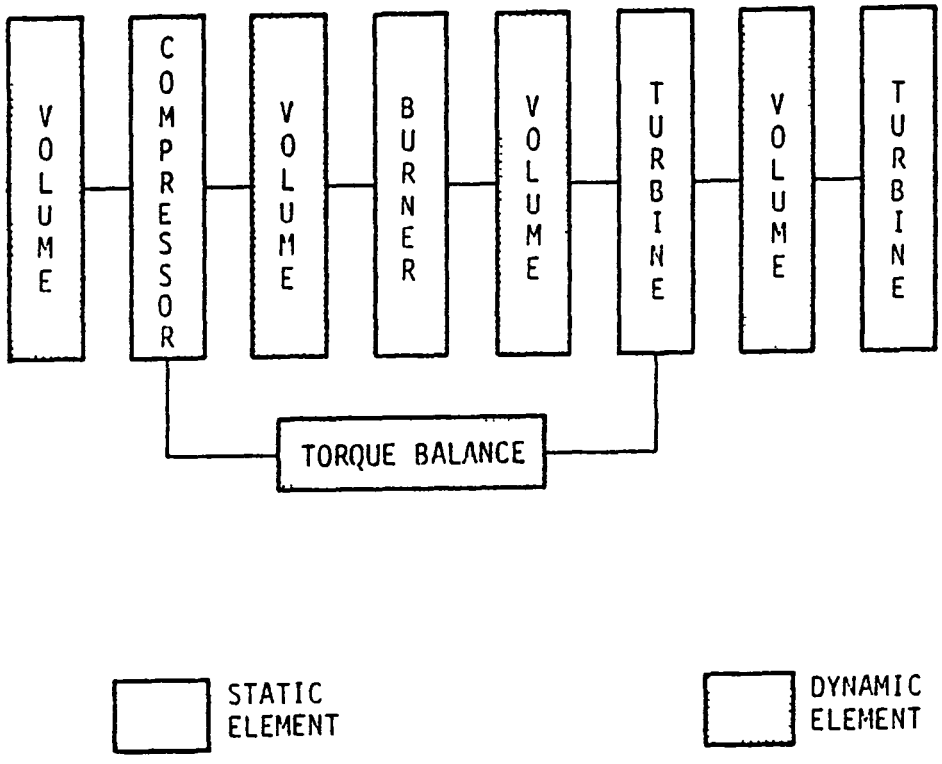

Figure 4.3 Typical Detailed Nonlinear Simulation Computational Flowpath

The development starts with a complete analysis of possible dynamic effects. Data are examined and unimportant or unexcited phenomena are removed. The remaining model terms are examined for bandwidth of response relative to the simulation requirement. Frequency effects outside the drive train and rotor bandwidths can be neglected. The resulting system represents a description of the response including both steady-state and dynamic performance whose parameterization is available from recorded measurements. This type of model can provide an excellent component module in a simulation used to analyze an integrated rotorcraft engine, fuel controller, drive train, and rotor system.

4.1.2 Modeling

The dynamics of the engine in the region near full power are nearly linear. Small perturbations in the state of the engine are characterized by changes in the speed of the power turbine and gas generator turbine. Previous analyses of engine dynamics have verified the linearity and the structure of the linear system representing this behavior [9-11].

Since rotorcraft engines typically have no variable geometry in the gas path, the primary dynamic exciter is the fuel flow which is metered by a hydromechanical governor. Fuel is chemically converted to heat in the combustor. This provides excess energy at the turbine entrance. The combustor lag is typically much faster than the dominant system response. The gas temperature at the entrance to the turbines is converted into work by the expansion through the rotating turbines. This energy is used to drive the compressor on the fixed shaft and the rotor on the free shaft. The dominant engine dynamical states can be associated with the rotating inertia of these elements. Newton's law for the shafts can be written in terms of the speeds and torques as follows:

$$\dot{N}_g = \frac{1}{I_g}\left(Q_{GTURB} - Q_{COMP}\right) \tag{4.1}$$

$$\dot{N}_p = \frac{1}{I_p}\left(Q_{PTURB} - Q_{ROTOR}\right) \tag{4.2}$$

where $(\ )_g$, $(\ )_p$ refer to the gas generator and power turbine turbine shafts. The torques are determined from the mass flow and pressure change across the component. The form of the expression is given below (for a compressor)

$$Q_{COMP} = \frac{T_{IN}\dot{m}\left(P_R^{\gamma} - 1/\gamma - 1\right)}{\eta_c N_g} \tag{4.3}$$

where the compression ratio, P_R, is determined by flow equilibrium through the engine and duct.

These equations can be used as the basis of a global nonlinear model of the engine. Maps of nonlinear parameter variations and detailed dynamical representations of nonequilibrium flow can model the continuity, energy, and mixing phenomena occurring in the gas path. However, these terms can be considered negligible if one is interested in system bandwidths characteristic of rotor and drive train dynamics.

For this study, modeling the engine behavior during moderate speed excursions by a linear set of dynamical equations provides an adequate representation. The form of the system equations can be simplified to second-order for most engines by considering the physical character of the motion. The linear system of constant coefficient equations which is constructed for the engine is shown in a Laplace transform block diagram in Figure 4.4 and collected in state variable form as follows:

$$\begin{bmatrix} \delta\dot{N}_p \\ \delta\dot{N}_g \end{bmatrix} = \begin{bmatrix} -1/\tau_p & C_{gp}(1-\alpha) \\ 0 & -1/\tau_g \end{bmatrix} \begin{bmatrix} \delta N_p \\ \delta N_g \end{bmatrix} + \begin{bmatrix} \alpha C_{Fg} C_{gp} \\ C_{Fg} \end{bmatrix} \delta W_f \tag{4.4}$$

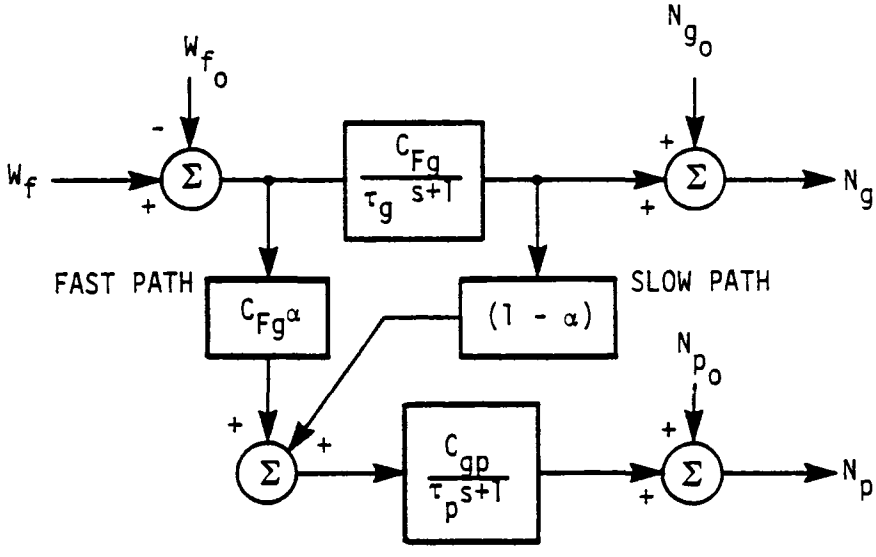

Figure 4.4 Linear Engine Model

where the five linear parameters, τ_p, τ_g, C_{gp}, C_{Fg}, and α, represent the dynamical behavior of the engine.

The dynamical equations are written for perturbations away from an equilibrium condition. A typical choice for this equilibrium point is 100 percent power.

The engine is not the only source of nonlinearity. The throttle linkage, electrical, and hydrodynamical fuel controls also represent limiting elements in the linearity of the response. The components are quite complex. Accurate representations of the internal dynamics are difficult to model with linear equations.

The hydromechanical fuel control is the most complex nonlinear element of the system. The fuel control meters fuel to the engine in response to throttle inputs and engine demand. Instability, temperature, speed, and airflow constraints are accommodated while producing specified performance at different temperatures, altitudes, and speeds.

Valid dynamic models describing the fuel control hardware need to be developed in a parameterized form consistent with Eq. (4.4). Yet, because of the control nonlinearity, this is not reasonable. The combination of nonlinear control equations with Eq. (4.4) will result in an engine/fuel control model suitable for analysis of the integrated rotorcraft system for the present study.

4.1.3 Data

SCT obtained the nonlinear, non-normalized versions of a small, 1500-shaft horsepower helicopter turbine engine and fuel control system. The simulations used relatively simple engine and control models and appeared to provide all the information required for the coupled model.

The engine simulation used four states:

(1) power turbine speed, N_p;

(2) gas generator speed, N_g;

(3) gas generator turbine inlet pressure, P_{41}; and

(4) power turbine inlet pressure, P_{45}.

(Subscripts 41 and 45 on the pressures correspond to stations along the engine as were shown in Figure 2.3.) The model used nonlinear maps and detailed dynamical representations to represent the continuity, energy, and mixing phenomena occurring in the turbine gas path.

The fuel control system consisted of two parts. The first part represented the hydromechanical part of the fuel control, and the second part represented the electromechanical part of the fuel control system.

The sections that follow describe the parameterization of the engine and fuel control models, for the coupled rotorcraft model, from this data.

4.2 ENGINE MODEL

A four-state linear perturbation engine model was derived in the present study to describe the performance of the small helicopter engine during moderate speed excursions from an operating trim of 100% N_p and 97% N_g. This corresponds to a 356-ft lb torque output. This model of the engine was consistent with system bandwidths characteristic of rotor and drive train dynamics.

The four states used in the model were the same ones used in the nonlinear simulation. The nonlinear maps and complex dynamical expressions used in the nonlinear model were to be replaced by constant coefficients evaluated about the operating trim condition. Parameters for the linear model were to be extracted from the nonlinear simulation by using the central

difference, state perturbation method. The outputs from the perturbation model were those required by the engine fuel control and by the drive train and fuselage dynamics models.

4.2.1 Parameterization of Generic Engine Model

4.2.1.1 Parameterization Method

A state perturbation method was used to parameterize the linear engine model. The state perturbation approach is described in Figure 4.5.

This method involves freezing the integrators in the nonlinear simulation after steady state is reached, then perturbing the states and controls one by one to compute the A, B, C, and D matrices of the linear state variable representation of the system. The approach is shown schematically in Figure 4.5.

In Figure 4.5(a), a block diagram of a linear model is shown. A linear scalar model is illustrated and discussed, but extension to a multivariable nonlinear formulation is straightforward.

The procedure for computing the parameters of the model is to integrate the nonlinear model to the steady-state operating condition, where $\dot{x}=0$. This implies that the system being modeled must be a stable, damped system. The integrators are then suppressed, as shown in Figure 4.5(b), and a perturbation, Δx, added to x. The perturbation will cause perturbations Δy and $\Delta\dot{x}$ in y and $\dot{x}$. The coefficients in the A and C matrices can be computed as

$$A = \frac{\Delta\dot{x}}{\Delta x} , \qquad C = \frac{\Delta y}{\Delta x} .$$

A similar perturbation, Δu, can be input to u to compute B and D (see Figure 4.5(c)). The procedure can be extended to

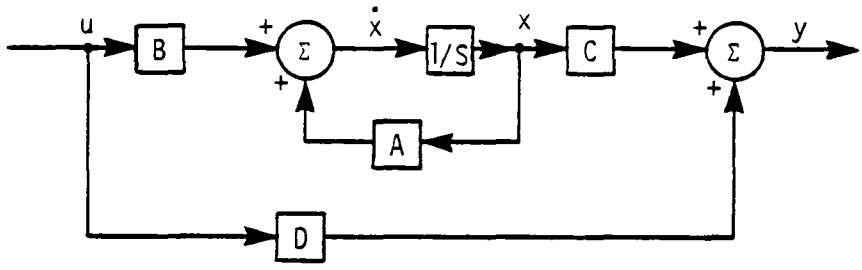

A. LINEAR MODEL

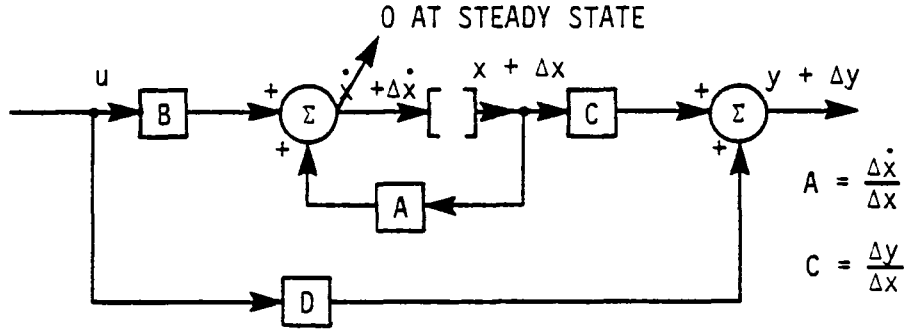

B. STEADY-STATE, INTEGRATION-SUPPRESSED, PERTURBED x

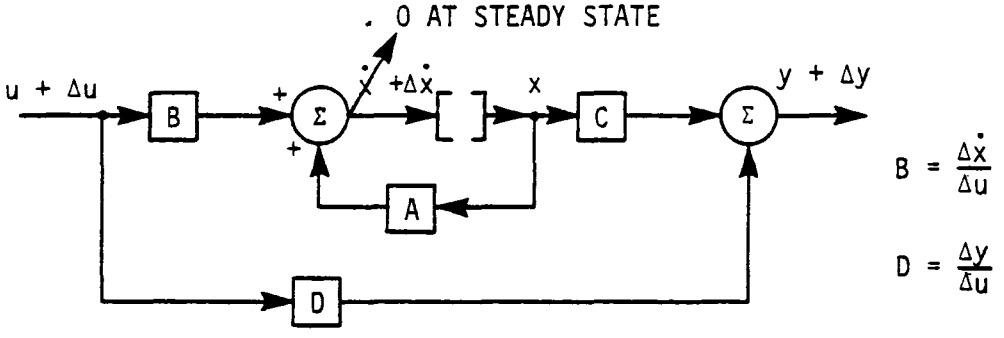

C. STEADY-STATE, INTEGRATION-SUPPRESSED, PERTURBED u

Figure 4.5 Linear Extraction by State Perturbation

vector $\bar{x}$ and $\bar{u}$ by independently incrementing each element of the $\bar{x}$ and $\bar{u}$ vectors.

The magnitude of the perturbations should be consistent with amplitudes expected in the real system. Results will generally vary with the magnitude of the perturbations used.

The approach is applicable to stable, damped systems where the integrators in the nonlinear simulations of the system are accessible and can be suppressed. The procedure may be tedious for large order systems. The procedure results in linear, dynamic equations in the perturbations

$$\Delta\dot{x} = A\,\Delta x + B\,\Delta u$$

$$\Delta y = C\,\Delta x + D\,\Delta u$$

4.2.1.2 Four-State Engine Model

A four-state linear perturbation engine model was extracted from the nonlinear engine simulation first. Figure 4.6 shows the form the linear equations were written in so they could easily be connected to fuel control and drive train models. The coefficients of the matrices used in the model are given in Figure 4.7.

The operating trim about which this linear engine model was developed was 100% N_p and 97% N_g at an altitude of 1000 feet and an ambient temperature of 34°F. This corresponds to a 356-ft lb torque output.

Figures 4.8(a) to (f) show the validation of the linear engine model with the nonlinear engine model results. As can be seen the fit is very good up until the engine reaches 110% shaft speed at time 15 seconds. The open-loop eigensystem of this linear engine model is shown in Table 4.1. All four eigenvalues of the model are non-oscillatory, exponentially decaying modes. The time constants of the modes range from 12.4 times the rotor period to 0.02 times the rotor period. The fastest mode (τ =

$$\Delta\dot{x}_E = A_{EE}\,\Delta x_E + B_{ET}\Delta y_T + B_{EF}\,\Delta y_F$$

$$\Delta y_E = C_{EE}\,\Delta x_E + D_{EF}\Delta y_F$$

WHERE $x_E = \left\{P_{41},\ N_g,\ P_{45},\ N_p\right\}^T$

= ENGINE STATES

$y_E = \left\{Q_E,\ T_{45},\ P_{S3},\ W_{45R}\right\}^T$

= ENGINE OUTPUTS

$y_T = \left\{Q_{P1},\ Q_{P2},\ \Omega_{TR},\ \dot{\Omega}_{MR}\right\}^T$

= DRIVE TRAIN OUTPUTS

$y_F = \left\{W_F\right\}$

= FUEL CONTROL OUTPUTS

A_{EE}, B_{ET}, B_{EF}, C_{EE}, D_{EF} = MATRICES OF COEFFICIENTS

$\Delta(\ )$ = PERTURBATION VALUE

Figure 4.6 Four-State Engine Model

$$A_{EE} = \begin{bmatrix} -3.95 & .0425 & 0. & 0. \\ 942. & -4.79 & -3790. & 0. \\ 27.4 & .0225 & -150. & 0. \\ -12.1 & -.0776 & 311. & -.283 \end{bmatrix}$$

$$B_{ET} = \begin{bmatrix} 0 & 0 & 0 & 0 \\ 0 & 0 & 0 & 0 \\ 0 & 0 & 0 & 0 \\ -15.92 & 0 & 0 & 0 \end{bmatrix}$$

$$B_{EF} = \begin{bmatrix} 1260. \\ 78600. \\ 2100. \\ 7790. \end{bmatrix}$$

$$C_{EE} = \begin{bmatrix} -.762 & -.00488 & 19.5 & -.0178 \\ -7.76 & -.0497 & 43.5 & 0. \\ .926 & .00156 & 0. & 0. \\ -4.87E-4 & -3.12E-6 & .00512 & 0. \end{bmatrix}$$

$$D_{EF} = \begin{bmatrix} 489. \\ 4980. \\ 0. \\ .313 \end{bmatrix}$$

Figure 4.7 Coefficients for Four-State Linear Perturbation Engine Model

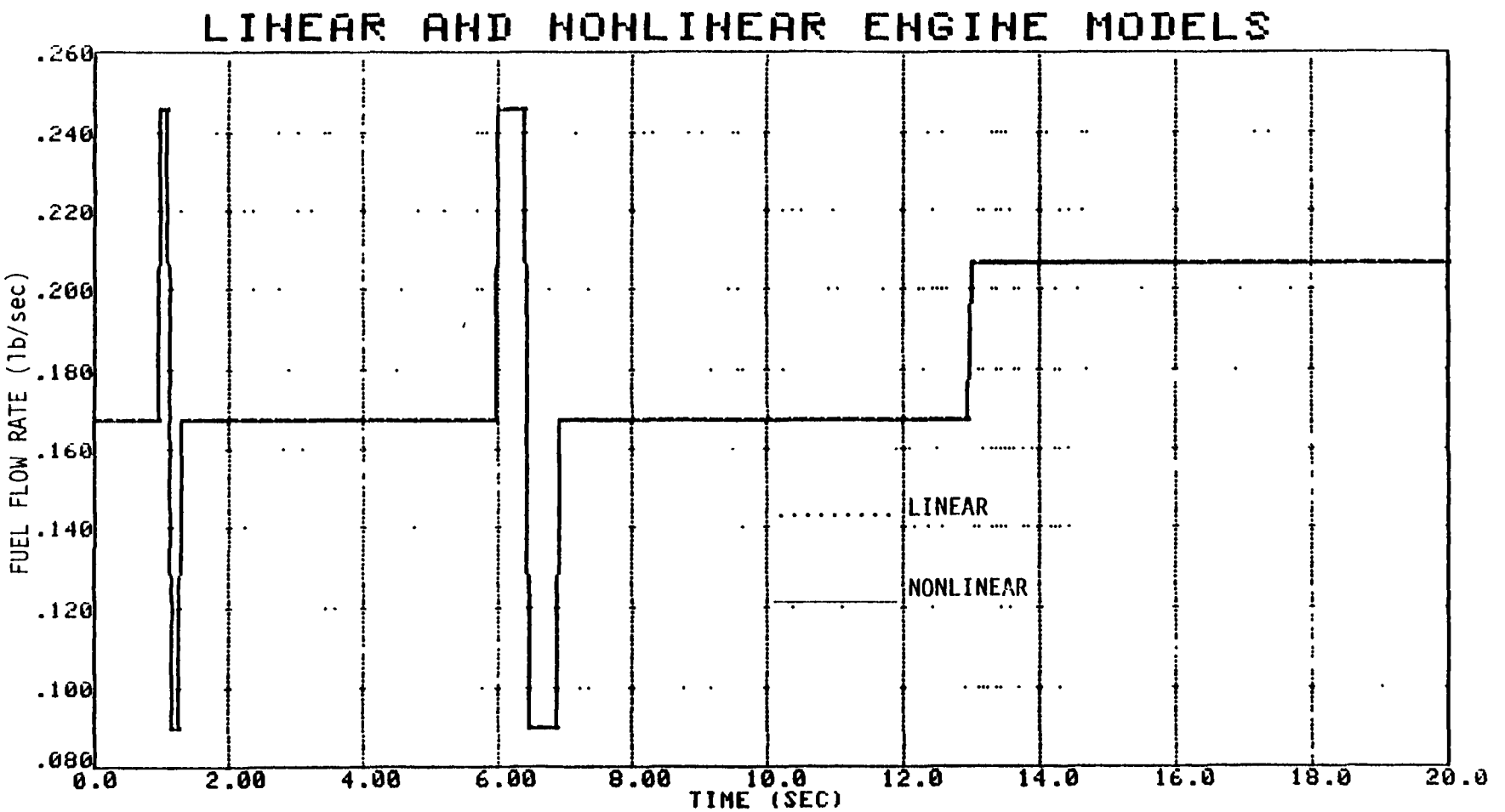

Figure 4.8a Validation of Four-State Linear Engine Model

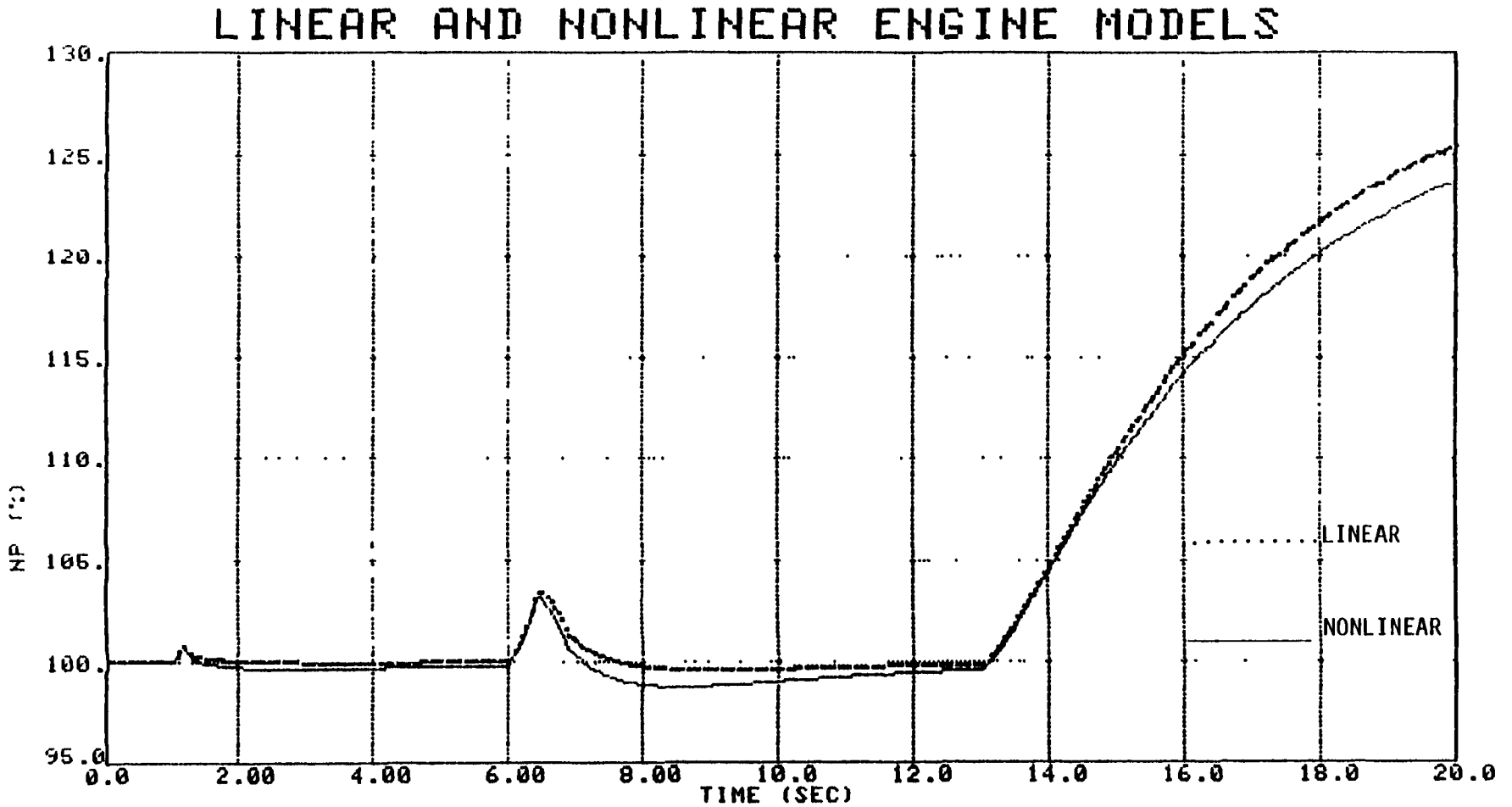

Figure 4.8b Validation of Four-State Linear Engine Model

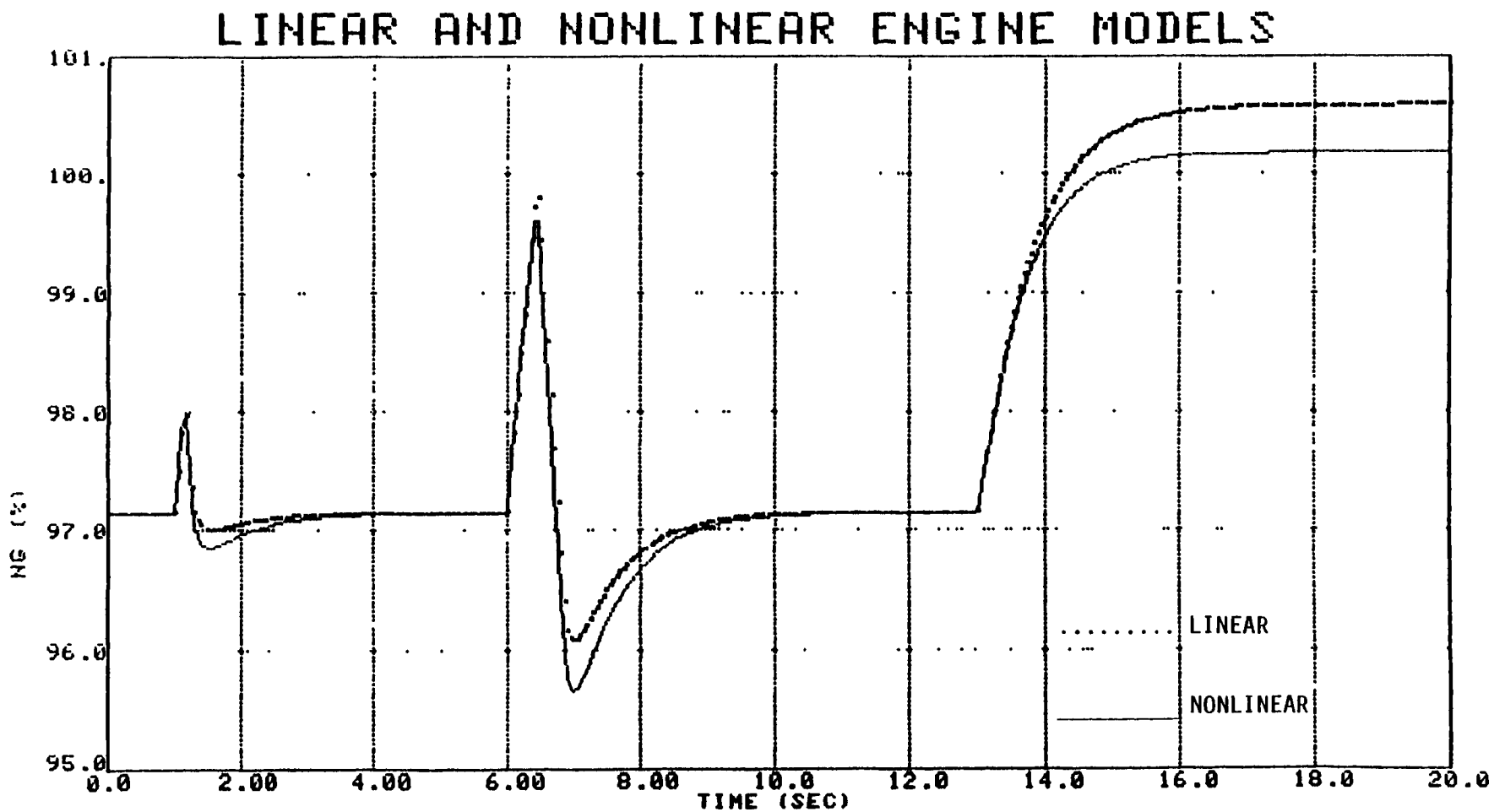

Figure 4.8c Validation of Four-State Linear Engine Model

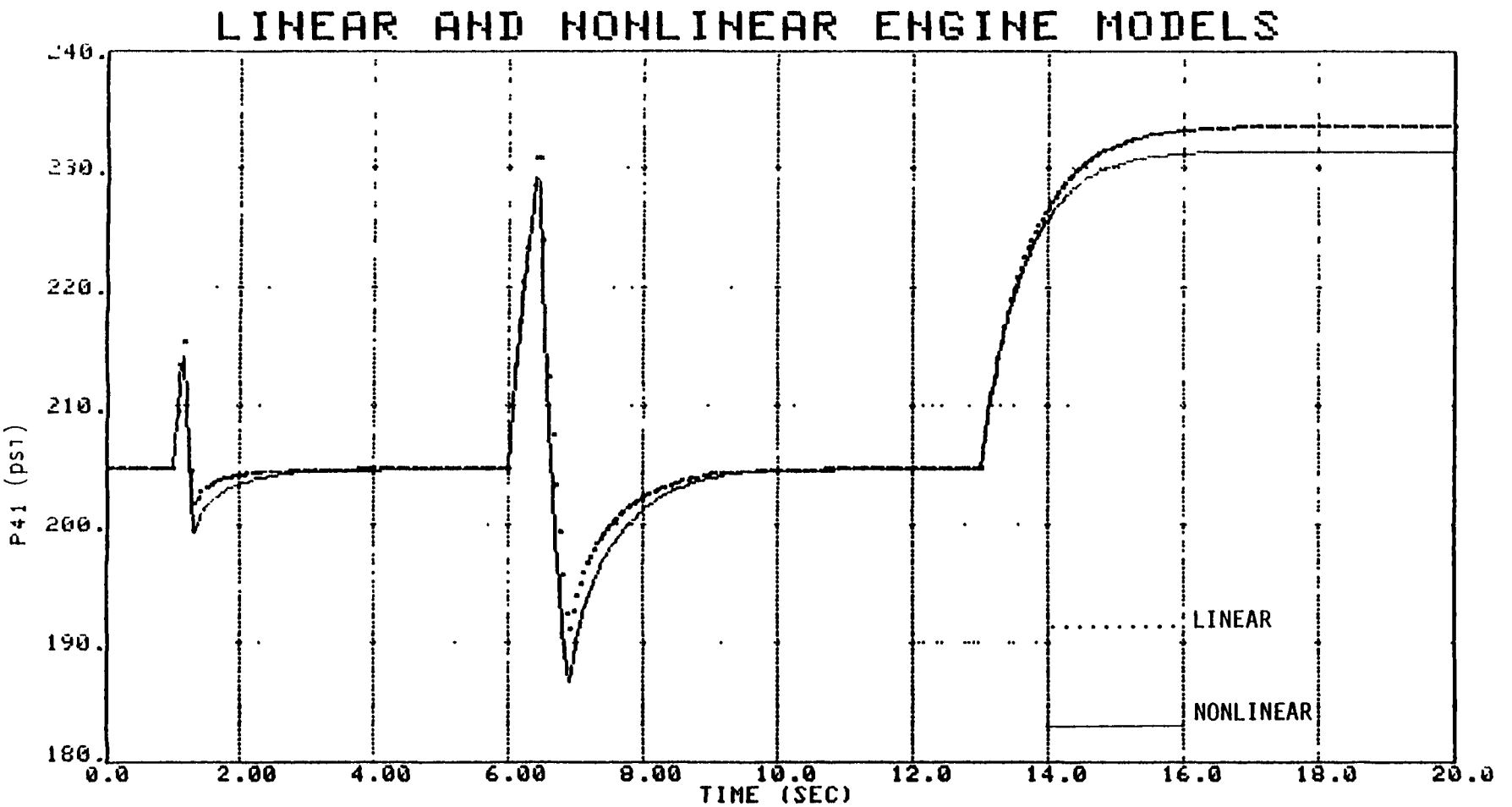

Figure 4.8d Validation of Four-State Linear Engine Model

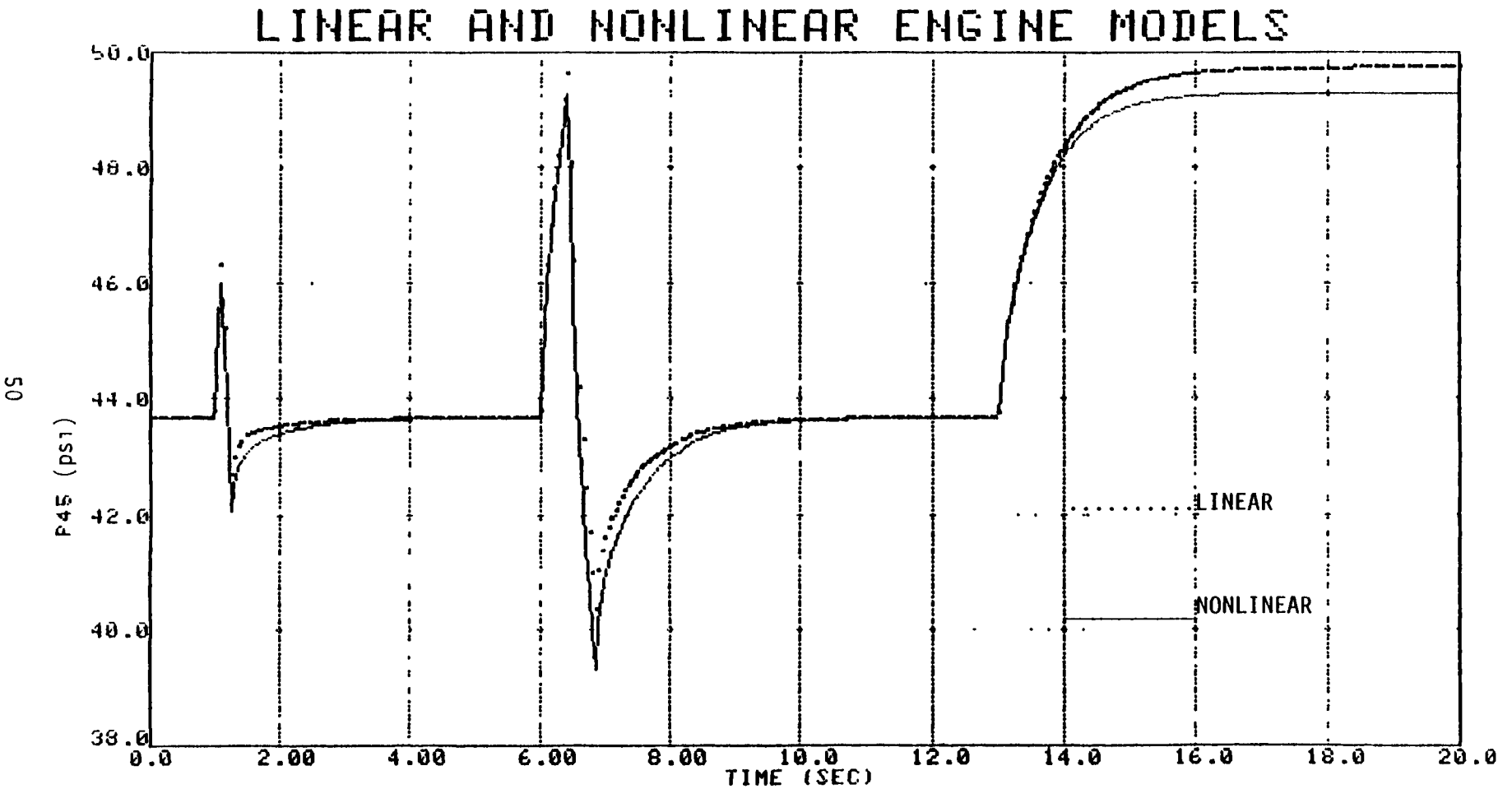

Figure 4.8e Validation of Four-State Linear Engine Model

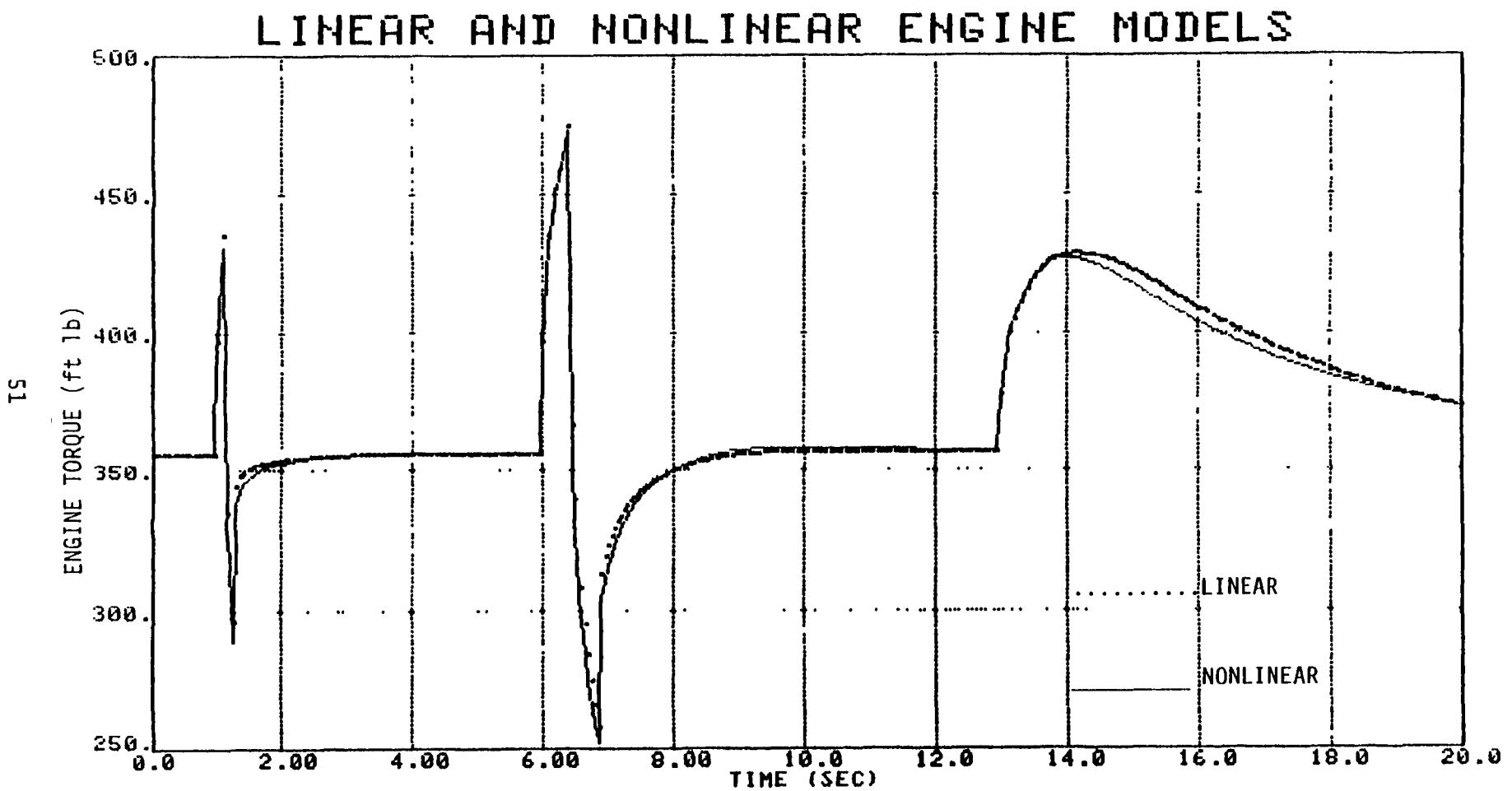

Figure 4.8f Validation of Four-State Linear Engine Model

Table 4.1

Eigensystem of Four-State Engine Model

NO.	EIGENVALUE	TIME CONSTANT (SEC)	MODE DESCRIPTION
1	-.28 + 0i	3.6	Power Turbine Speed (N_p)
2	-1.4 + 0i	.71	First Turbine Stage Inlet Pressure (P_{41})
3	-7.8 + 0i	.13	Gas Generator Speed (N_g)
4	-150. + 0i	.007	Power Turbine Inlet Pressure (P_{45})

NOTE: $\frac{1}{\Omega_{MR}}$ = .028 SEC/CYCLE

.007 sec) is faster than the dynamics required of the generic rotorcraft model and was determined to be unneccessary.

4.2.1.3 Model Reduction

Model reduction was applied to the four-state linear engine model to simplify it. Two states were proposed (see Section 4.1.2, Eq. (4.4)) for the generic model structure, but four states were used originally. It was reasonable that the number of states in the four-state model be reduced since the model contained higher frequency characteristics than necessary, and would be inconsistent with modeling assumptions of the other subsystems. By setting the derivatives of faster states to zero, model order reduction was used to remove the faster mode. This approach is described in Figure 4.9.

Figure 4.9 illustrates model order reduction for a two-state model. The first equation in the figure is the state equation for the system. Suppose it is found analytically (or in an eigenanalysis) that x_2 is much faster than x_1 (i.e. $\dot{x}_2 \gg \dot{x}_1$). Then x_2 is assumed to change instantaneously with respect to x_1, and $\dot{x}_2$ is set to zero. The equation for $\dot{x}_2$ can then be solved for x_2 in terms of x_1 and u. This result is substituted into the equation for $\dot{x}_1$ to remove x_2 from the equation (as shown in the last equation of Figure 4.9). The approach can easily be extended to a many degree-of-freedom system and also applied to remove unwanted state(s) from output equations.

Table 4.2 shows the eigensystem of the three-state model that resulted after model order reduction was applied. Note that the eigensystem for the three states left in the model was practically the same as that of the three slowest modes before the fast mode was removed (see Table 4.1). Plots of the responses of the three-state model were indistinguishable from those of the four-state model for the inputs and plotting scales

$$\begin{Bmatrix} \dot{x}_1 \\ \dot{x}_2 \end{Bmatrix} = \begin{bmatrix} a_{11} & a_{12} \\ a_{21} & a_{22} \end{bmatrix} \begin{Bmatrix} x_1 \\ x_2 \end{Bmatrix} + \begin{bmatrix} b_1 \\ b_2 \end{bmatrix} \{u\}$$

WHERE: $\dot{x}_2$ MUCH FASTER THAN $\dot{x}_1$

SET $\dot{x}_2 = 0$

$$\dot{x}_2 = 0 = [a_{21} \quad a_{22}] \begin{Bmatrix} x_1 \\ x_2 \end{Bmatrix} + b_2 \{u\}$$

OR

$$x_2 = -a_{22}^{-1} a_{21} x_1 - a_{22}^{-1} b_2 \{u\}$$

THUS

$$\dot{x}_1 = [a_{11} - a_{12} a_{22}^{-1} a_{21}] \{x_1\} + [b_1 - b_2 a_{22}^{-1} b_2] \{u\}$$

Figure 4.9 Model Order Reduction

Table 4.2

Eigensystem of Three-State Engine Model

NO.	EIGENVALUE	TIME CONSTANT (SEC)	MODE DESCRIPTION
1	-.28 + 0i	3.6	Power Turbine Speed (N_p)
2	-1.3 + 0i	.77	First Turbine Stage Inlet Pressure (P_{41})
3	-8.0 + 0i	.13	Gas Generator Speed (N_g)

NOTE: $\frac{1}{\Omega_{MR}}$ = .028 SEC/CYCLE

used in Figures 4.8(a) through 4.8(f), so no new plots for the three-state model are shown.

Figure 4.10 shows the form of the generic model structure for the three-state engine model. Coefficients for the model are given in Figure 4.11.

It is reasonable that only one pressure state be used in the three-state model. Theoretical fluid mechanics indicate that a quasi-steady relationship exists between pressures. Any disturbance of the relationship among pressures is quickly corrected, so only one pressure state is needed.

4.2.1.4 Engine Subroutine

The three-state engine model become one subsystem component of the rotorcraft/propulsion simulation. Trim values were added back onto the perturbational engine states and output variables in the model so total as well as perturbational outputs would be available. Figure 4.12 shows a flowchart of this engine simulation.

4.3 FUEL CONTROL MODEL

The fuel control simulation with the nonlinear engine simulation was converted directly into a subroutine for use in the generic rotorcraft/propulsion model. It was not linearized or simplified. A flowchart of the fuel control model subroutine is shown in Figure 4.13. This fuel control simulation could be used to control either one of the linear or the nonlinear engine simulations.

4.4 DRIVE TRAIN MODEL

Figure 4.14 shows the proposed generic structure for the drive train model. The equations for this model are described in

$$\Delta\dot{x}_E = A_{EE}\,\Delta x_E + B_{ET}\Delta y_T + B_{EF}\,\Delta y_F$$

$$\Delta y_E = C_{EE}\,\Delta x_E + D_{EF}\Delta y_F$$

WHERE $x_E = \left\{ P_{41},\ N_g,\ N_P \right\}^T$

= ENGINE STATES

$y_E = \left\{ Q_E,\ T_{45},\ P_{S3},\ W_{45R} \right\}^T$

= ENGINE OUTPUTS

$y_T = \left\{ Q_{P1},\ Q_{P2},\ \Omega_{TR},\ \dot{\Omega}_{MR} \right\}^T$

= DRIVE TRAIN OUTPUTS

$y_F = \left\{ W_F \right\}$

= FUEL CONTROL OUTPUTS

A_{EE}, B_{ET}, B_{EF}, C_{EE}, D_{EF} = MATRICES OF COEFFICIENTS

$\Delta(\ )$ = PERTURBATION VALUE

Figure 4.10 Three-State Engine Model

$$A_{EE} = \begin{bmatrix} -3.95 & .0425 & 0. \\ 250. & -5.36 & 0. \\ 44.7 & -.031 & -.283 \end{bmatrix}$$

$$B_{ET} = \begin{bmatrix} 0 & 0 & 0 & 0 \\ 0 & 0 & 0 & 0 \\ -15.92 & 0 & 0 & 0 \end{bmatrix}$$

$$B_{EF} = \begin{bmatrix} 1260. \\ 25500. \\ 12100. \end{bmatrix}$$

$$C_{EE} = \begin{bmatrix} 2.8 & -.00196 & -.0178 \\ .187 & -.0432 & 0. \\ .926 & .00156 & 0. \\ .000448 & -2.35E-6 & 0. \end{bmatrix}$$

$$D_{EF} = \begin{bmatrix} 762. \\ 5590. \\ 0. \\ .385 \end{bmatrix}$$

Figure 4.11 Coefficients for Three-State Linear Perturbation Engine Model

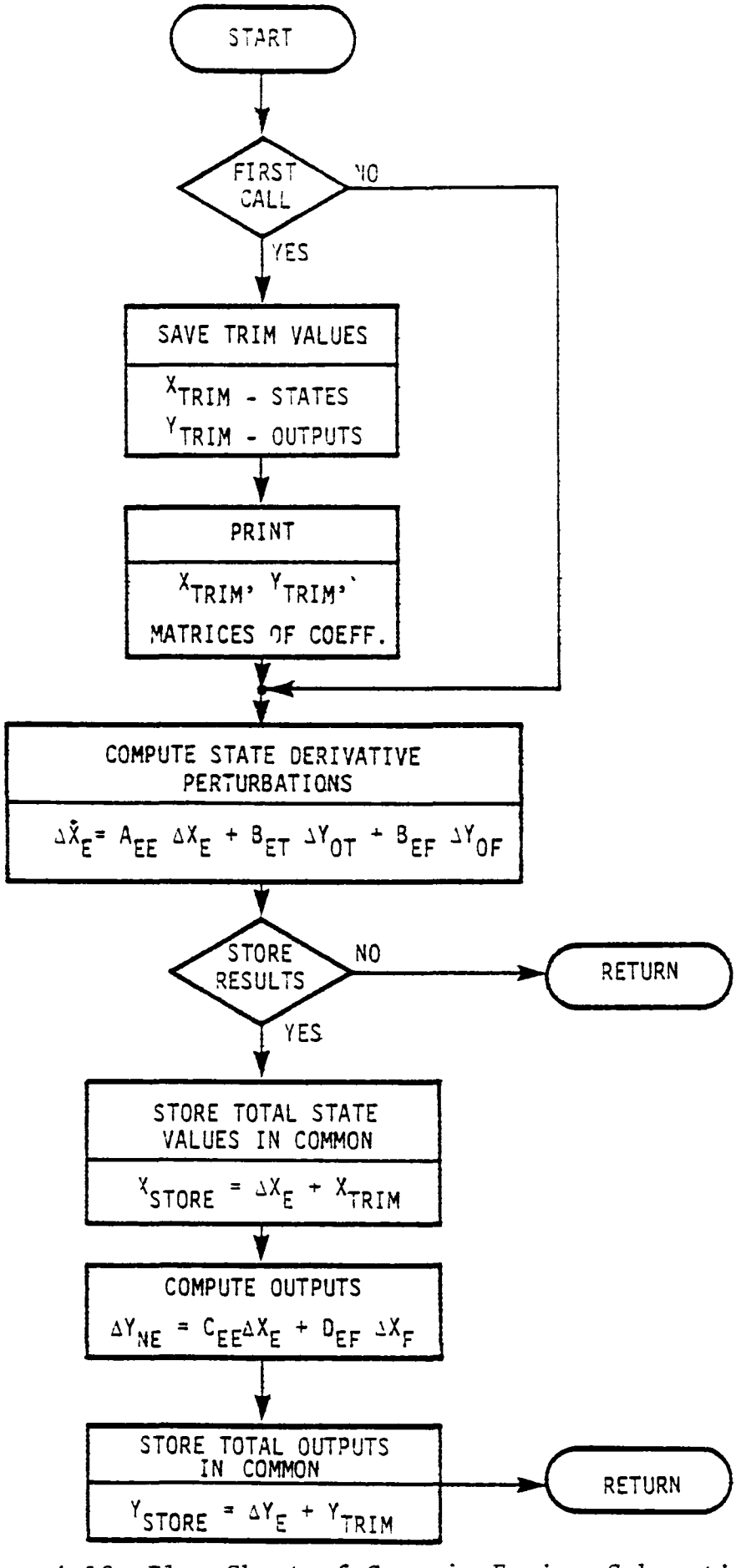

Figure 4.12 Flow Chart of Generic Engine Subroutine

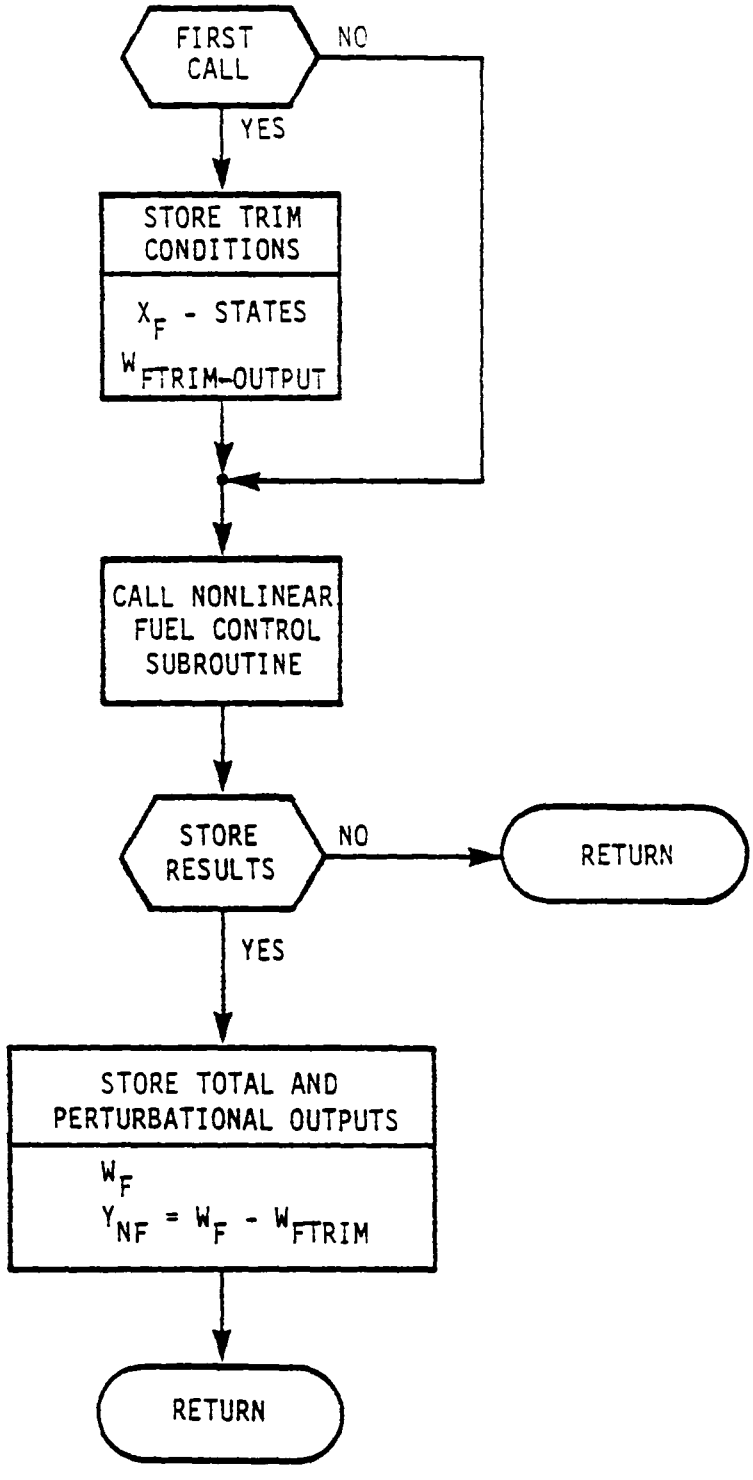

Figure 4.13 Flow Chart of Generic Fuel Control Subroutine

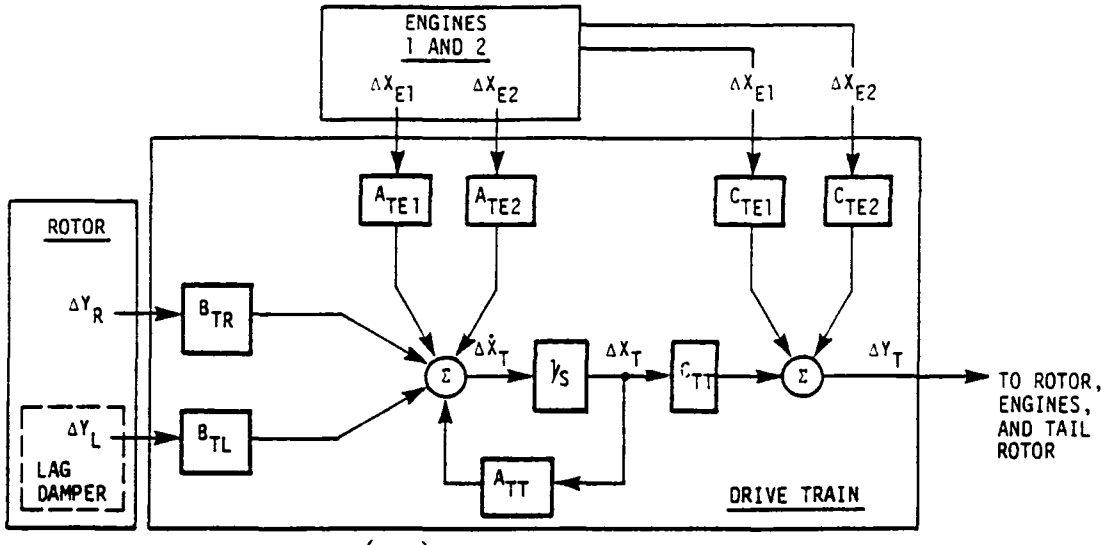

WHERE $\Delta X_T = \begin{Bmatrix} \Omega_{MR} \\ \epsilon_1 \\ \epsilon_2 \end{Bmatrix}$ = DRIVE TRAIN STATES

$$\Delta Y_T = \begin{Bmatrix} Q_{P1} \\ Q_{P2} \\ \Omega_{TR} \\ \dot{\Omega}_{MR} \end{Bmatrix} = \text{DRIVE TRAIN OUTPUTS}$$

ΔX_{E1}, ΔX_{E2} = ENGINE STATES FOR TWO ENGINES

ΔY_R = ROTOR OUTPUTS

ΔY_L = LAG DAMPER OUTPUTS

A_{TE1}, A_{TE2}, A_{TT}, B_{TR}, B_{TL}, C_{TT}, C_{TE1}, C_{TE2} = COEFFICIENTS

Figure 4.14 Form of Generic Drive Train Model

Figure 4.15. The derivation of the equations is straight forward and similar to that used to derive the equations in [12].

The drive train model is shown schematically in Figure 4.16. Note that the transmission inertia has been lumped into the rotor hub inertia. This simplification was made because numerical data were not available for modeling the transmission separately. The power turbine inertias shown in the figure are not really in the transmission equations, Figure 4.15, because they were already included in the engine model equations.

The parameters used in the model are representative of a small, twin turbine helicopter. They do not correspond to any one helicopter. Although this drive train is not the one connected to the engine, fuel control, and rotor being used in consideration, it is thought to be sufficiently representative for the purposes of demonstrating the simulation model. Figure 4.17 lists the parameters used in the model.

Damping parameters were not available. Small values of damping were used to assure that the system would be stable.

4.5 MODEL CHECKOUT

The propulsion system model was checked out by executing it independent of the rest of the rotorcraft simulation. The propulsion system that was constructed includes two engine subroutines, two fuel controllers, and a drive train subroutine. A rotor load torque time history was specified to excite the propulsion system dynamics. The results of a checkout run are plotted in Figure 4.18. The plots in this figure show the responses of the propulsion system with both full nonlinear and three-state linear engine models.

It might be useful in the future to perform an eigenanalysis of the engine/drive train/engine part of the simulation to determine its frequency content. It might be shown possible to

STATE

$$\begin{bmatrix} I_h & 0 & 0 \\ 0 & 1 & 0 \\ 0 & 0 & 1 \end{bmatrix} \begin{Bmatrix} \dot{\Omega}_{MR} \\ \dot{\varepsilon}_1 \\ \dot{\varepsilon}_2 \end{Bmatrix} = \begin{bmatrix} (-d_H - 2d_{HE}) & -k_{HE} & -k_{HE} \\ 1 & 0 & 0 \\ 1 & 0 & 0 \end{bmatrix} \begin{Bmatrix} \Omega_{MR} \\ \varepsilon_1 \\ \varepsilon_2 \end{Bmatrix} + \begin{bmatrix} d_{HE}r_{H1} & d_{HE}r_{H2} & -1 \\ -r_{H1} & 0 & 0 \\ 0 & -r_{H2} & 0 \end{bmatrix} \begin{Bmatrix} N_{P1} \\ N_{P2} \\ Q_{MR} \end{Bmatrix}$$

OUTPUT

$$\begin{Bmatrix} Q_{P1} \\ Q_{P2} \\ \Omega_{TR} \\ \dot{\Omega}_{MR} \end{Bmatrix} = \begin{bmatrix} r_{H1}d_{HE} & r_{H1}k_{HE} & 0 \\ r_{H2}d_{HE} & 0 & r_{H2}k_{HE} \\ C_1 & 0 & 0 \\ (-d_H-2d_{HE})/I_h & -k_{HE}/I_h & -k_{HE}/I_h \end{bmatrix} \begin{Bmatrix} \Omega_{MR} \\ \varepsilon_1 \\ \varepsilon_2 \end{Bmatrix} + \begin{bmatrix} (-d_E-d_{HE}r_{H1}^2) & 0 & 0 \\ 0 & (-d_E-d_{HE}r_{H2}^2) & 0 \\ 0 & 0 & 0 \\ d_{HE}r_{H1}/I_h & d_{HE}r_{H2}/I_h & -1/I_h \end{bmatrix} \begin{Bmatrix} N_{P1} \\ N_{P2} \\ Q_{MR} \end{Bmatrix}$$

Figure 4.15 Equations For Drive Train Model

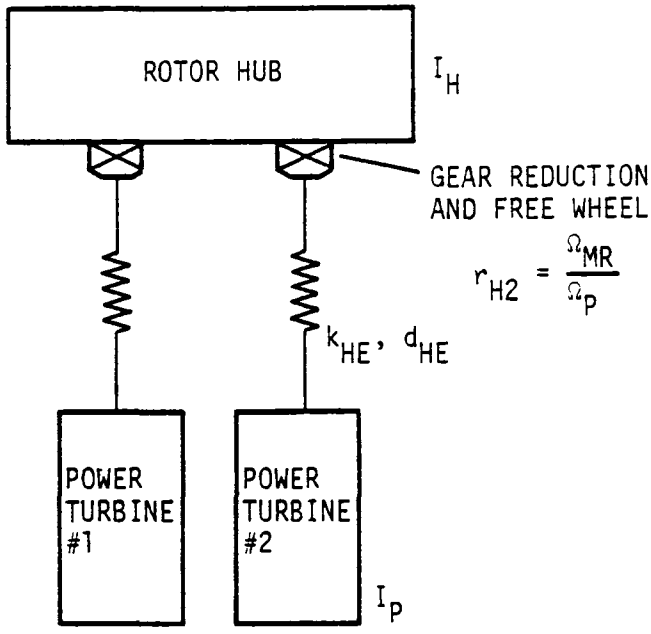

Figure 4.16 Drive Train Model

d_E = 0.

d_H = 0.

d_{HE} = 1070. ft lb sec (referenced to hub)

I_h = 880. ft lb sec^2 (referenced to hub)

k_{HE} = 64930. ft lb/rad (referenced to hub)

$r_{H1} = r_{H2} = .010572$

Figure 4.17 Drive Train Model Parameters

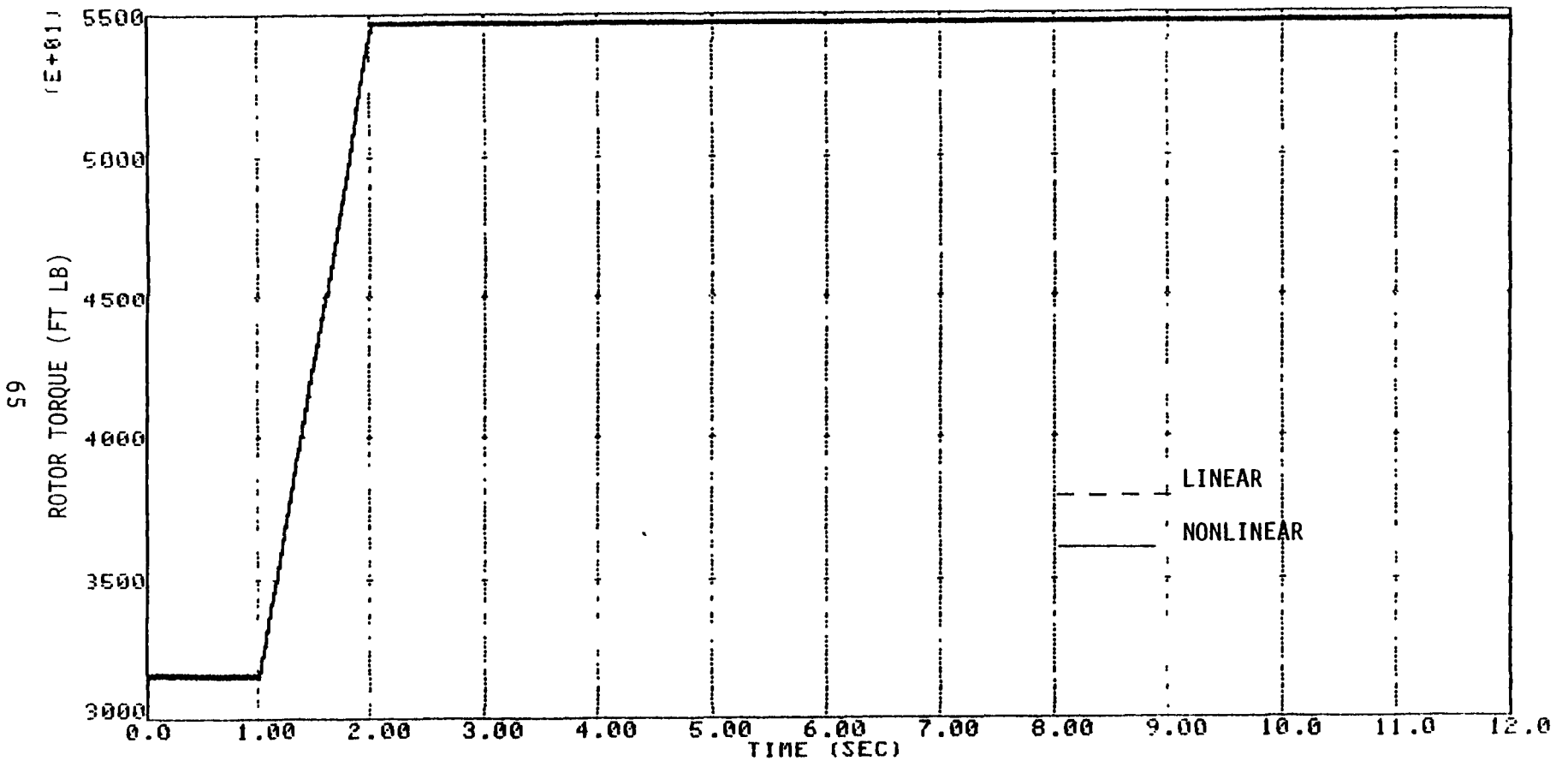

Figure 4.18a Linear and Nonlinear Propulsion Systems

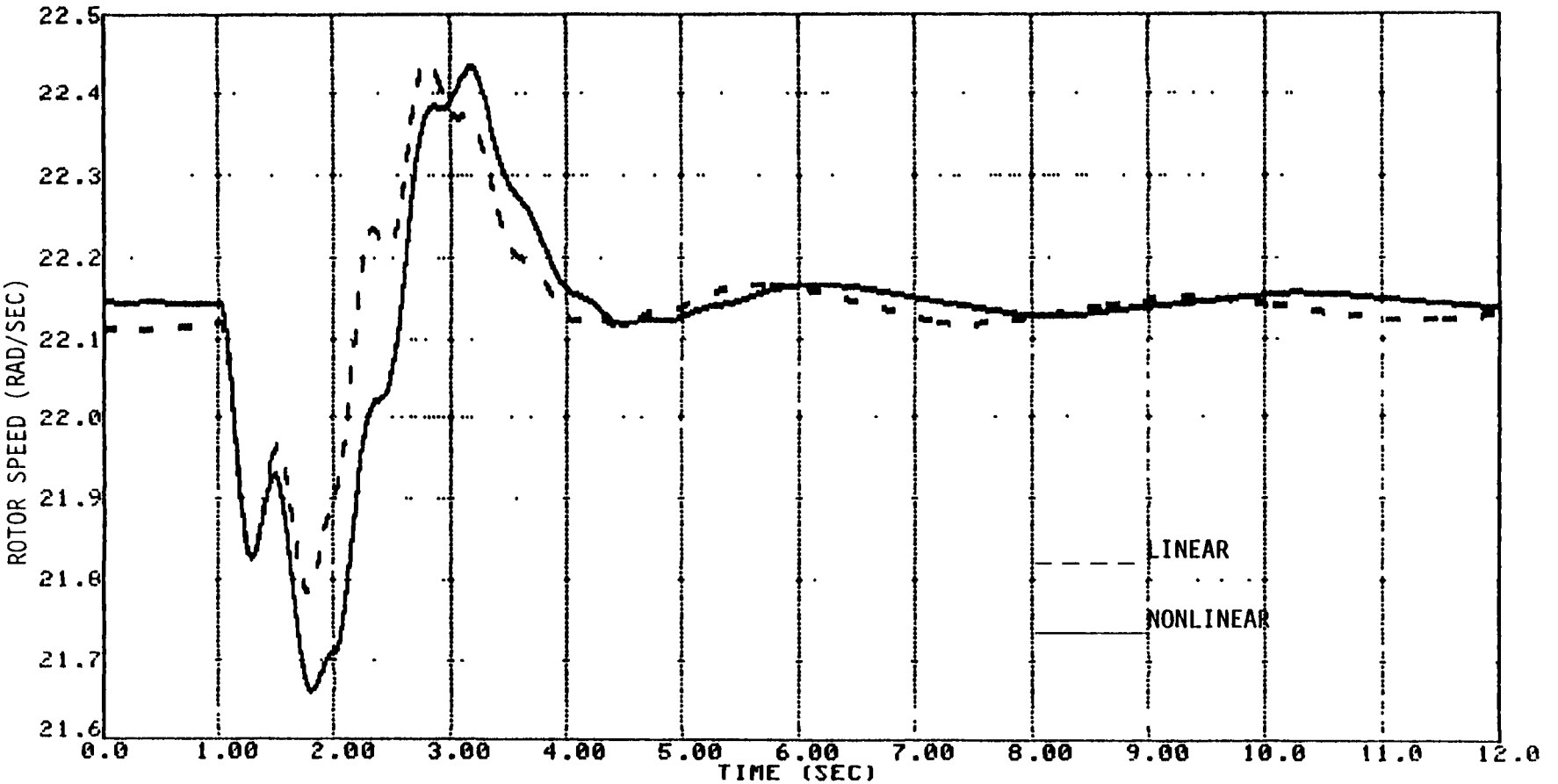

Figure 4.18b Linear and Nonlinear Propulsion Systems

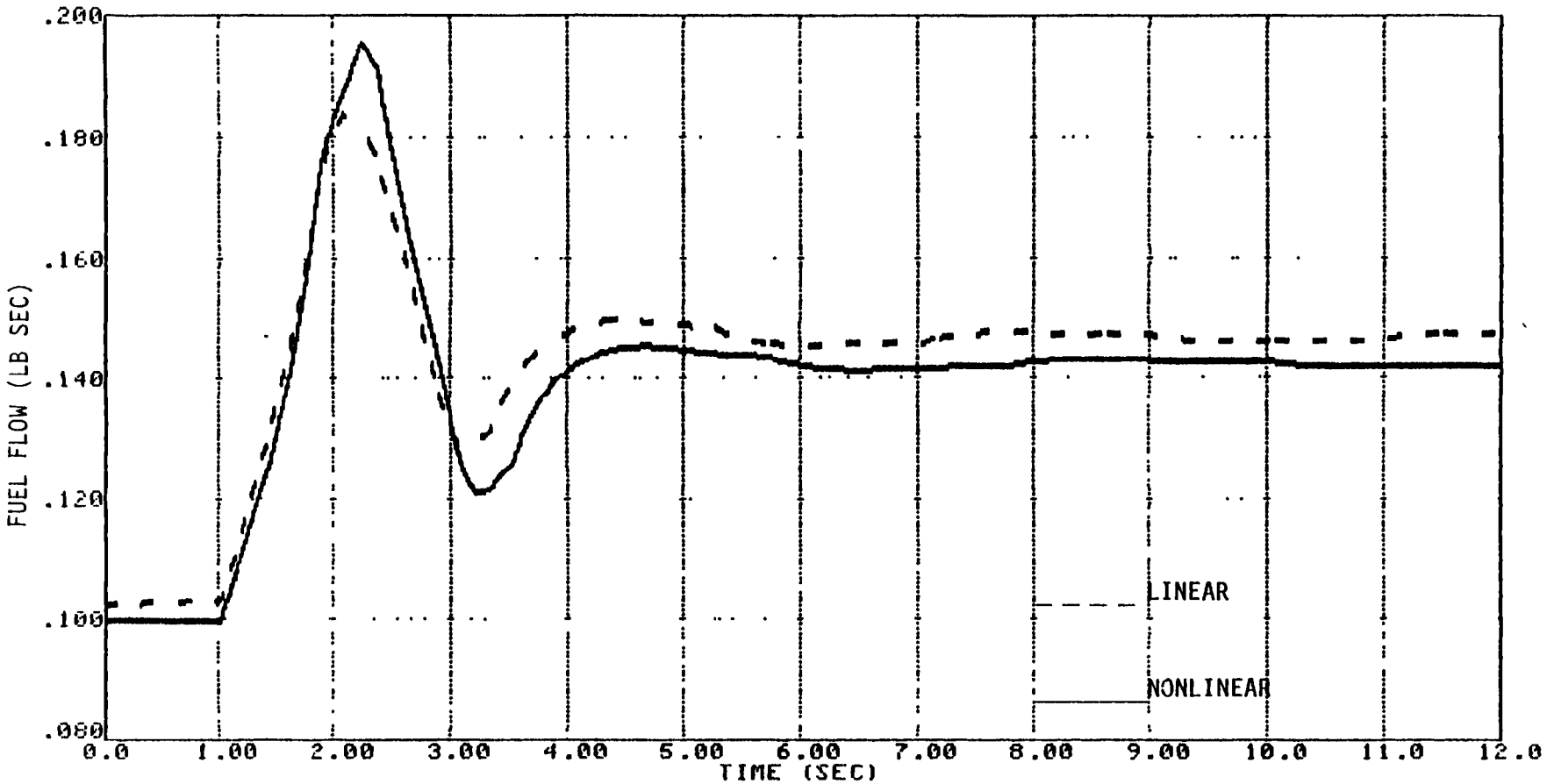

Figure 4.18c Linear and Nonlinear Propulsion Systems

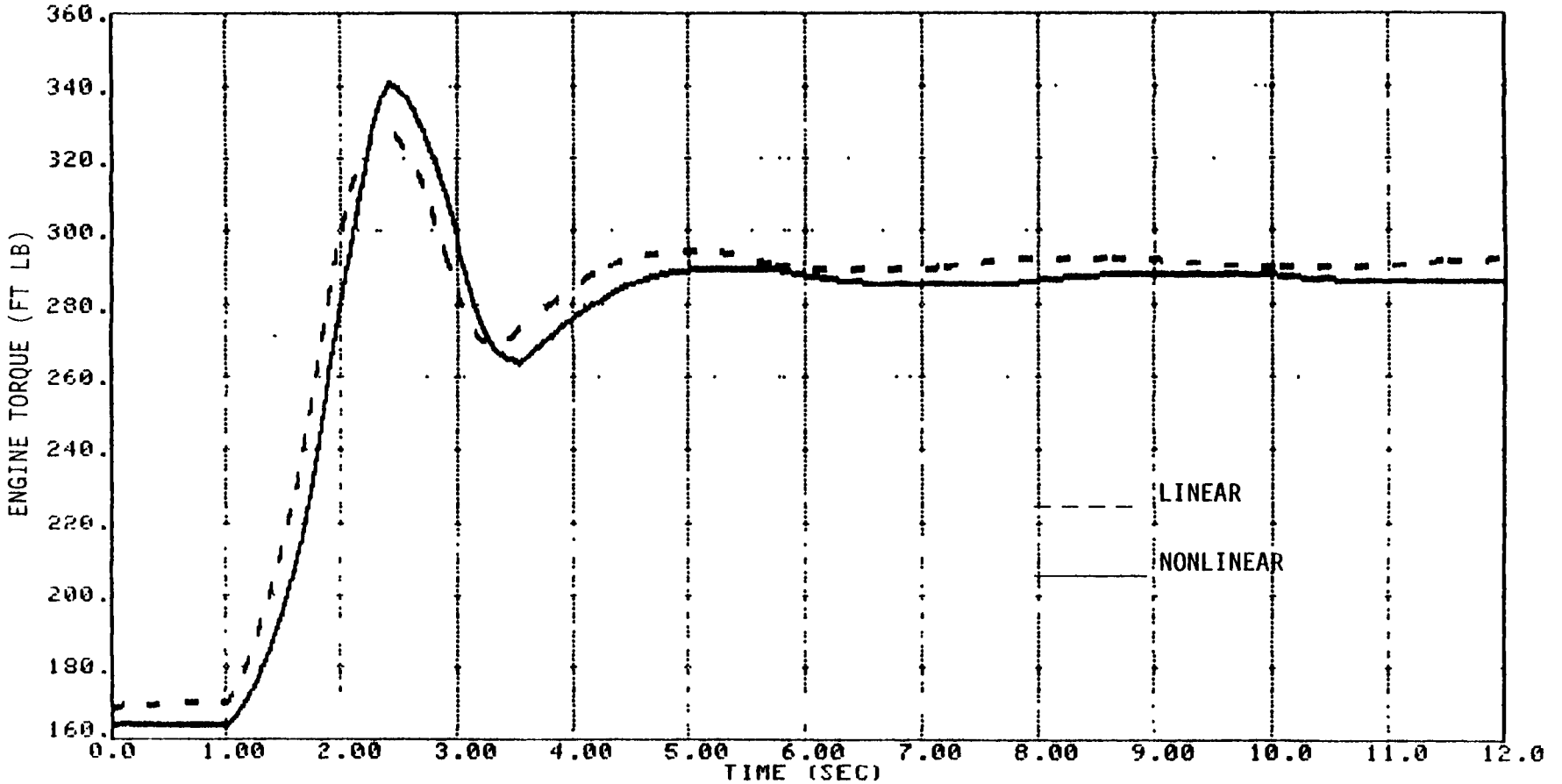

Figure 4.18d Linear and Nonlinear Propulsion Systems

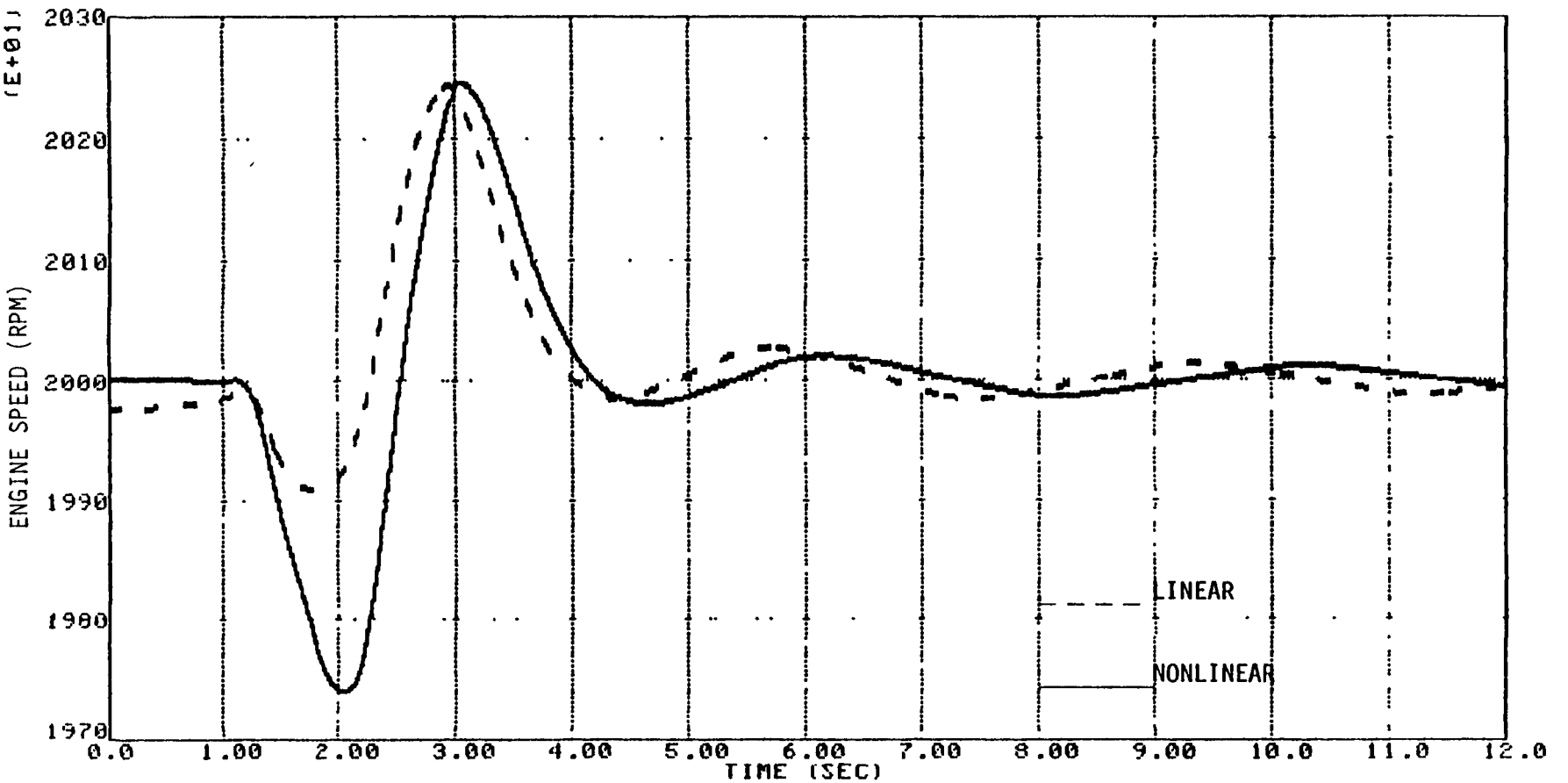

Figure 4.18e Linear and Nonlinear Propulsion Systems

reduce the order of this system by a few states, and still cover the desired frequency range.

Additional system dynamics, not demonstrated in the plots of Figure 4.18, are the engine hunting modes. Future propulsion system runs should be performed that perturb one engine differently from the other, and thus excite engine hunting. The damping of the engine hunting mode could be observed after the excitation was removed.

4.6 SUMMARY

A rotorcraft propulsion system model of a particular engine, fuel control, and drive train combination was constructed. A methodology for parameterizing linear versions of the model was discussed, and parameters for a linear engine model developed.

V. ROTOR SYSTEM MODELING

This chapter describes a methodology for constructing a rotor/fuselage model. The form of the generic model structure is also described. The model is based on the structure defined in Chapter III. Model parameters of a particular rotorcraft, used to demonstrate the model, are obtained from a nonlinear simulation of a research helicopter. Regression techniques are used to obtain these parameters.

5.1 ROTOR/FUSELAGE GENERIC MODEL FORM

The rotor/fuselage generic model equations were constructed in the input-output form shown in Figure 3.3. This form allowed the model to be plugged into the modular framework for the coupled system that was described in Figure 3.2. This input-output approach also allowed the rotor and fuselage models to be developed separately from the other modules (e.g. engine, drive train) of the rotorcraft system.

The states used in the rotor model were multi-blade coordinates (e.g. β_0, β_{1C}..., ξ_0, ξ_{1C},...). The states in the fuselage model were the six rigid-body rates (u, v, w, p, q, r) and the three rigid-body Euler angles (ϕ, θ, ψ).

The rotor and fuselage models were interconnected through the rotor hub forces and the fuselage states. The forces were outputs of the rotor model.

The forces (and moments) acting on a helicopter fuselage include aerodynamic forces, main rotor forces and tail rotor forces. These forces were kept separate in the model to provide a better framework for identifying the structure of these forces and to provide flexibility in the model.

The dynamics of the fuselage and rotor model and the fuselage aerodynamic forces were described using perturbational

quantities, as was done for the propulsion system. Trim values were added back onto the perturbational quantities in the subroutines, as was also done for the propulsion system. The trim values were added back on after integration so total response will be available.

5.2 GENHEL RSRA SIMULATION

The GENHEL RSRA simulation was used in parameterizing the perturbational rotor and fuselage models. It is a fully nonlinear simulation of the main rotor, tail rotor, fuselage and control system of the Rotor Systems Research Aircraft (RSRA). It does not include rotor propulsion system dynamics (i.e. engine, fuel control, drive train dynamics). The equations in the simulation originated from Sikorsky Aircraft's General Helicopter Simulation (GENHEL) which is documented in [13,14]. The main rotor mathematical model in the simulation is a rotating blade element model of an articulated rotor system. Rotor blade and airframe flexibility are not taken into account. Flapping and lagging hinges are assumed coincident. A Bailey model [15] is used for the tail rotor.

The control system represented in the simulation includes a full complement of helicopter controls. It includes the pilot's control system and the stability augmentation system (SAS).

The GENHEL simulation has a modular format, as shown in Figure 5.1. It is well documented and is easily accessible on a CDC-7600 batch computer.

5.3 PARAMETERIZATION METHODOLOGY

The parameters (or coefficients) for the rotor and fuselage equations were obtained from time history data generated by the nonlinear GENHEL simulation. A stepwise regression algorithm, in

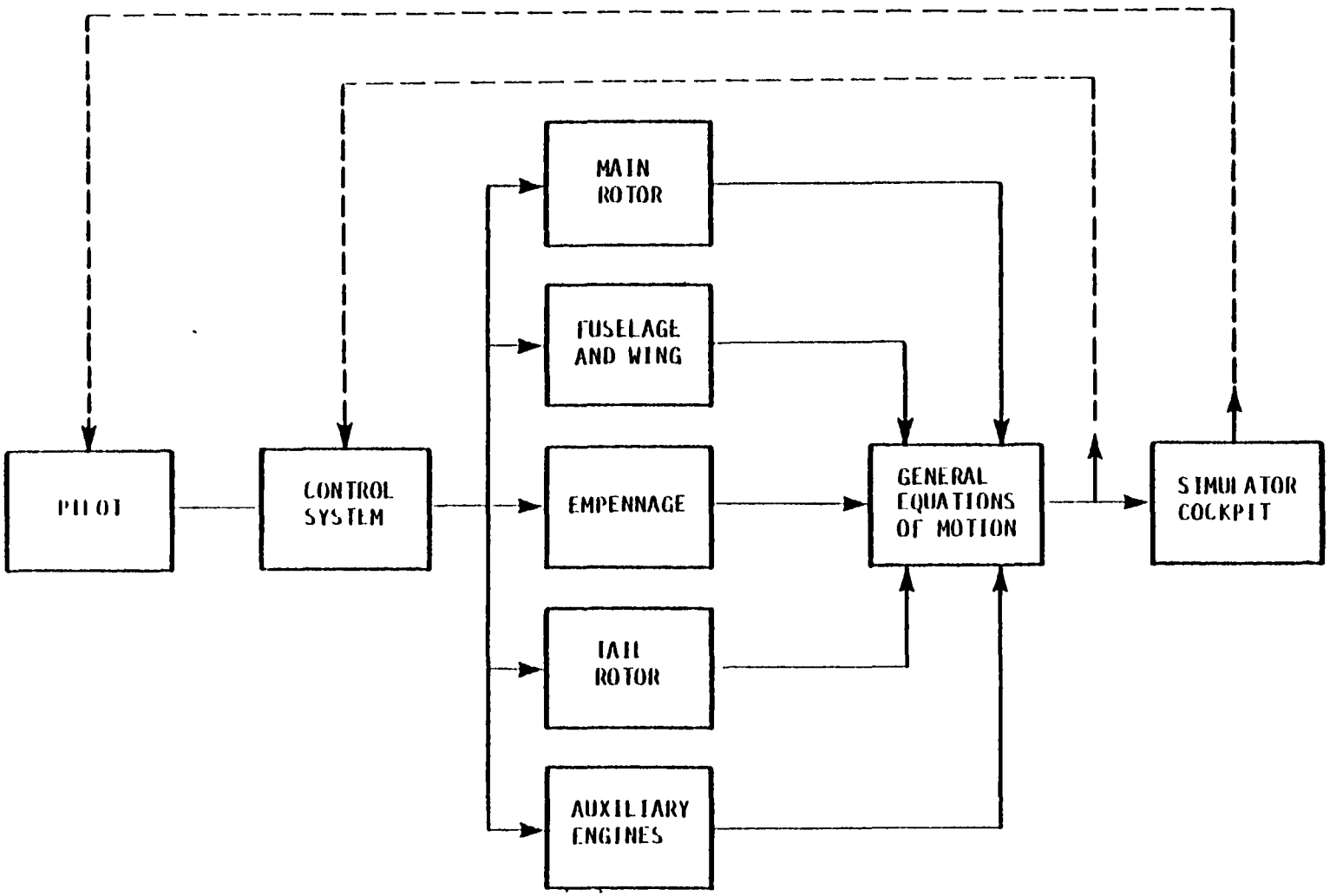

Figure 5.1 Simplified Block Diagram of GENHEL Simulation [14]

use at SCT, called OSR was used to compute the coefficient values.

The stepwise regression method, OSR (Optimal Subset Regression), requires as input the time histories of the states, state derivatives, and control inputs. These inputs are the data that can be generated by the GENHEL simulation.

Conceptually, the use of OSR involves setting up an equation for each acceleration term, mx, as

$$m\ddot{x}_1 = \Sigma F_i$$

$$= c_1 x_1 + c_2 \dot{x}_1 + c_3 u + \ldots$$

where the terms x_1, $\dot{x}_1$, u, etc., are candidate independent variables and the coefficients $(c_1, c_2, c_3 \ldots)$ are unknown. The variables $\ddot{x}_1$, $\dot{x}_1$, x_1, u_1, etc., are input to OSR as time histories. OSR then determines the subsets of the candidate independent variables which best represent the data for the dependent variable, $m\ddot{x}_1$. OSR also computes estimates of the unknown coefficients of the independent variables in the subset. The subset independent variables and variable coefficients are chosen to minimize the mean square error between the $m\ddot{x}_1$, time history and the subset time history. Thus, the "fit" of the linear equations is a mean square minimization.

The stepwise regression procedure implemented in OSR is not applied to data from the steady state performance of the system, but is applied to data from specific trajectories or maneuvers. The trajectories are defined by sets of control inputs chosen to excite the system performance that is to be modeled.

A single maneuver is often insufficient to properly excite all the states so a sequence of maneuvers is performed with the rotorcraft returned to its trim condition between maneuvers.

Subset regression has an advantage over perturbation methods in that it automatically averages over a time interval or period. This averaging is important when identifying constant coefficients for a system that has significant periodic

coefficient effects. An additional advantage of the subset regression method is that it can easily handle a large number of states.

The stepwise regression method as formulated above applies to a linear or non-linear model of the motions of a dynamic system from test or simulation data. The approach can also be used to determine a perturbation model (i.e., where the states are perturbation motions about a nominal or trim state rather that total motions).

Difficulties are often encountered in the application of this approach when there is a high correlation between any of the states and/or controls. Correlation causes a reduction in the linear independence of the regression variables and degrades the identification process.

5.4. ROTOR MULTIBLADE EQUATIONS

The perturbational rotor model was defined in the multi-blade coordinate system. Recall that the nonlinear GENHEL simulation defined the rotor blade dynamics in the rotating coordinate system. Multiblade coordinates are preferred for the perturbational model because they are constant in steady flight (except for higher harmonics) and because they provide accurate information on the magnitude and direction of the thrust of the rotor. They are useful in modeling and gaining a better physical understanding of the coupling between the rotor and the fuselage. They are also useful in feedback control synthesis. Rotating blade coordinates on the other hand allow a better physical understanding of the forces on, and dynamics of, a single blade, but do not provide for easy understanding of the effects on the fuselage.

The transformation from the rotating blade coordinate system to the multi-blade coordinate system is described in Appendix A

for a five-bladed rotor system. This appendix also discusses the form of the resulting equations which were parameterized.

5.5 ROTOR/FUSELAGE EQUATIONS

The final forms of the fuselage aerodynamic and rotor equations are shown in Figures 5.2 and 5.3. More detailed descriptions of the matrices in the rotor equations are given in Appendix A where the multi-blade transformation is discussed. Parameterization for the models is discussed in the following section.

The unknown or uncertain portion of the fuselage dynamics is the aerodynamics. Rigid body dynamics are well understood. Standard simulations are available. A regression to identify a fuselage model need only identify the particular form of the aerodynamic equations.

In the current study the fuselage aerodynamic forces are separated from the hub forces and identified as a separate module.

5.6 PARAMETERIZATION OF ROTOR AND FUSELAGE MODELS

Parameters for the linear rotor and fuselage aerodynamics models were obtained by applying OSR to the perturbation data generated by executing the GENHEL simulation. This section describes this work.

The trim condition about which the GENHEL-RSRA simulation was operated was as follows:

- forward speed = 120 knots
- altitude = 1000 feet
- gross vehicle weight = 19,600 pounds
- ambient temperature = 59°F
- ambient pressure = 14.7 psi

$$\Delta x_R = A_{RR}\,\Delta x_R + A_{RT}\,\Delta x_T + A_{RFU}\,\Delta x_{FU} + B_{RC}\,\Delta u + B_{RFU}\,\Delta y_{FU}$$

$$+ B_{RT}\,\Delta y_T + B_{RL}\,\Delta y_L + \begin{bmatrix} 0 & 0 \\ (\dot{J} - J^2) & 2J \end{bmatrix} \Delta x_R$$

$$\Delta y_R = C_{RR}\,\Delta x_R + C_{RT}\,\Delta x_T + C_{RFU}\,\Delta x_{FU} + D_{RT}\,\Delta y_T + D_{RC}\,\Delta u$$

$$+ D_{RR1}\,\Delta y_{1R} + D_{RFU}\,\Delta y_{FU}$$

where

A_{RR}, A_{RT}, A_{RFU}, B_{RC}, B_{RFU}, B_{RT}, B_{RL}, C_{RR}, C_{RT}, C_{RFU}, D_{RT},

D_{RC}, D_{RR1}, D_{RFU} = matrices of coefficients

J = axis transform matrix (see Eq. (A.4) in Appendix A)

u = rotor controls
$= \{\theta_C, A_{1s}, B_{1s}, \theta_{TR}\}^T$

x_{FU} = fuselage states
$= \{u, v, w, p, q, r, \phi, \theta, \psi\}^T$

x_R = rotor states
$= \{\beta_0, \ldots, \beta_{2s}, \xi_0, \ldots, \xi_{2s}, \dot{\beta}_0, \ldots, \dot{\beta}_{2s}, \dot{\xi}_0, \ldots, \dot{\xi}_{2s}\}^T$

x_T = drive train states

y_{FU} = fuselage outputs
$= \{\dot{u}, \dot{v}, \dot{w}, \dot{p}, \dot{q}, \dot{r}, /v/\}^T$

y_R = rotor force and torque outputs
$= \{H, J, T, L_H, M_H, Q_H\text{-}Q_{LD}\}^T$

y_T = drive train outputs

y_{1R} = $\{\ddot{\beta}_0, \ldots, \ddot{\beta}_{2s}, \ddot{\xi}_0, \ldots, \ddot{\xi}_{2s}\}^T$

Figure 5.2 Form of Rotor Perturbational Equations

$$\Delta y_A = C_{AFU}\,\Delta x_{FU} + C_{AR}\,\Delta x_R + D_{AC}\,\Delta u + D_{AT}\,\Delta y_T + D_{AFU}\,\Delta y_{FU} + D_{AR1}\,\Delta y_{1R}$$

where:

C_{AFU}, C_{AR}, D_{AC}, D_{AT}, D_{AFU}, D_{AR1} = coefficient matrices

u = rotor controls

x_{FU} = fuselage states
$= \{u, v, w, p, q, r, \phi, \theta, \psi\}^T$

x_R = rotor states

y_A = fuselage aerodynamic force outputs
$= \{x_F, y_F, z_F, L_F, M_F, N_F\}^T$

y_{FU} = fuselage outputs
$= \{\dot{u}, \dot{v}, \dot{w}, \dot{p}, \dot{q}, \dot{r}, /v/\}^T$

y_T = drive train outputs

y_{1R} = rotor accelerations

Figure 5.3 Form of Fuselage Aerodynamicss Perturbation Equations

The data generated by the GENHEL simulation was stored on a computer disk to be used in the regression analysis. These data included the states, state derivatives and control inputs.

5.6.1 Control Inputs

The control inputs were defined so they would excite all of the rotor and fuselage dynamics in the frequency range 0 to $2\ \Omega_{MR}$, where Ω_{MR} is the main rotor speed. Five different control inputs were used. These included

θ_C - main rotor collective

A_{1s} - main rotor lateral cyclic

B_{1s} - main rotor longitudinal cyclic

θ_{TR} - tail rotor collective

Q_E - engine torque on rotor hub

The engine torque, Q_E, on the rotor hub, was included because the GENHEL simulation did not have a rotor propulsion system. The engine torque was used to vary the rotor speed and to thus excite the rotor dynamics that needed to couple with propulsion system dynamics.

A doublet was used as the form for the control input perturbations. Doublets at four different frequencies were used in order to excite all response frequencies of the rotor and fuselage between zero and $2\Omega_{MR}$. The shape and duration of these doublets are shown in Figure 5.4.

5.6.2 Attitude Control

The GENHEL simulation contained a Stability Augmentation System (SAS) to stabilize the fuselage dynamics. The SAS would not "fly" the simulation, though. Some type of pilot-in-the-loop was required to keep the helicopter from flying off erratically. A simple attitude controller was coupled with the SAS in order to

(a) TRIM CONDITION

- ALTITUDE = 1000 FEET
- FORWARD SPEED = 120 KNOTS
- TEMPERATURE = $59^{O}F$

(b) INPUT FORM

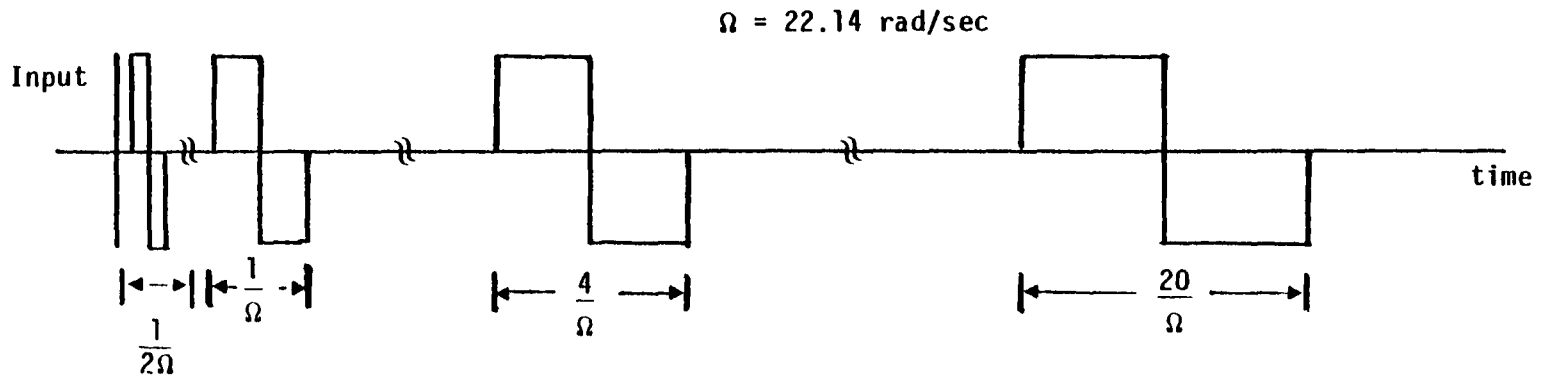

Figure 5.4 Generation of GENHEL Data for OSR

keep the helicopter near the nominal trim flight condition that was being modeled.

The attitude controller consisted of a simple proportional controller applied to the roll and pitch axes of the fuselage. A schematic of the controller for the roll axis is shown in Figure 5.5. The gains for the roll and pitch controllers were chosen to be small so as not to wash out the transient effects of the control perturbations.

5.6.3 Data Generation

Table 5.1 summarizes the data runs used to generate data for the regression analysis. Twenty data generation runs were made (five different controls times four doublet periods). The run times and sampling rates are also given in Table 5.1. The data from these twenty runs was catenated end-to-end to create one long time history of 3950 time points.

5.6.4 Dependent and Independent Variables

Table 5.2 summarizes the dependent and independent variables that were used in the regression analysis. The independent variables are the ones that are collected into equations to describe each dependent variables time history. Table 5.3 describes the nomenclature used in Table 5.2.

Some additional constraints, pertaining to which dependent variables were allowed into the equations, were applied that are not shown in this table. These constraints forced the diagonal matrix form, found in Eq. (A.10) of Appendix A, into the regression equations.

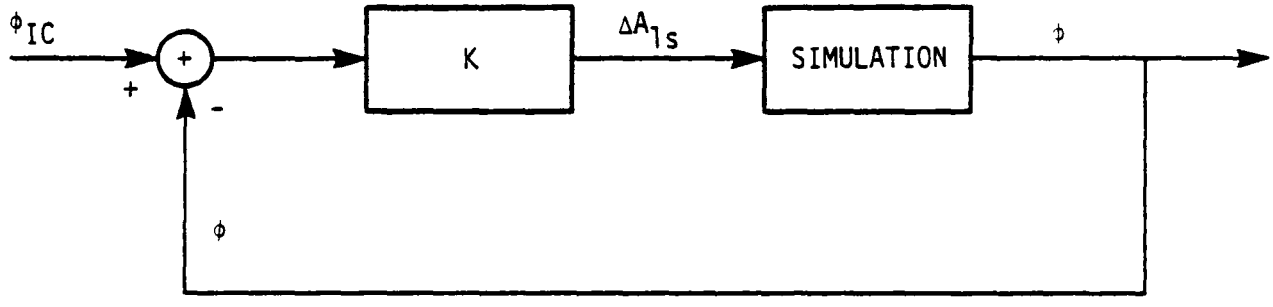

Figure 5.5 Attitude Control For Roll Axis

Table 5.1

Description of Data Runs Used to Generate Data for OSR

a. CONTROL DISTURBANCES

NO.	CONTROL	NOMINAL VALUE	PERTURBATION
1.	θ_C- COLLECTIVE	11°	1.5°
2.	A_{1S}- LAT. CYC.	-1.5°	0.3°
3.	B_{1S}- LONG. CYC.	9.3°	0.9°
4.	θ_{TR}- TAIL ROTOR COLL.	5.9°	-2.2°
5.	Q_E- ENG. TORQ. ON HUB	31630 FT. LB.	3160 FT. LB.

b. DISTURBANCE FORMS

NO.	PERIOD (SEC)	LENGTH t_f (SEC)	SAMPLE INTERVAL τ (SEC)
1.	.142 (2/Ω)	.5	.02
2.	.284 (1/Ω)	1.0	.02
3.	1.14 (.25/Ω)	6.0	.05
4.	5.68 (.02/Ω)	20.	.10

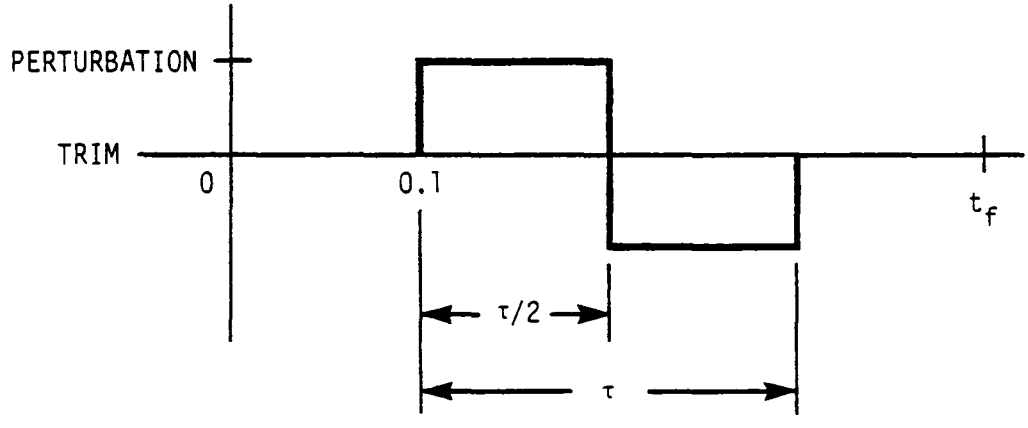

Table 5.2
Regression Model Setup

DEPENDENT VARIABLE	INDEPENDENT VARIABLES
ΔX_F	- GROUP 1 (Δu, Δv, Δw, Δp, Δq, Δr)
ΔY_F	
ΔZ_F	- GROUP 2 ($\Delta\beta_0,\ldots, \Delta\beta_{2s}, \Delta\xi_0,\ldots, \Delta\xi_{2s}$, $\Delta\dot{\beta}_0,\ldots, \Delta\dot{\beta}_{2s}, \Delta\dot{\xi}_0,\ldots, \Delta\dot{\xi}_{2s}$)
ΔL_F	
ΔM_F	- GROUP 3 ($\Delta\ddot{\beta}_0,\ldots, \Delta\ddot{\beta}_{2s}, \Delta\ddot{\xi}_0,\ldots, \Delta\ddot{\xi}_{2s}$)
ΔN_F	- GROUP 4 ($\Delta\dot{u}$, $\Delta\dot{v}$, $\Delta\dot{w}$, $\Delta\dot{p}$, $\Delta\dot{q}$, $\Delta\dot{r}$, $\Delta\lvert v\rvert$)
	- GROUP 5 (Δe_{TR}, $\Delta\Omega_{TR}$)
$*\Delta\ddot{\beta}_0$	- GROUP 1
$*\Delta\ddot{\beta}_{1c}$	- GROUP 2
$*\Delta\ddot{\beta}_{1s}$	- GROUP 4
$*\Delta\ddot{\beta}_{2c}$	- GROUP 6 ($\Delta\theta_c$, ΔA_{1s}, ΔB_{1s}, $\Delta\Omega_{MR}$)
$*\Delta\ddot{\beta}_{2s}$	
$*\Delta\ddot{\xi}_0$	
$*\Delta\ddot{\xi}_{1c}$	
$*\Delta\ddot{\xi}_{1s}$	
$*\Delta\ddot{\xi}_{2c}$	
$*\Delta\ddot{\xi}_{2s}$	
ΔH	- GROUP 1
ΔJ	- GROUP 2
ΔT	- GROUP 4
ΔL_H	- GROUP 6
ΔM_H	- GROUP 7 ($\Delta\dot{\Omega}_{MR}$)
$\Delta Q_H - \Delta Q_{LD}$	

Table 5.3

Nomenclature For Table 5.2

$\Delta(\ )$ - PERTURBATION VALUE

$*(\ )$ - DOES NOT INCLUDE AXIS TRANSFORMATION "J" TERMS (SEE APPENDIX A) OR LAG DAMPER TORQUES

$X_F, \ldots, N_F$ - AERODYNAMIC BODY-FIXED FORCES AND MOMENTS ON FUSELAGE

$\beta_0, \ldots \beta_{2S}$ - ROTOR FLAPPING MULTIBLADE COORDINATES FOR 5 BLADES

$\zeta_0, \ldots, \zeta_{2S}$ - ROTOR LAGGING MULTIBLADE COCRDINATES FOR 5 BLADES

$H, \ldots, Q_H$ - HUB FORCES ON ROTOR IN SHAFT COORDINATES

Q_{LD} - LAG DAMPER TORQUE FOR 5 BLADES

u, v, w, p, q, r -FUSELAGE RATES IN BODY-FIXED COORDINATES

θ_C, A_{1S}, B_{1S} - MAIN ROTOR COLLECTIVE, LATERAL CYCLIC AND LONGITUDINAL CYCLIC CONTROL INPUTS

θ_{TR} - TAIL ROTOR COLLECTIVE INPUT

Ω_{MR}, Ω_{TR} - MAIN ROTOR AND TAIL ROTOR SPEEDS

5.6.5 Results

5.6.5.1 Coefficients

The coefficients for the fuselage and rotor models that were obtained from the data are listed in Volume II.

Identification of the fuselage aerodynamic models (equations for $X_F, Y_F, .., N_F$) and for the rotor hub forces and moments (equations for H, J, T, L_H, M_H, Q_H) were straightforward and proceeded without difficulty. OSR runs were made using the dependent and independent variables listed in Table 5.2. Very good fits to the data were obtained.

Significant difficulty was encountered in attempting to identify coefficients for the rotor dynamics model. Initial OSR runs were made with the "axis transformation" terms (the terms involving "J" in Eq. (A.8) of Appendix A) removed from the regression. "Removed from the regression" means the terms were known beforehand and were subtracted off of the acceleration term before attempting to fit an equation to the acceleration term. All of the blade states, fuselage states, controls (except for the tail rotor), and fuselage accelerations were allowed in the analysis during the initial runs. No attempt was made to force the diagonal matrix coefficient form of Eq. (A.10) of Appendix A into the analysis. The analysis results of Appendix A were not available until the completion of this study.

The model identified in the initial regression analysis (just described), had very high mean squared fit values but was unstable when integrated. Since the nonlinear model equations were stable, the identified model was definitely wrong. Although the mean squared (and also the F-test) fit measures said the fit was good, it was not. It is known, though, that when there is no uncorrelated noise in the data, as was true for this data, the F-test is of questionable value. Also, the mean squared fit value increases with each variable allowed into the regression.

A good fit, although not necessarily physically reasonable, can always be obtained by allowing enough variables into the regression.

Several attempts were made to obtain better equations. In the first attempts, the number of blade states was reduced. The 2c and 2s blade lagging states were dropped, then the 2c and 2s blade flapping states were dropped. It was thought that perhaps there was insufficient information on these states in the data or that identification of these states was corrupted by high frequency (greater than $2\Omega_{MR}$) responses in the data. No significant improvement in the resulting model resulted from these changes.

Other changes in the regression that also yielded no improvement were;

(1) filtering the data to remove responses with frequencies higher than approximately $4\Omega_{MR}$,

(2) using larger control input perturbations to try to excite more inplane (lag) response, and

(3) not allowing the fuselage accelerations into the analysis.

The results shown in Volume II were finally computed by forcing the diagonal form of the coefficient matrices, shown in Eqs. (A.8) and (A.10) of Appendix A, into the regression analysis while also analytically subtracting off the fuselage acceleration terms before performing the regression analysis. These acceleration terms were found analytically by linearizing and partially transforming the GENHEL equations into multi-blade coordinates. The rotor equations thus constructed using the regression analysis were stable, although when integrated, did not fit the nonlinear response particularly well. A sample of the results is shown and discussed in the next section.

The reason for the difficulty in obtaining the parameters for the rotor equations is now understood. It was uncovered during the analysis of the multi-blade transformation discussed in Appendix A.

The difficulty was caused by periodic effects in the rotor dynamics. Generally, periodic effects in the rotor dynamics are considered to be small and can be neglected up to rotor advance ratios of = 0.3 [18]. The flight condition analysed in this contract was a helicopter forward speed of 120 knots, which corresponded to an advance ratio of 0.3. Thus, periodic effects should have been expected to be significant.

The problem was that the periodic effects were not handled correctly in the initial analysis. As shown in Eq. (A.11) of Appendix A, trim for helicopters at forward speeds where periodic effects are present is not time-independent. The trim state is given by the sum of a steady, non-accelerating term and a periodic, time-varying term. When computing perturbations from a trim state, the periodic portion of the trim must be removed as well as the time-independent portion. This periodic portion of the trim was not removed when the perturbational data for the regression analysis was saved.

The procedure used in this study to subtract off the trim values was as follows. First the GENHEL simulation was trimmed out. Then second, a "snapshot" of the states, responses and controls at this trim condition was taken and stored. Third, this "snapshot" of the data was subtracted off of the data as it was stored during the helicopter maneuvers to create the perturbation data.

This approach was in error because the "snapshot" of the data was distorted by the time-dependent trim effects. This is shown in Figure 5.6. The correct procedure would have been to subtract off the steady part of the trim value, labelled in Figure 5.6, and the periodic trim signal. The "snapshot" could occur during any phase of the periodic motion so it could error from the steady trim by up to $\pm$ the amplitude of the periodic motion if the trim values are not removed correctly. The magnitudes of these amplitudes are observable in the plots in the next section. If it is only possible to remove the steady

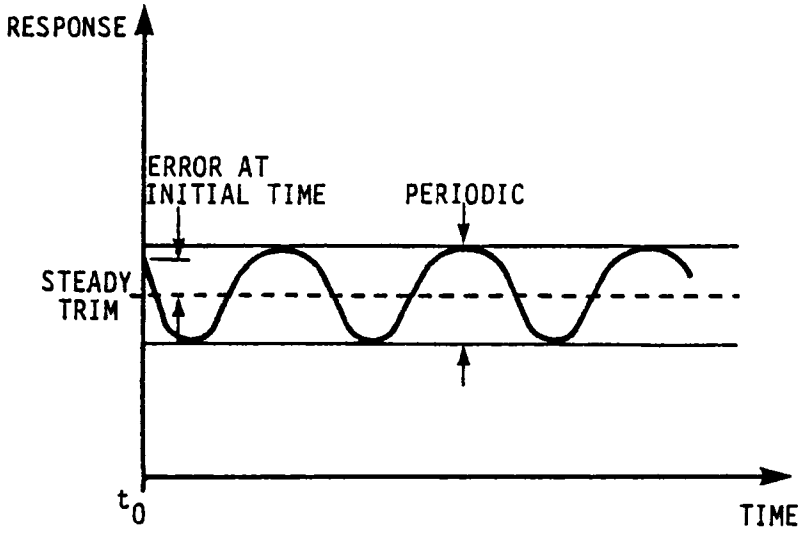

Figure 5.6 Example of Trim in a Periodic System

portion of the trim, OSR may successfully average out the rest, assuming the steady portion is removed correctly.

The error in removing the steady trim caused the perturbation data that was stored to be biased. Each channel (or variable) in the data had a different bias value.

The correct way to compute the perturbation values would have been to save the trim response for a period of time. Then, average the data to find the steady trim value and fit a sine to the periodic portion of the trim signal. Finally, subtract off the steady trim value and the sine from the maneuver data to leave the perturbation values.

There were insufficient resources left in the contract at the end to redo the rotor model parameterization and correctly consider the periodic effects. This was because the regression data had been originally taken incorrectly.

5.6.5.2 Simulation Results

The linear rotor and fuselage models that were extracted from the GENHEL simulation were appended back to the GENHEL simulation for checkout. A nonlinear lag damper model in multi-blade coordinates was added to complete the rotor model. The parameter values in the linear perturbation models are given in Volume II.

The plots in Figure 5.7 show the comparison of the linear perturbation rotor and fuselage results with those of the GENHEL simulation. Both sets of results were computed assuming a constant rotor speed (i.e, no propulsion dynamics). The trim condition is 120 knots forward speed, 1000 ft altitude, which is the same trim for which the perturbational data were developed. The plots in Figure 5.7 show the response to a pilot longitudinal cyclic input. The input is ramped up from 78% pilot stick position to 88% over one second.

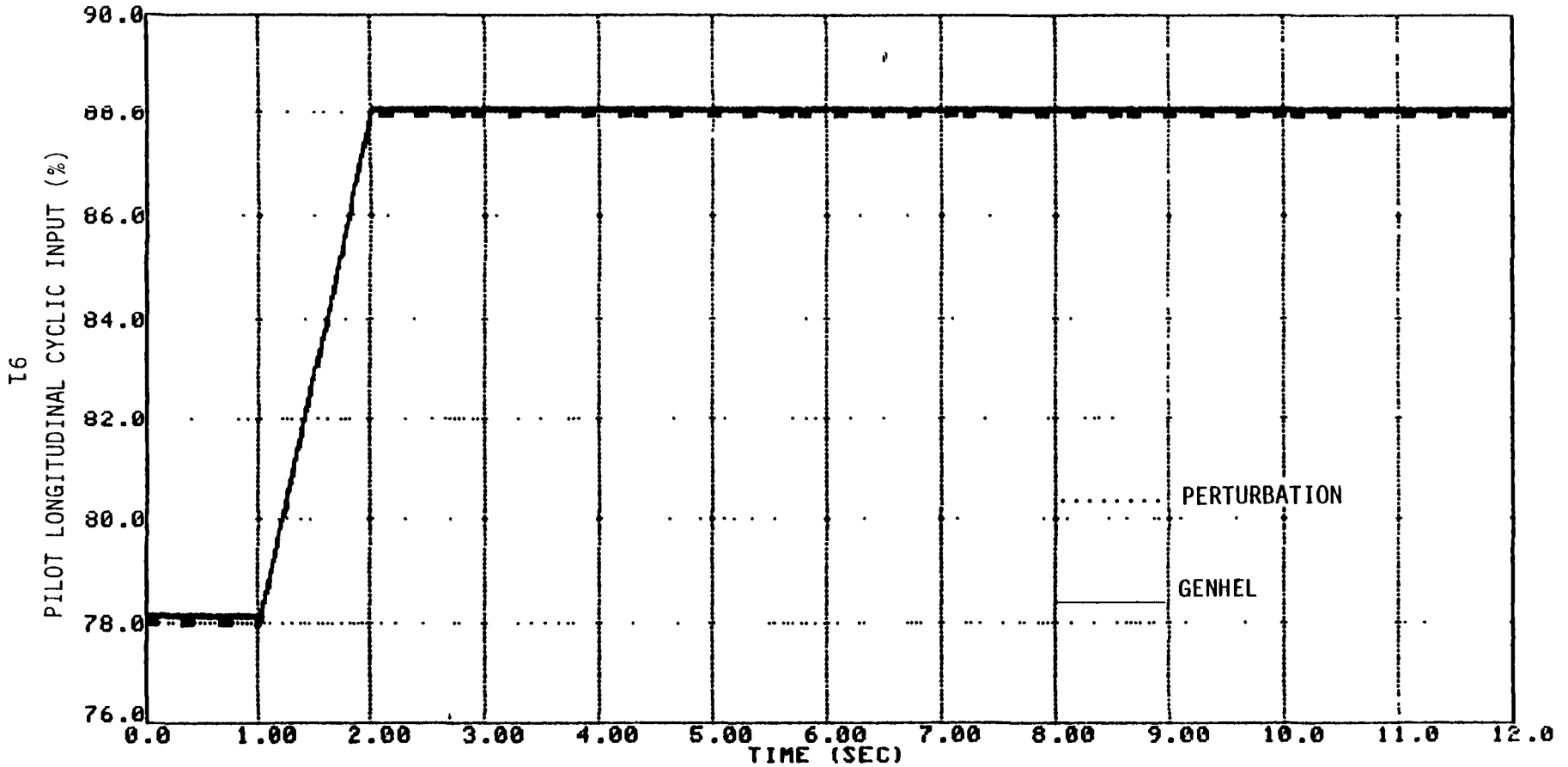

Figure 5.7a Rotor/Fuselage With Long Cyc Input

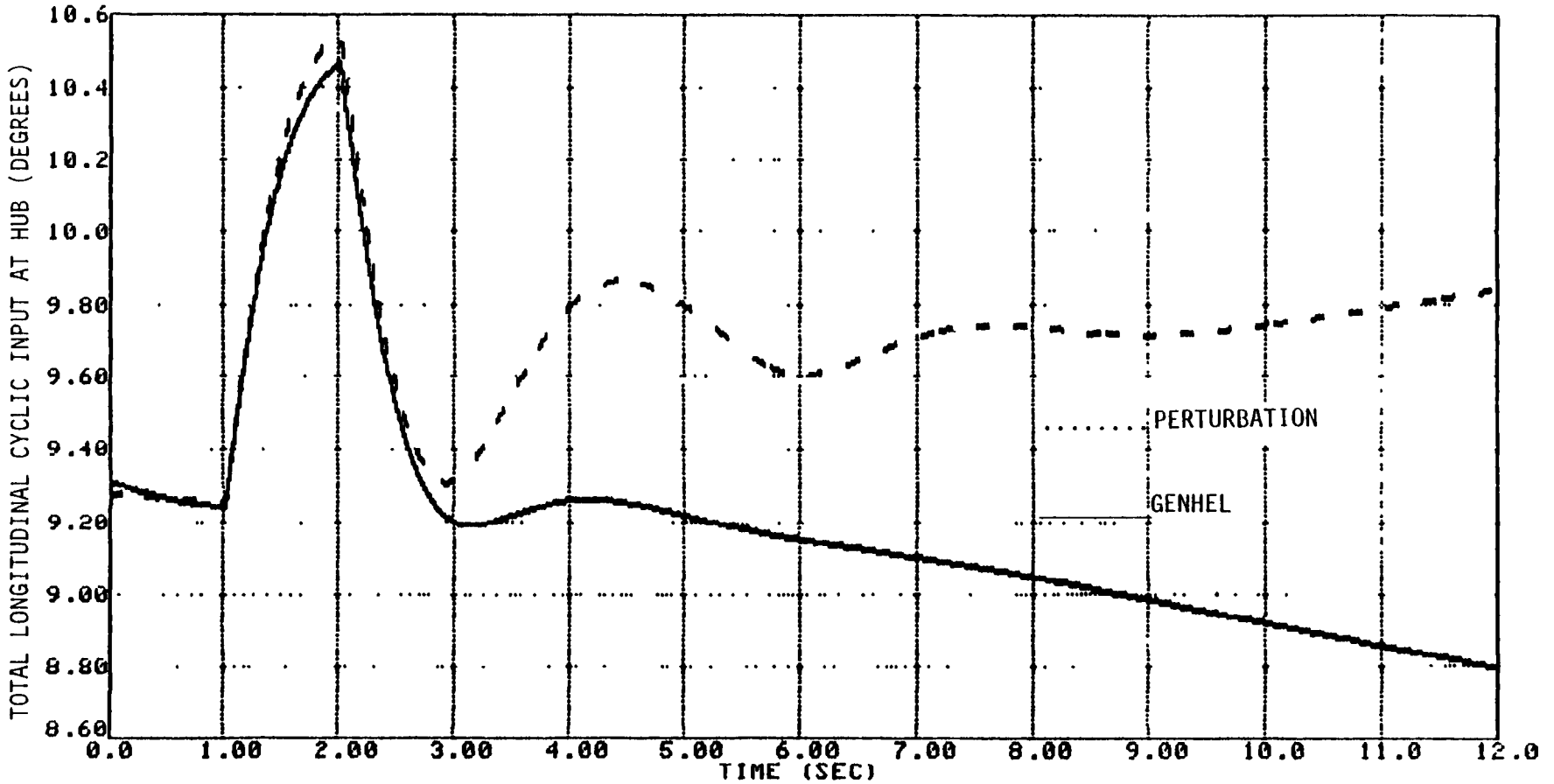

Figure 5.7b Rotor/Fuselage With Long Cyc Input

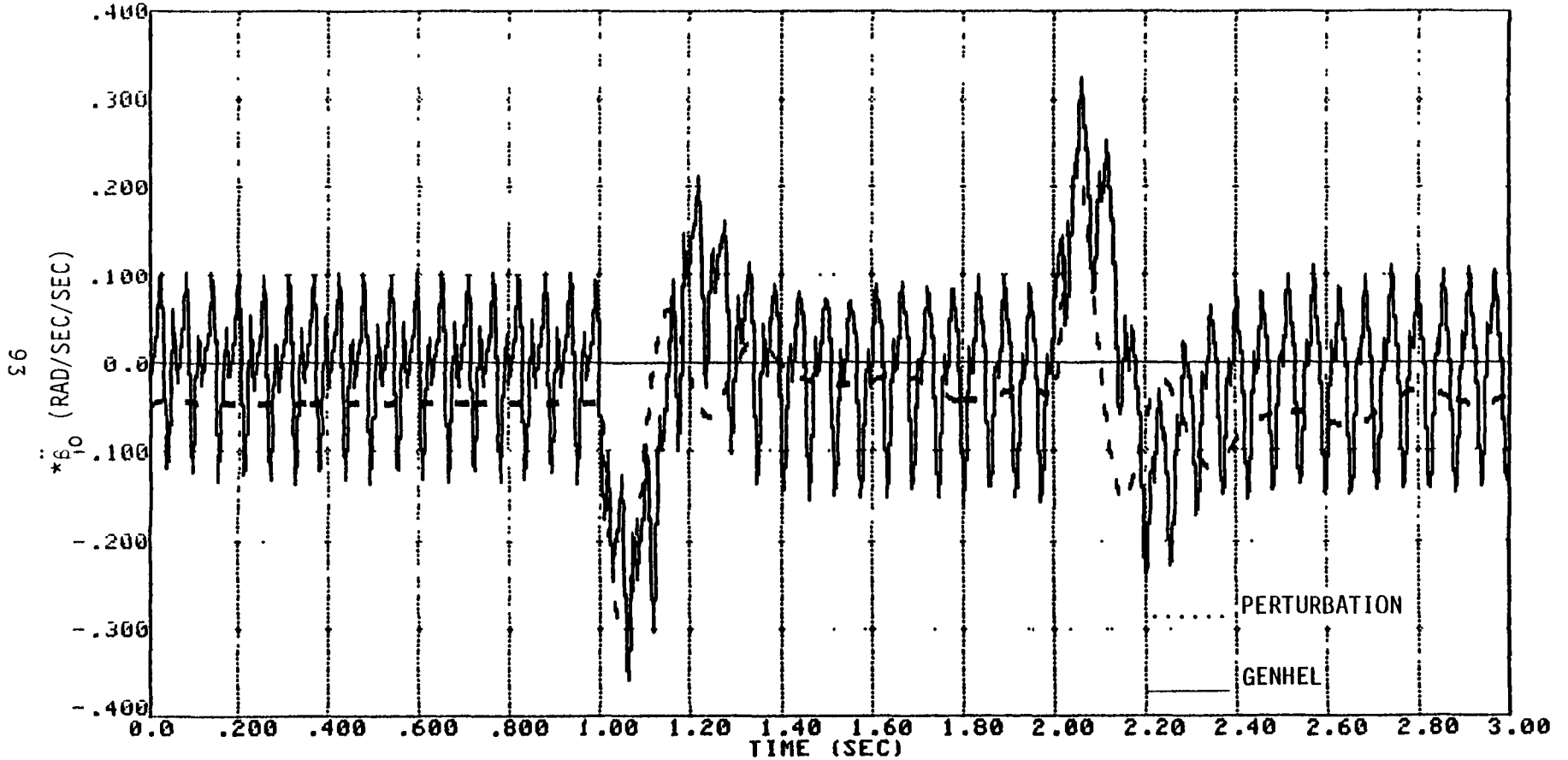

Figure 5.7c Rotor/Fuselage With Long Cyc Input

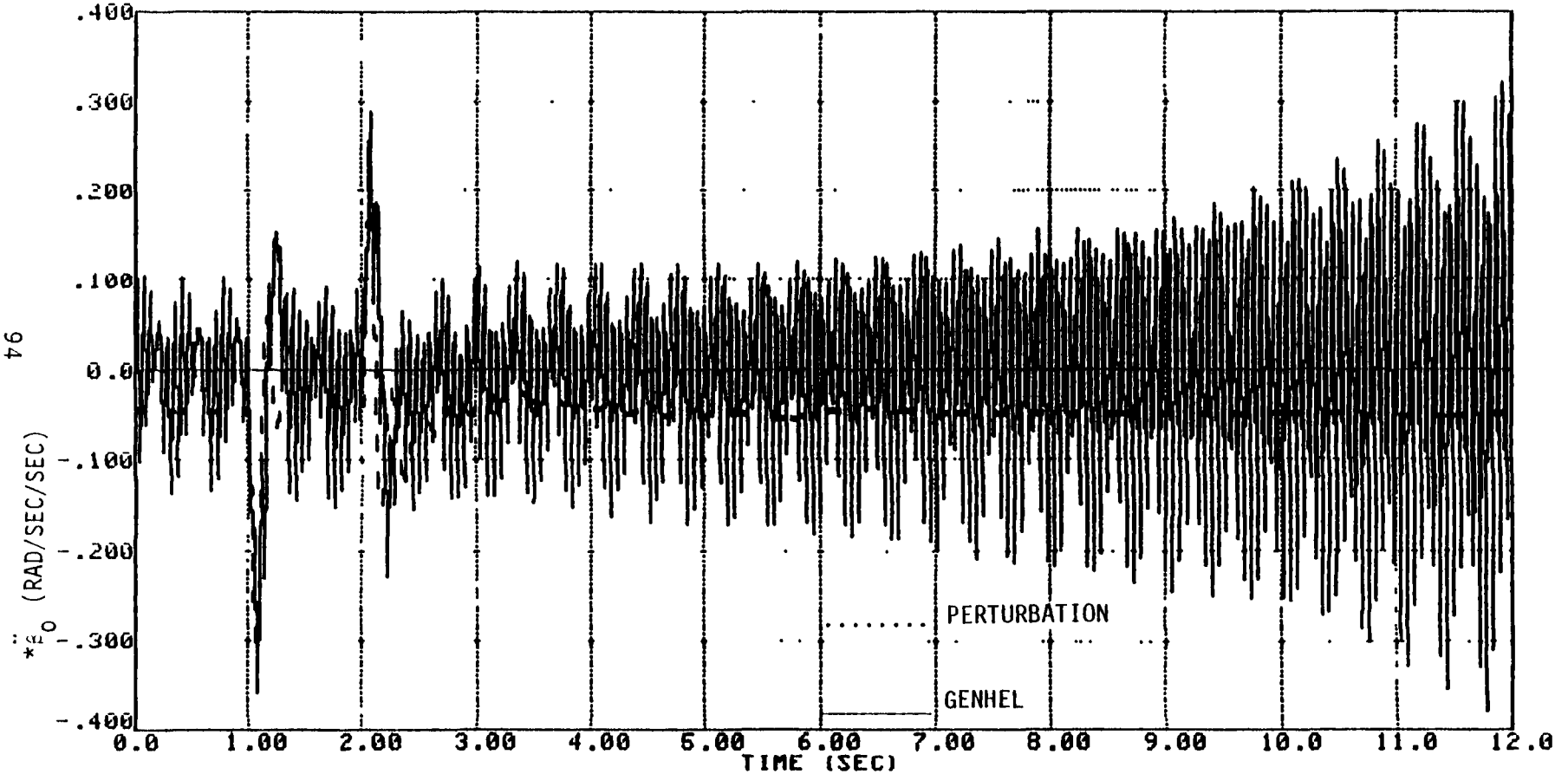

Figure 5.7d Rotor/Fuselage With Long Cyc Input

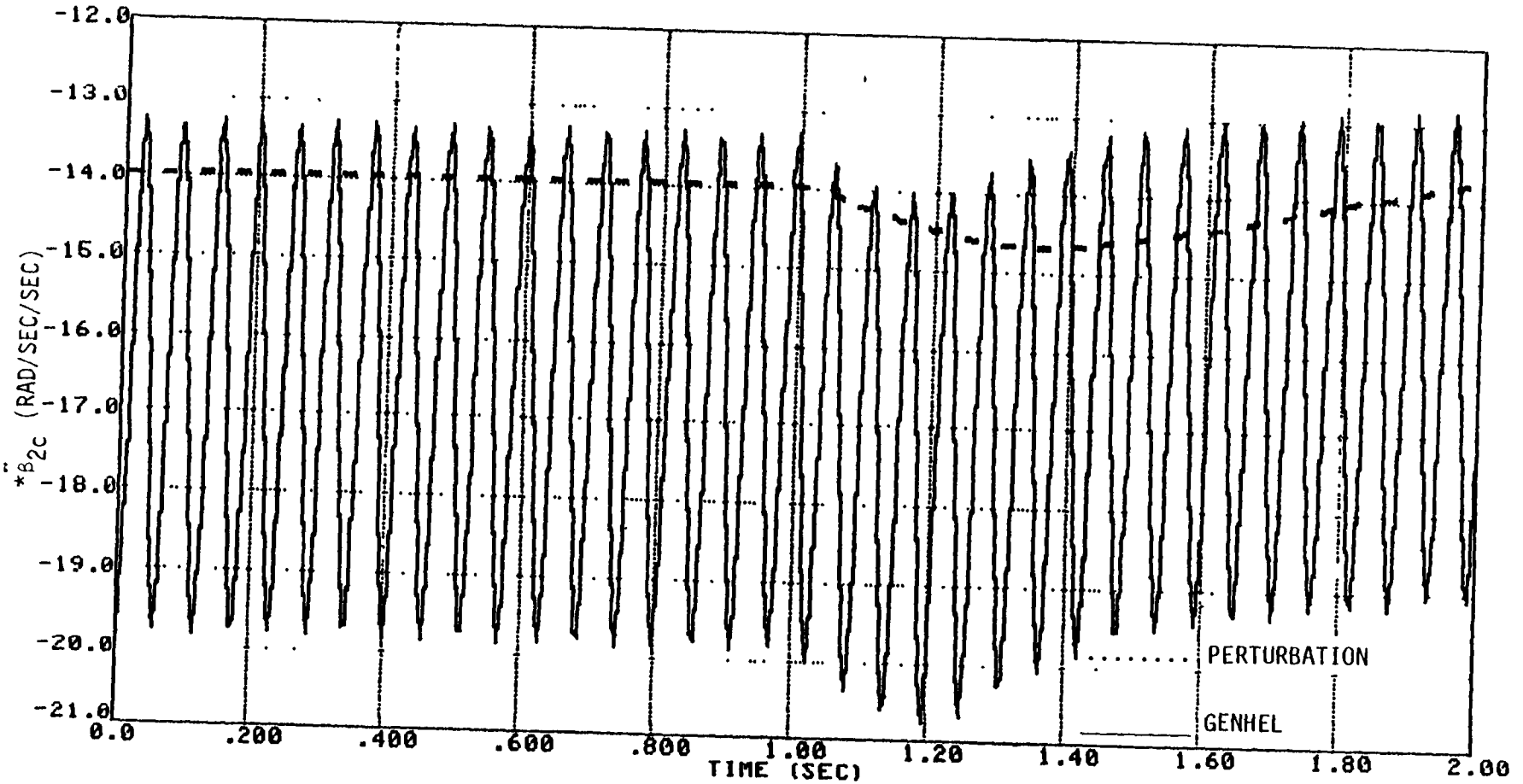

Figure 5.7e Rotor/Fuselage With Long Cyc Input

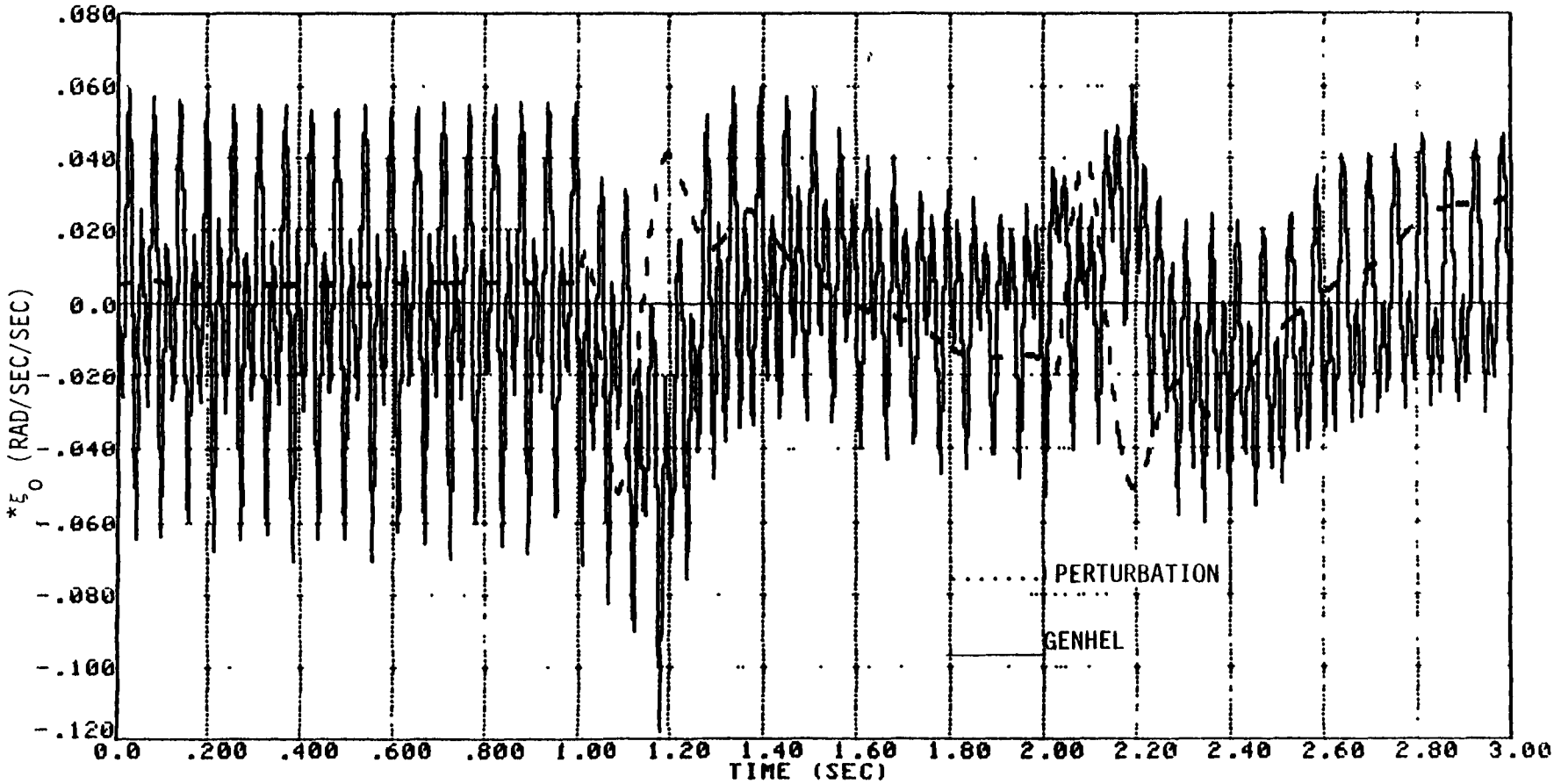

Figure 5.7f Rotor/Fuselage With Long Cyc Input

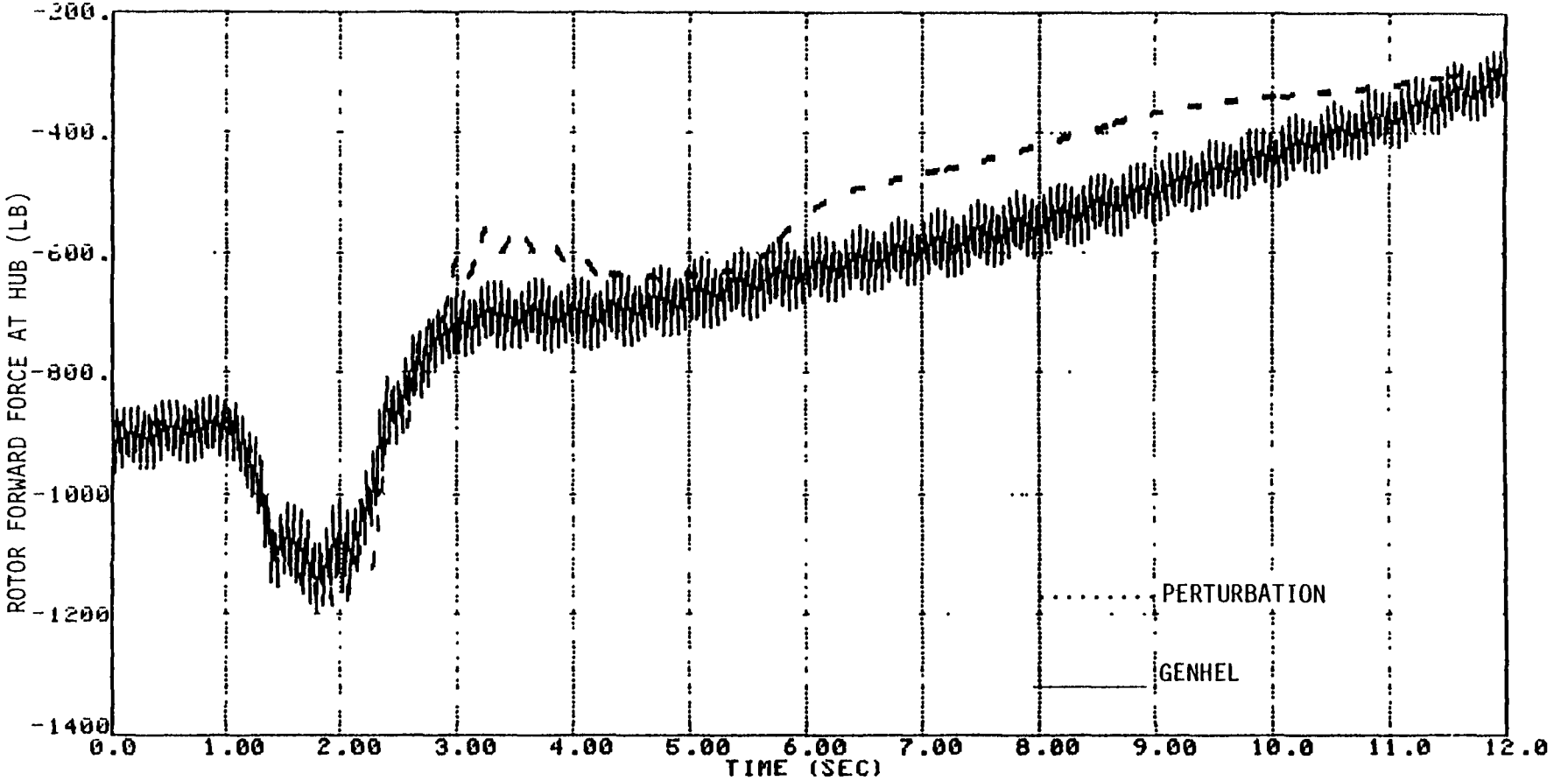

Figure 5.7g Rotor/Fuselage With Long Cyc Input

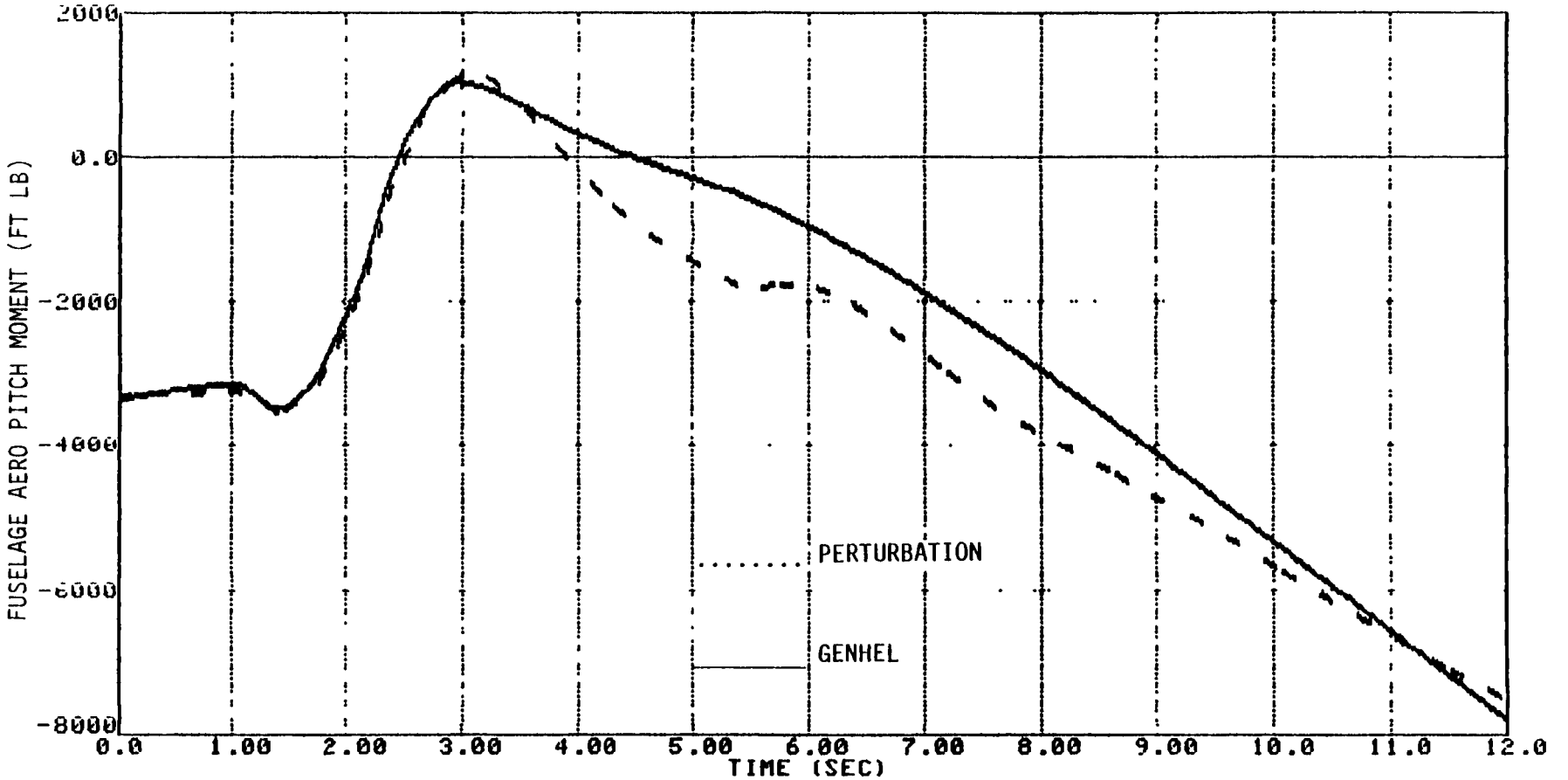

Figure 5.7h Rotor/Fuselage With Long Cyc Input

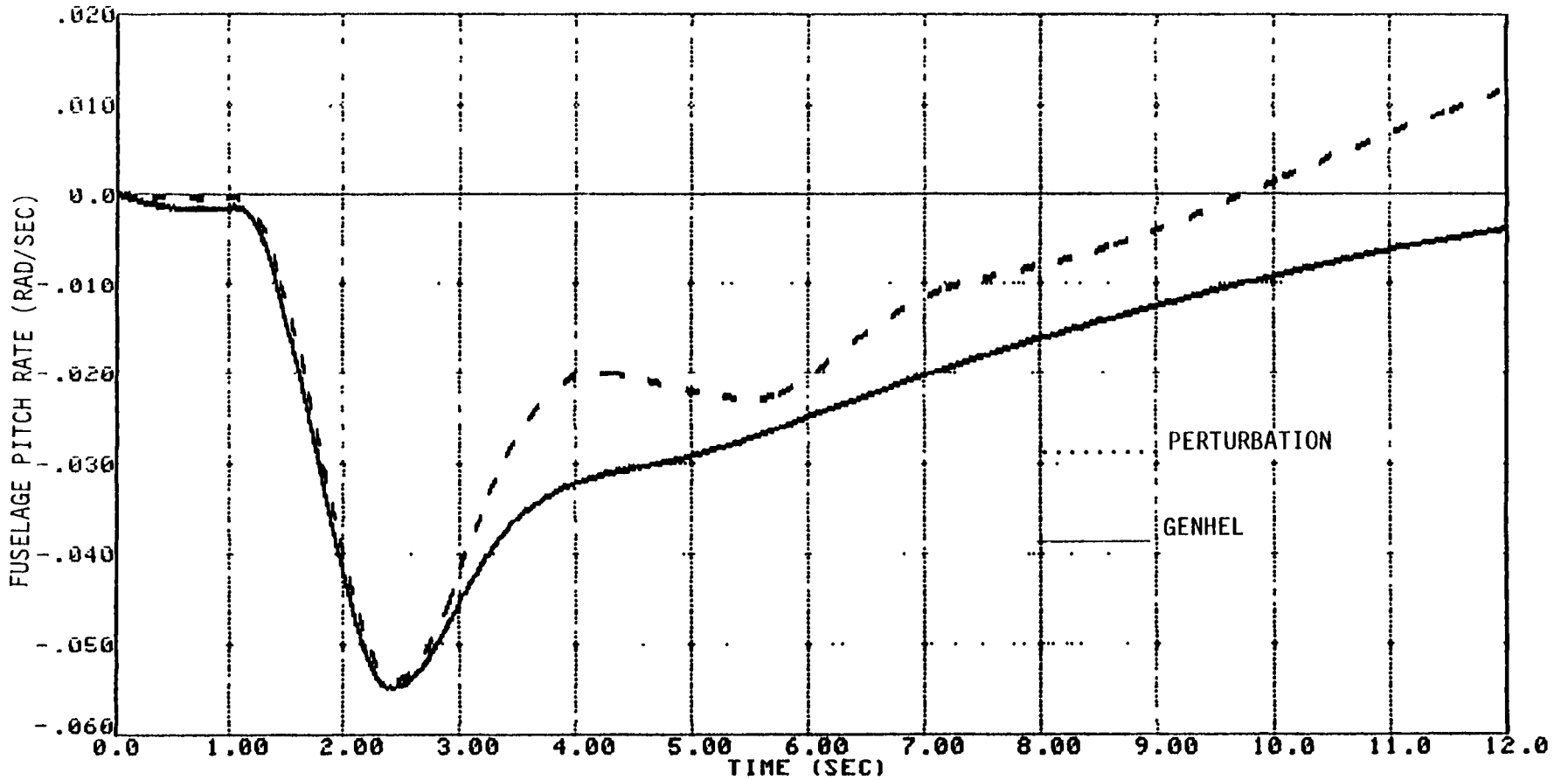

Figure 5.7ı Rotor/Fuselage With Long Cyc Input

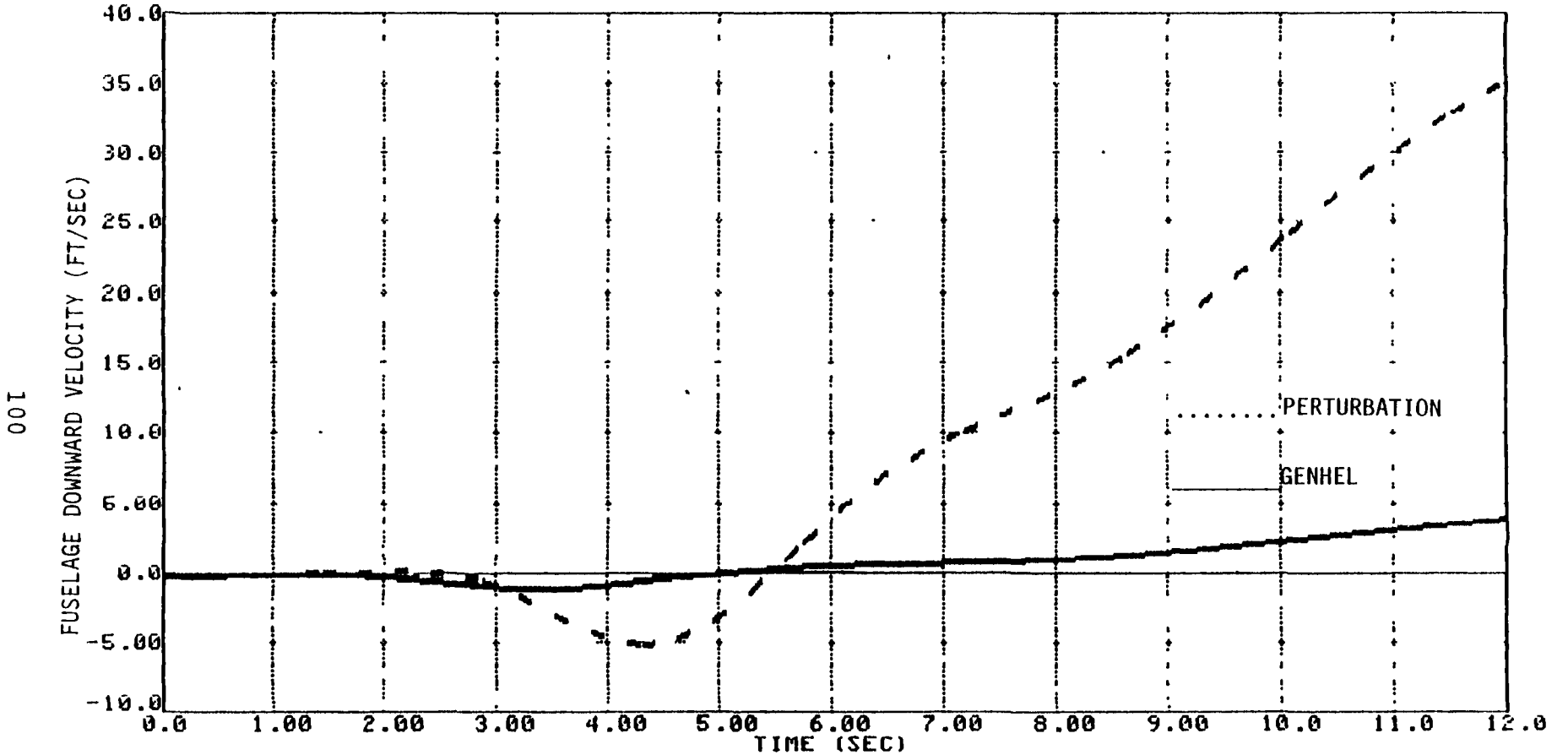

Figure 5.7j Rotor/Fuselage With Long Cyc Input

The effect of the poor rotor model parameters is apparent. Figure 5.7(a) shows the pilots longitudinal cyclic input. Figure 5.7(b) shows the total longitudinal cyclic input at the rotor hub, including pilot input, SAS input and attitude controller input. Figures 5.7(c) to 5.7(f) show some of the blade accelerations. The ones shown are $*\ddot{\beta}_0$, $*\ddot{\beta}_{2c}$ and $*\ddot{\xi}_0$. The "*" symbol implys that the terms are not total accelerations, and the "axis transform" or "J" terms in Eq. (A.8) of Appendix A have not been added on. This was the approach taken in Ref. 20.

The periodic effects are quite apparent for the nonlinear rotor simulation in Figures 5.7(c) to 5.7(f). These effects have a major effect at the $5\Omega_{MR}$ = 17.6 Hz frequency. Note that time scales on some of the plots have been expanded to allow this frequency to be eyeballed.

The effect of the periodic motion on the choice of the trim condition is especially apparent in Figure 5.7(e). Here, trim data was taken near the peak of the periodic motion of this response.

The remaining figures, Figure 5.7(g) to 5.7(j) show some of the forces and fuselage motions. The periodic effects are mostly filtered out before they reach these responses, although they are still quite apparent in the rotor hub forces. These four plots also show that the perturbational model is drifting off in error due to the poor rotor fit as time increases.

5.7 SUMMARY AND RECOMMENDATIONS

A generic methodology was defined for developing a simplified rotor/fuselage model from detailed nonlinear simulations. The approach is generic in that it can be applied to any helicopter or rotorcraft. The modular structure used in the approach also allows parts (i.e. rotor, fuselage or lag damper) of the total model to be obtained from different data

sources, then combined into a single simulation. The simulation itself, used here as a test case, was not generic as it applied to one particular twin engine, single main rotor rotorcraft simulation.

There were problems in the parameterization of the rotor model. The rotor model did not fit the source data very well. The problem was attributed to initial lack of knowledge about the effect of periodic rotor dynamics. The periodic effects were subsequently studied and found to cause a component of the trim solution to be periodic. This periodic trim was not correctly accounted for when the perturbation data was taken.

An analysis of the transformation from rotating blade coordinates to multi-blade coordinates was performed. This analysis showed the form of the rotor equations in multi-blade coordinates and also the existence and equation form of the periodic terms. The analysis is documented in Appendix A. Periodic effects cannot be modeled by constant coefficient linear equations. The new information on the periodic effects can be used to obtain better multi-blade coordinate rotor models. The periodic effects can be either averaged out, now that their structure is known, or included in the model.

VI. SYSTEM MODEL FORMULATION

The rotorcraft model developed in this contract was appended to the nonlinear GENHEL simulation to form a single simulation. This was done for two reasons. First, the perturbation model developed in this contract needed a flight control system to "fly" it. The GENHEL simulation had a flight control system which could be used for this purpose. Second, combining the simulations together facilitated their comparison. Checkout of a parameterization of the generic model structure could be accomplished by running the nonlinear and the perturbation models with the same controller and then comparing the output directly.

Formulation of the combined perturbation and GENHEL simulations into one simulation was divided into two steps. Step one consisted of appending nonlinear engine, fuel control and drive train subroutines onto the GENHEL simulation. This step was taken to provide a full nonlinear helicopter model capable of simulating the dynamic interactions between the rotor and propulsion systems. The second step was to append the perturbation model equations to the GENHEL simulation.

The sections that follow in this chapter describe (1) the addition of the nonlinear propulsion system dynamics simulation to the GENHEL simulation, (2) the formulation of the combined perturbation and GENHEL simulations, and (3) demonstration and discussion of the resulting model. User's notes and common block descriptions for the augmented GENHEL simulation are given in Volume II.

6.1 ADDITION OF NONLINEAR PROPULSION DYNAMICS TO GENHEL SIMULATION

The nonlinear engine, fuel control and drive train subroutines discussed in Chapter IV were appended to the GENHEL simulation on the CDC 7600 at NASA-Ames. This addition created a

helicopter simulation that could model the interactions between the propulsion system and the rotor system.

The nonlinear propulsion subroutines (engines, fuel controls, drive train) were connected to the ROTOR subroutine in the GENHEL simulation. A simplified flow chart of the GENHEL simulation was shown in Figure 5.1. The propulsion subroutines contained their own fourth order Runge Kutta integration package. Options were written into the GENHEL simulation so the simulation could be run assuming the following three propulsion system models:

(1) constant rotor speed,

(2) constant engine torque on rotor hub, and

(3) nonlinear engine, fuel control and transmission dynamics.

Figures 6.1(a) through (i) demonstrate the response of the resulting augmented simulation. The change in rotor collective due to a ramp input of 20% to the pilots collective control is shown in Figure 6.1(a). Figure 6.1(b) shows the rotor speed droop. The two curves in this figure correspond, in one case, to a constant speed rotor model, and in the other case, to the nonlinear engine/fuel controller model with the collective input fed forward to the fuel control. The plots that follow these two show the fuel flow rate, rotor torque, rotor moments, and fuselage motions for the two configurations. The addition of propulsion system dynamics had little effect on the response of the system except for the effects on yaw rates, as shown in Figure 6.1(g).

A paper [21] written in conjunction with this report provides additional results and a discussion of the influence of the propulsion system dynamics on this model.

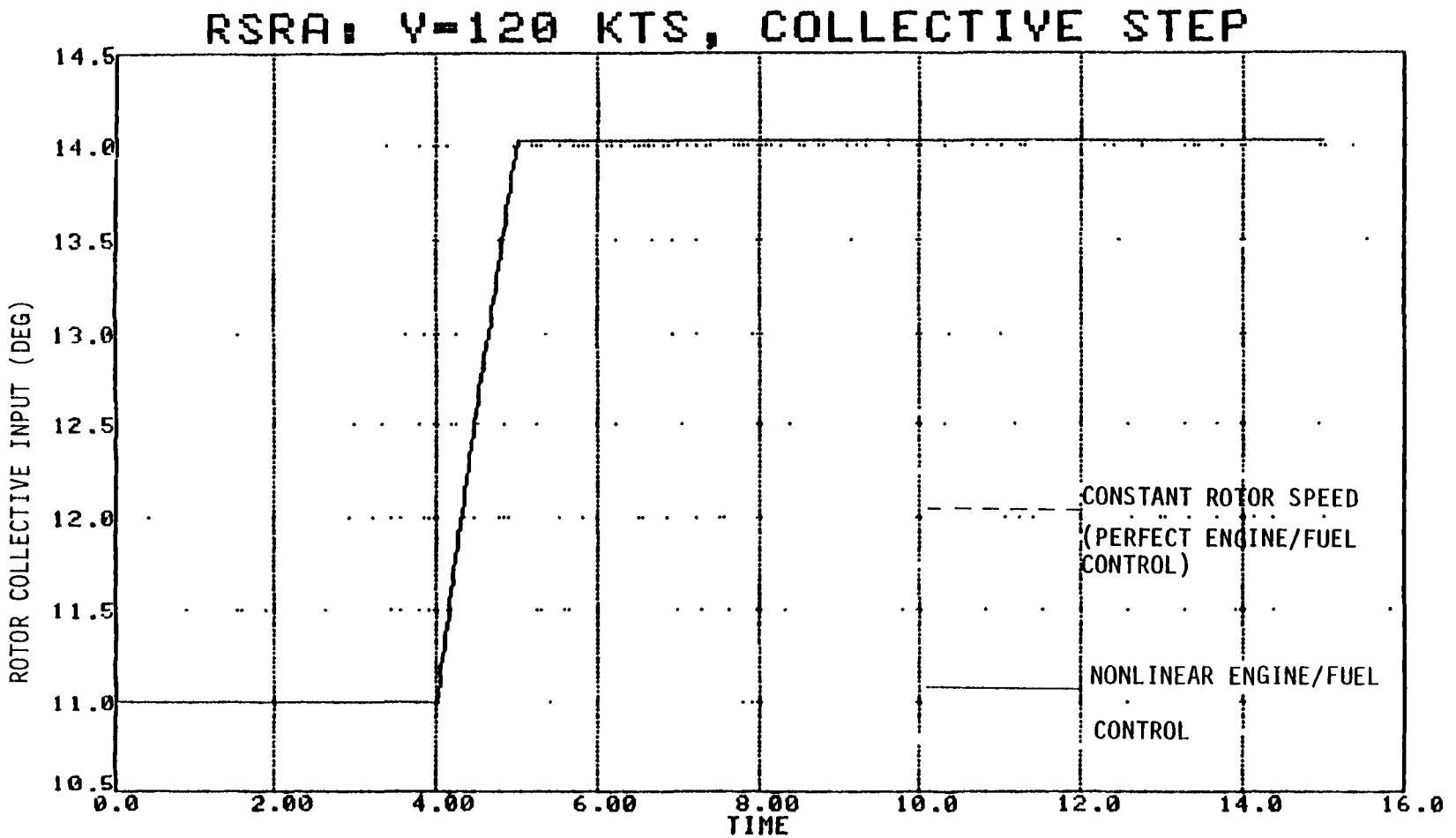

Figure 6.1a Nonlinear Rotor/Propulsion System With Collective Input, Collective Input

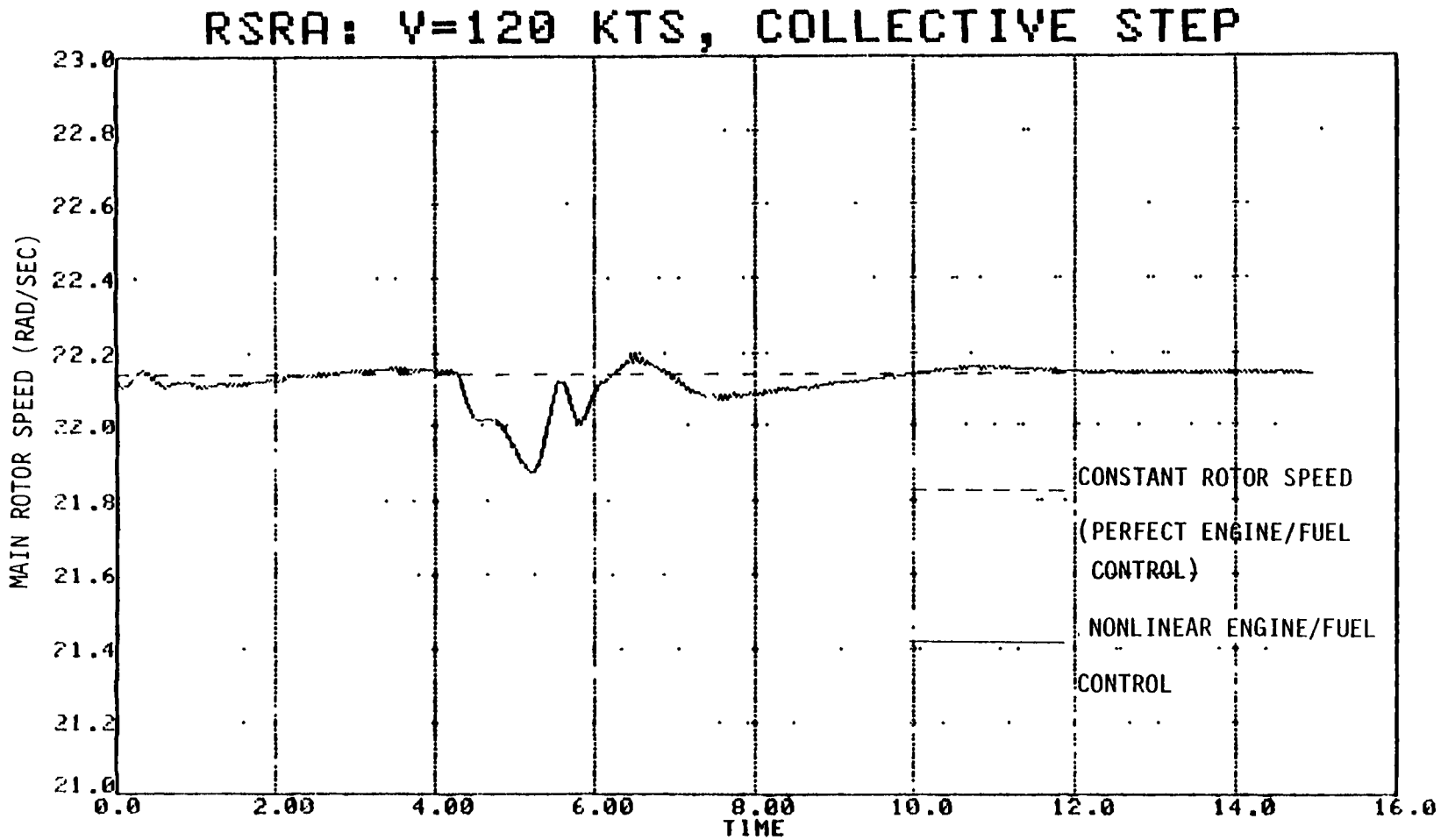

Figure 6.1b Nonlinear Rotor/Propulsion System With Collective Input, Rotor Speed

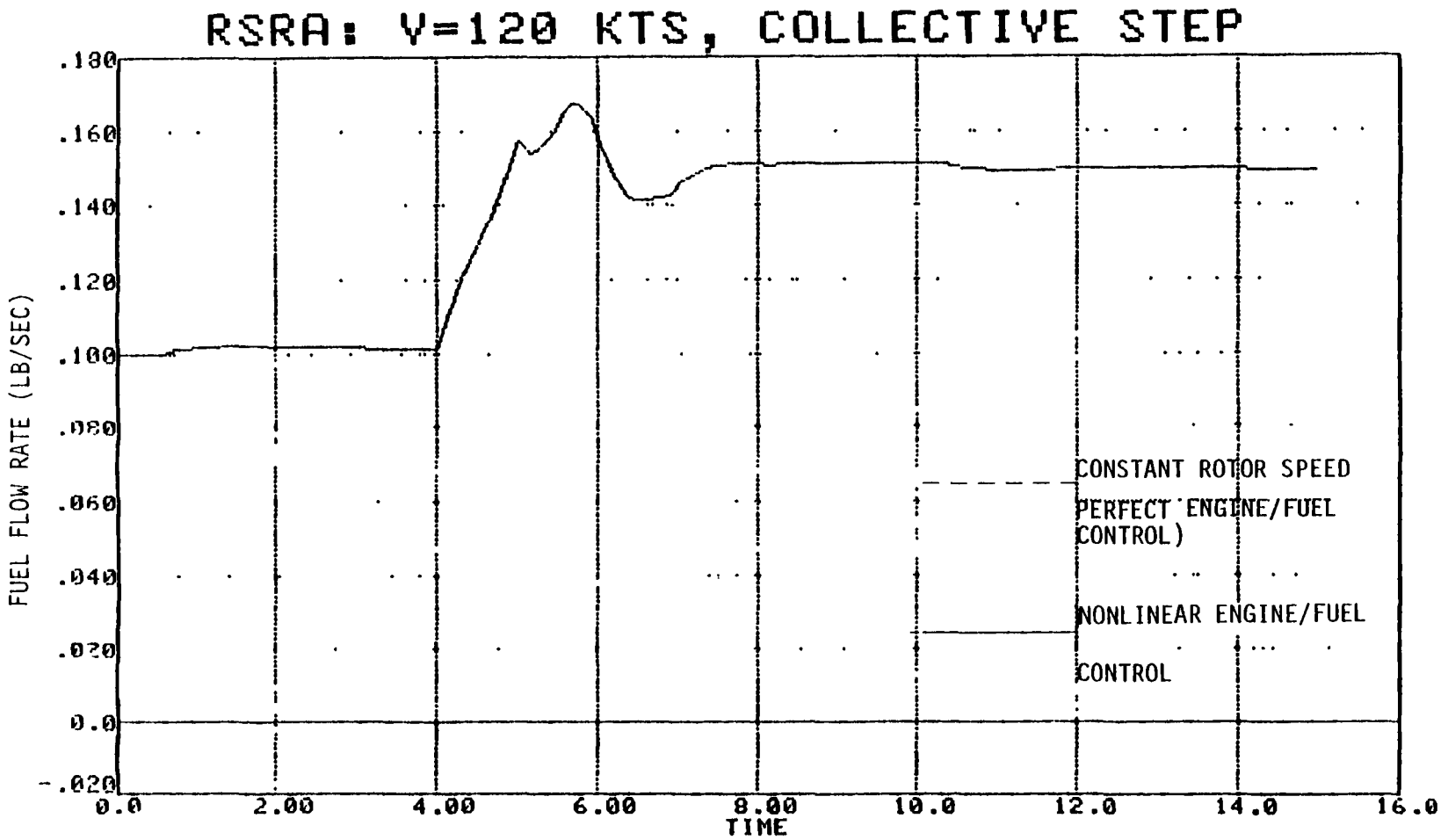

Figure 6.1c Nonlinear Rotor/Propulsion System With Collective Input, Fuel Flow

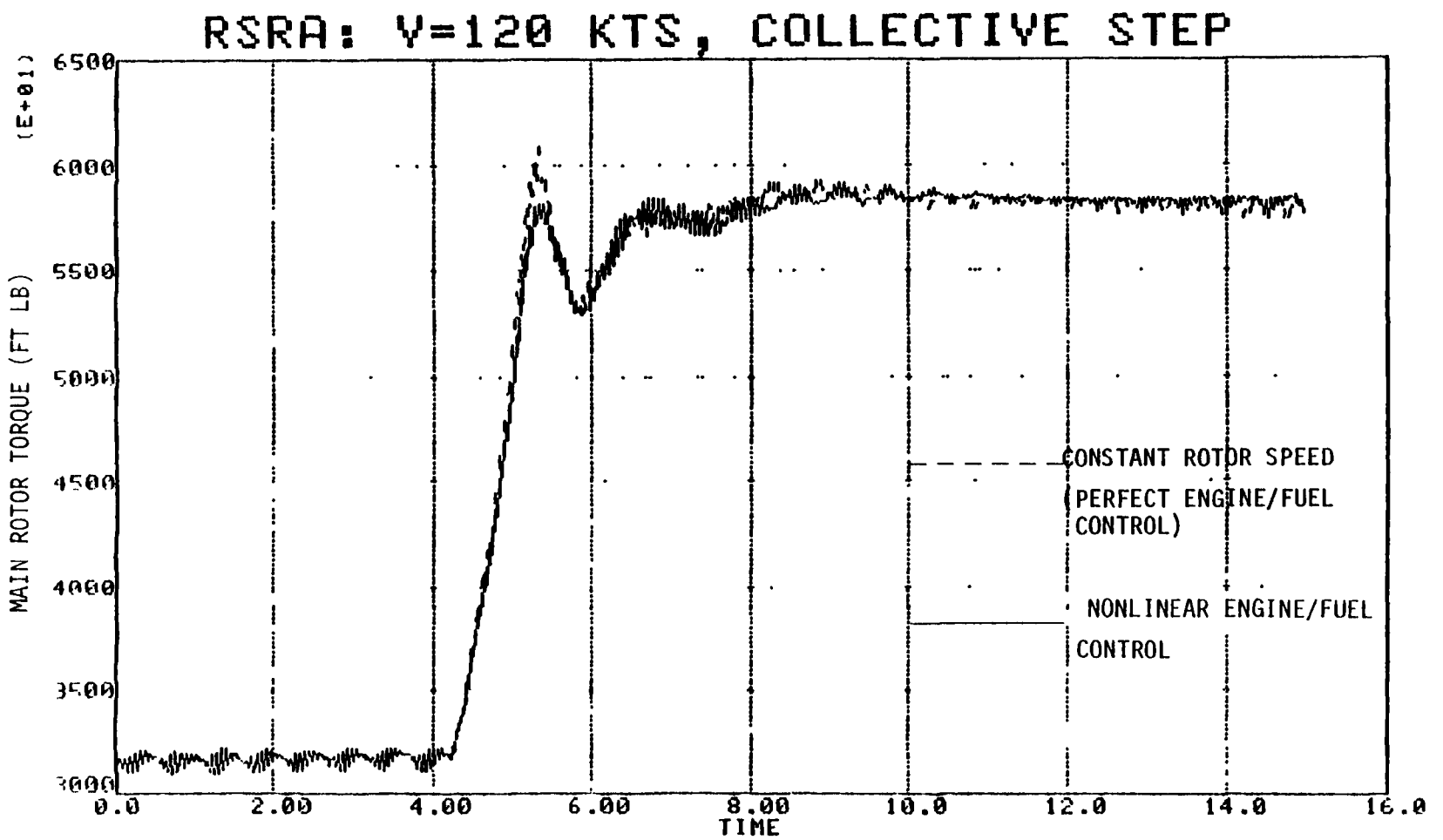

Figure 6.1d Nonlinear Rotor/Propulsion System With Collective Input, Rotor Torque

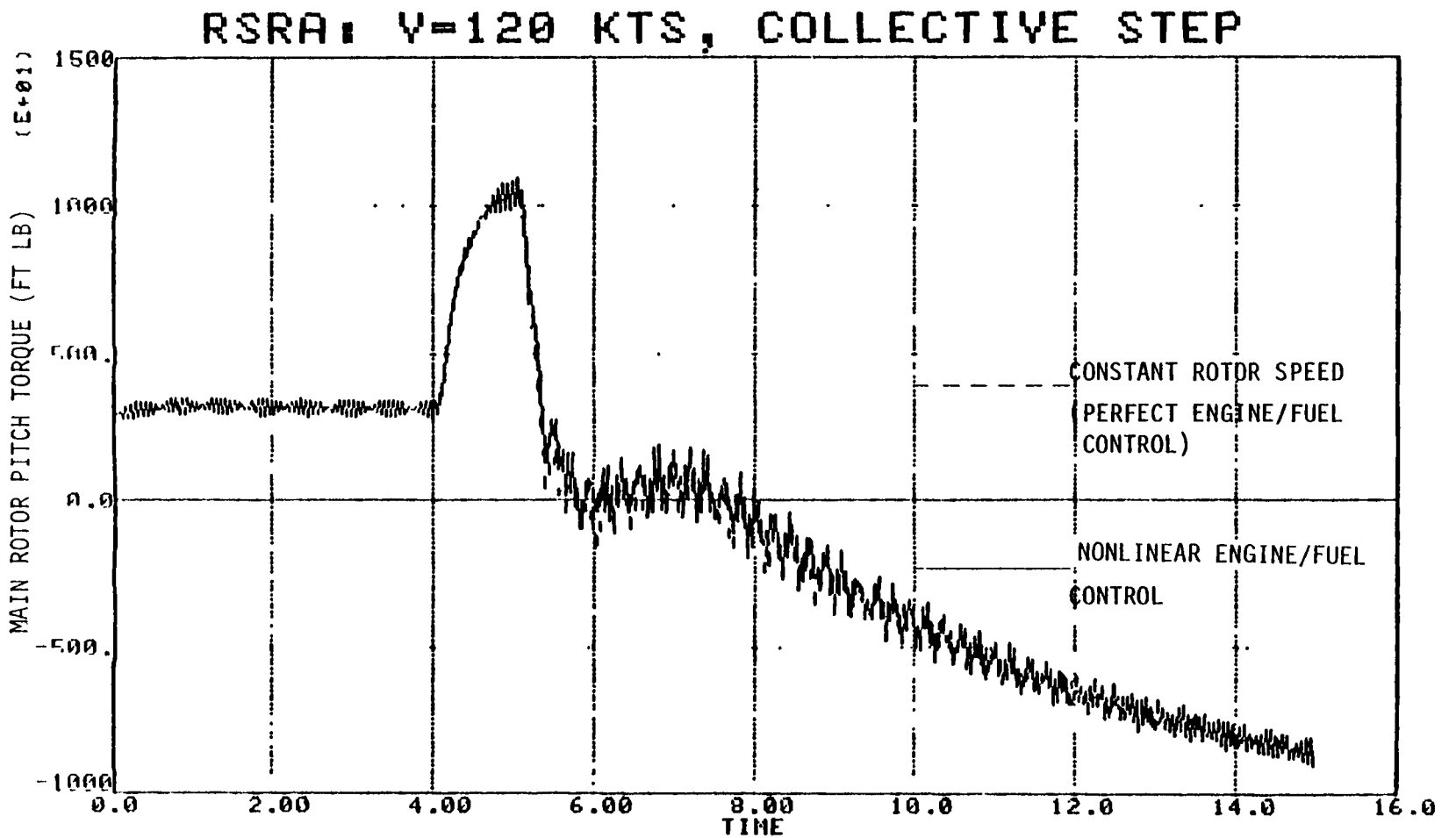

Figure 6.1e Nonlinear Rotor/Propulsion System With Collective Input, Body Axis Pitch Moment

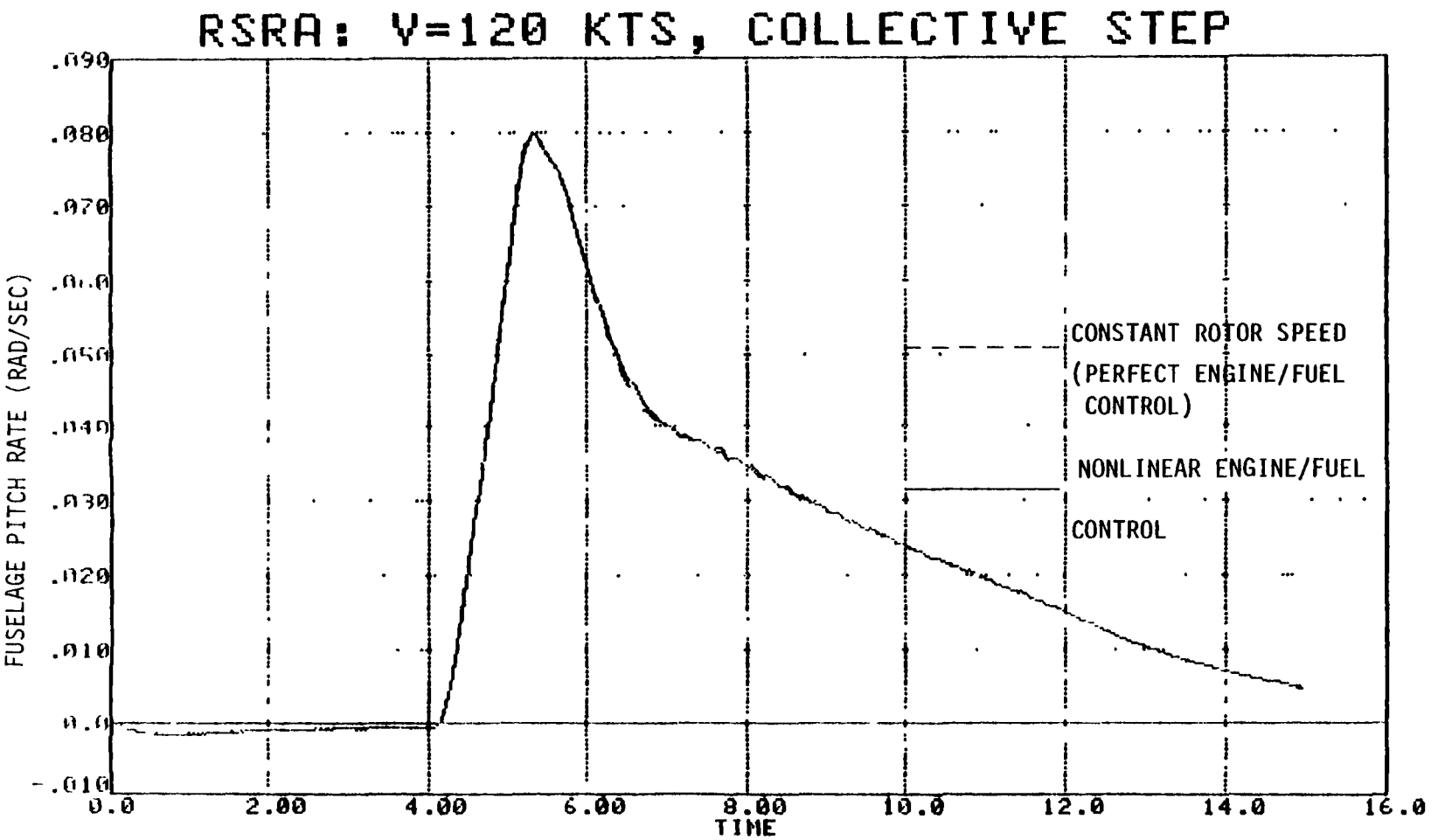

Figure 6.1f Nonlinear Rotor/Propulsion System With Collective Input, Body Pitch Rate

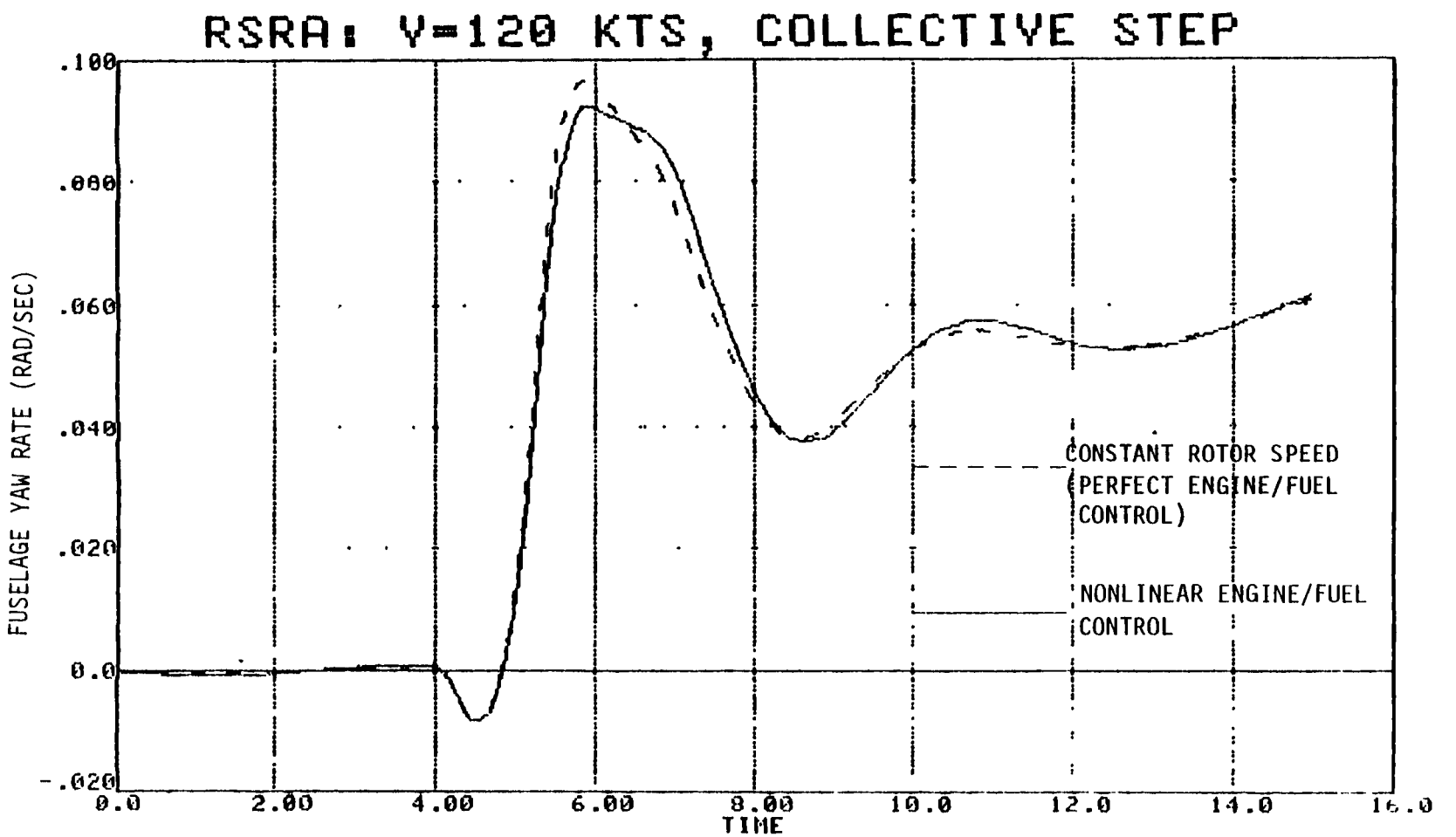

Figure 6.1g Nonlinear Rotor/Propulsion System With Collective Input, Body Yaw Rate

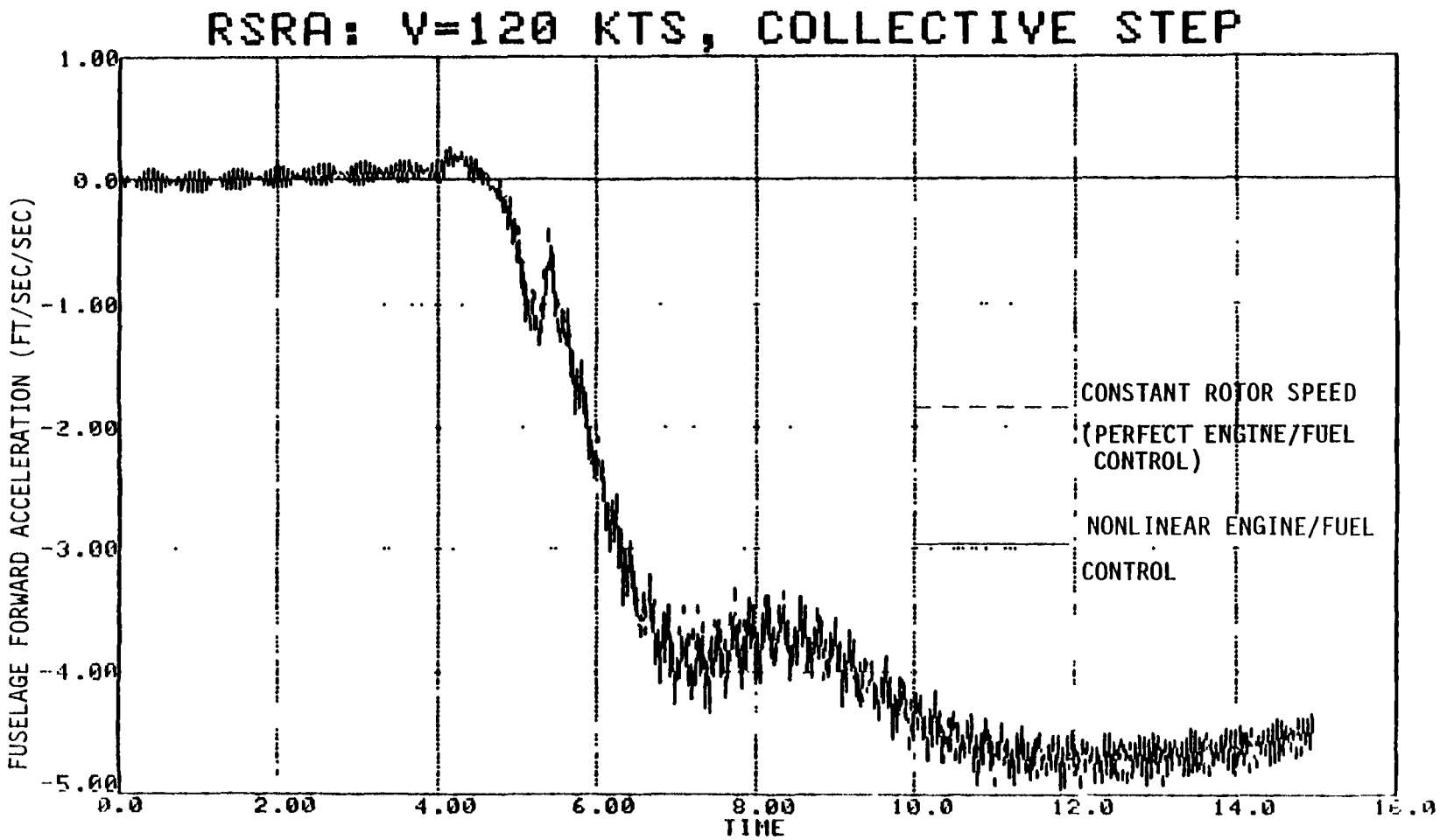

Figure 6.1h Nonlinear Rotor/Propulsion System With Collective Input, Body Forward Velocity

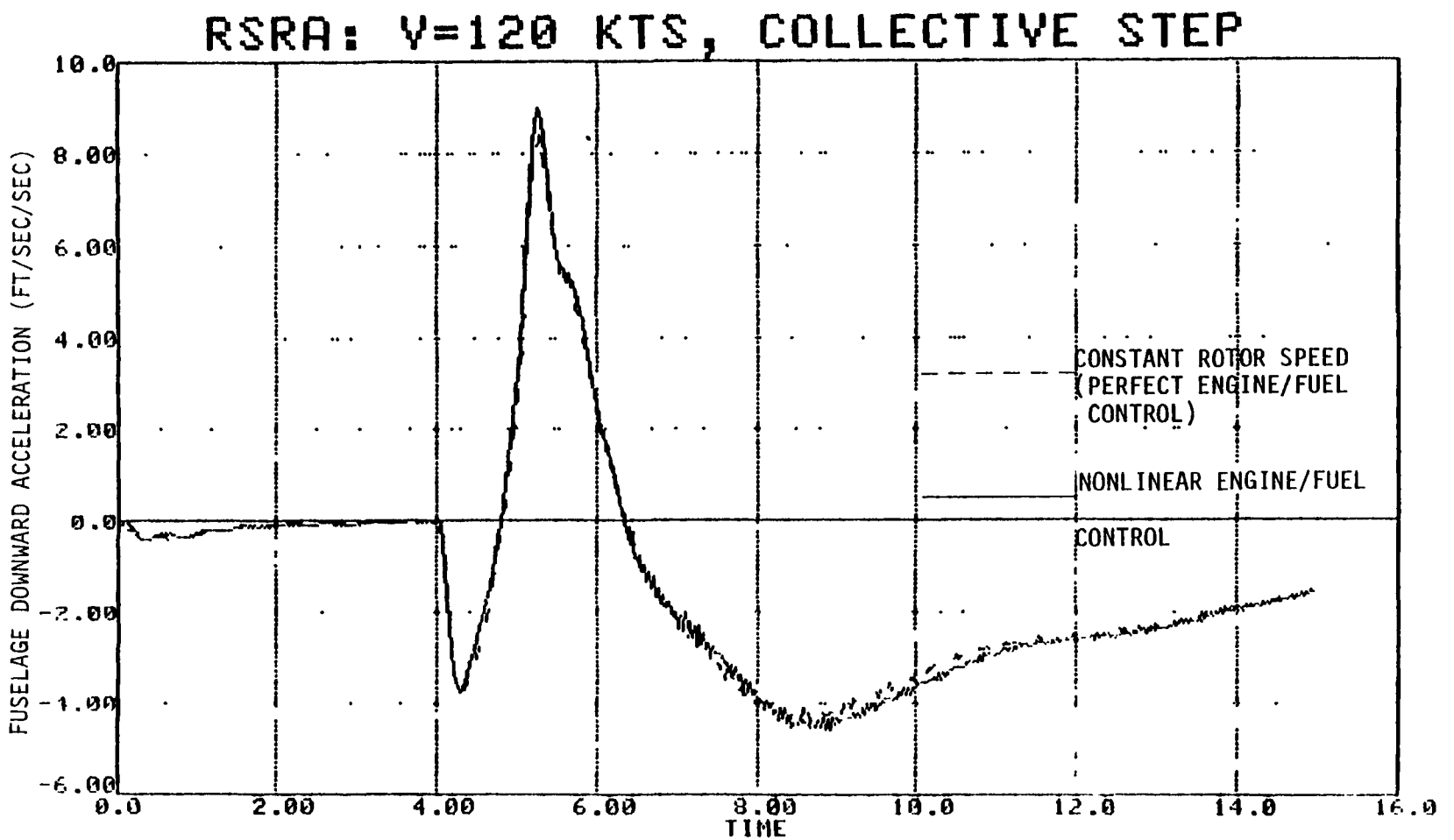

Figure 6.1i Nonlinear Rotor/Propulsion System With Collective Input, Body Downward Velocity

6.2 COMBINED PERTURBATIONAL AND GENHEL SIMULATIONS

The perturbational rotorcraft/propulsion model was appended to the GENHEL simulation. The perturbational model consisted of the propulsion system constructed in Chapter IV and the rotor/fuselage system constructed in Chapter V. The perturbational model was connected so, at the option of the person running the program, the perturbational rotor, fuselage aerodynamics, and propulsion subroutines would replace those of the GENHEL simulation. The organization of the resulting model is shown in Figure 6.2. Note that there are two possible paths. The first is through the existing GENHEL nonlinear rotor and attached propulsion subroutines, and the second is through the perturbational subroutines.

Recall that the perturbational equations do not yield total values. The perturbational equations are integrated separately from the GENHEL equations. After the perturbational equations are integrated, trim values are added to the perturbation values to yield total values which can be compared with the GENHEL predictions.

Figure 6.3 compares the responses predicted by the perturbational equations with those of the GENHEL simulation. The trim condition here is the same one used previously; 120 knots forward speed, 1000 feet altitude. The solid lines in the figures are the GENHEL results and the dashed lines are the perturbational model results. Note that the problems caused by a poor fit of the rotor equations (this was discussed in the previous chapter) appear here also.

6.3 DISCUSSION

A mostly linear perturbational model for modeling the interactions between the rotor system and the propulsion system of a helicopter was developed and demonstrated. The program that

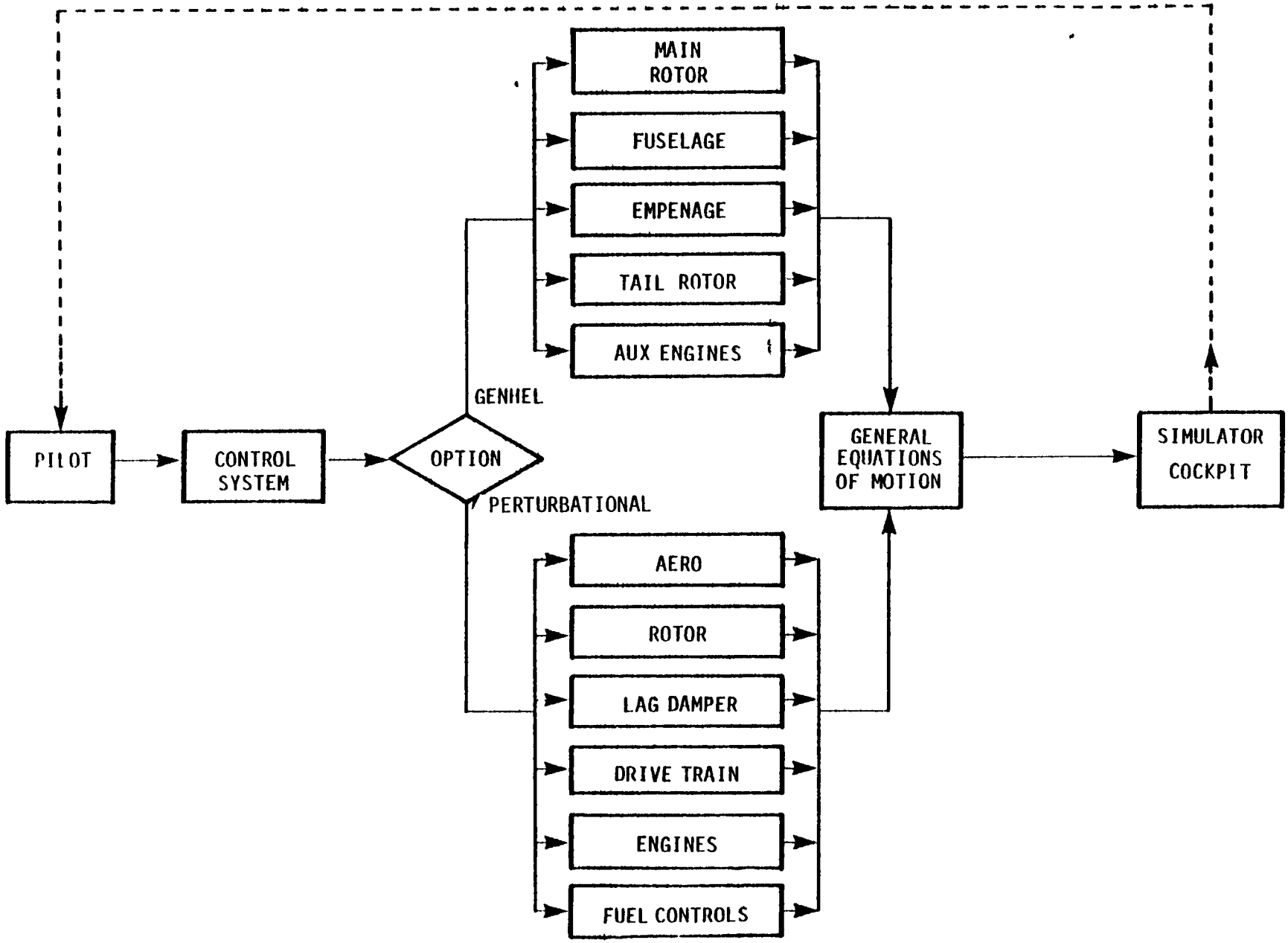

Figure 6.2 Organization of Coupled GENHEL and Perturbational Simulation

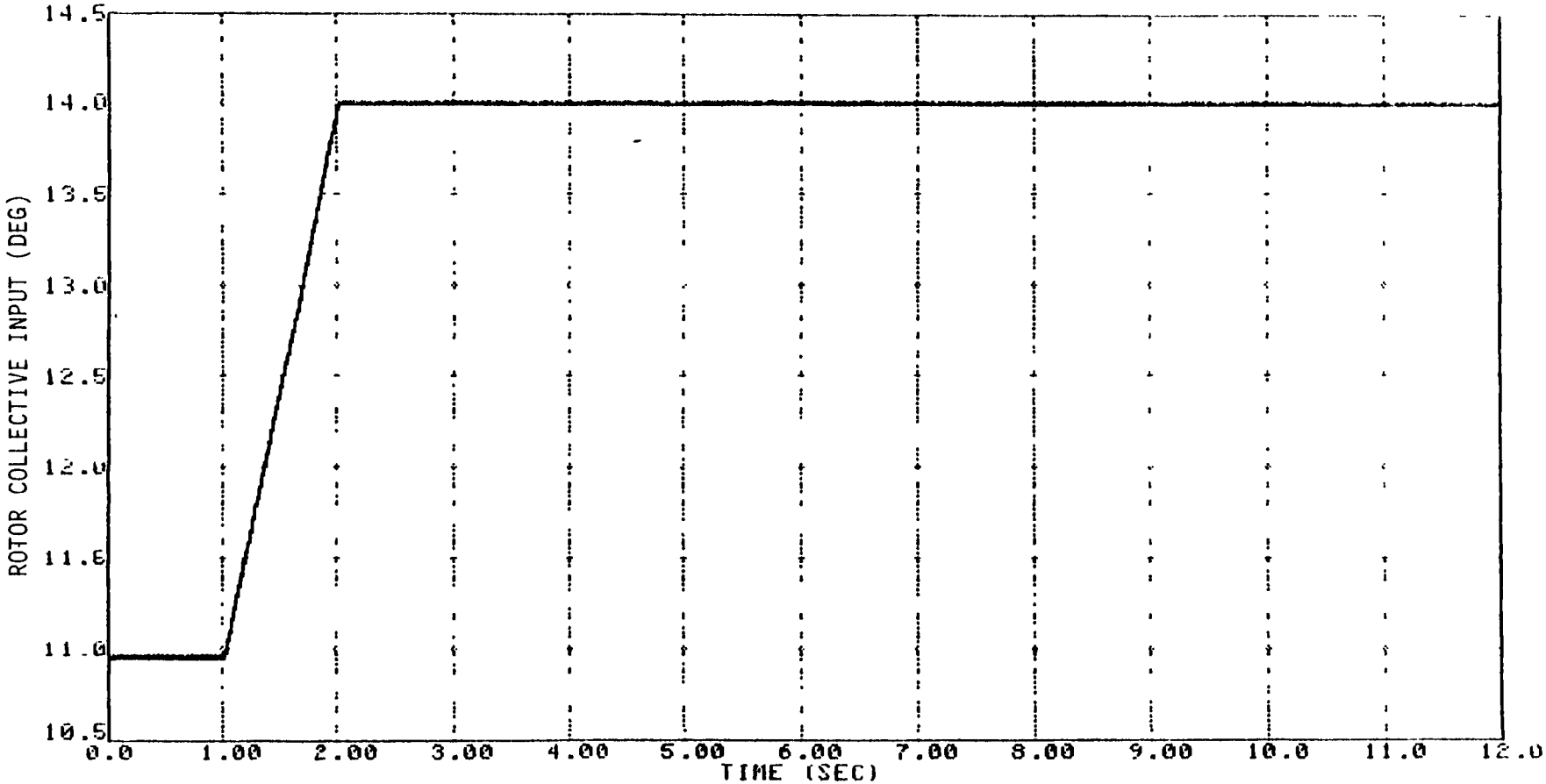

Figure 6.3a Rotor/Propulsion System, Collective Input

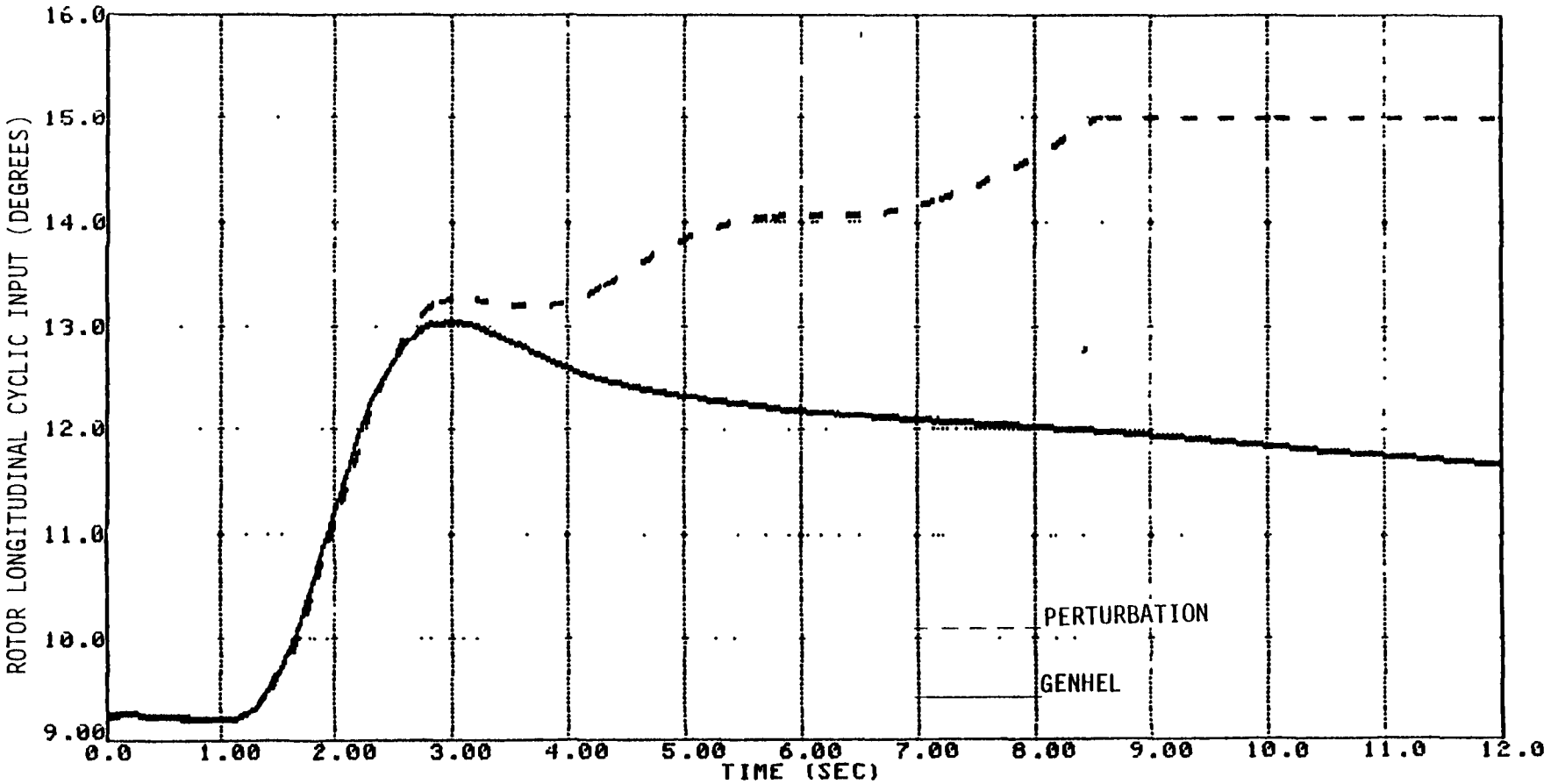

Figure 6.3b Rotor/Propulsion System, Longitudinal Cyclic Input

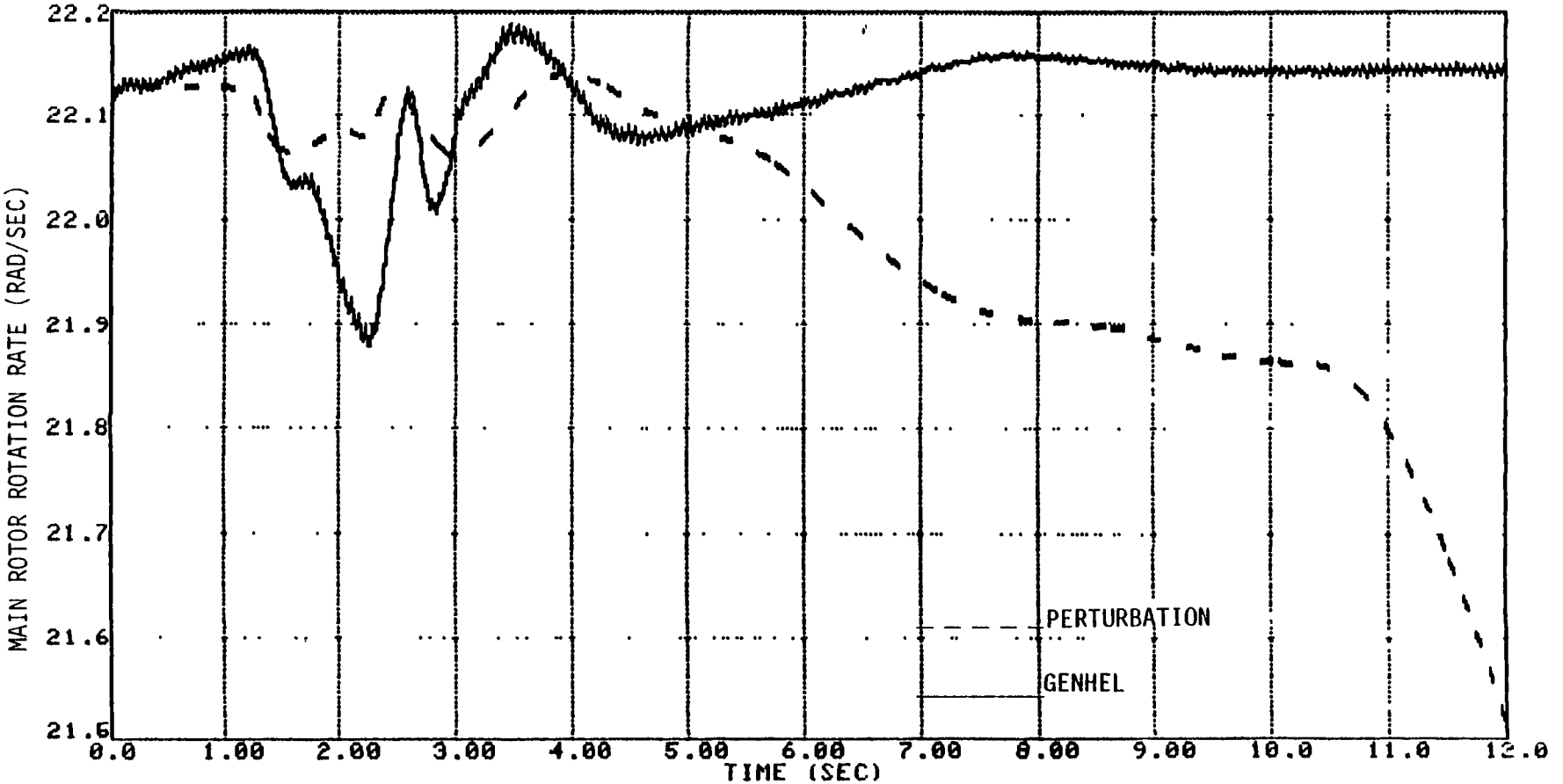

Figure 6.3c Rotor/Propulsion System, Fuselage Roll Rate

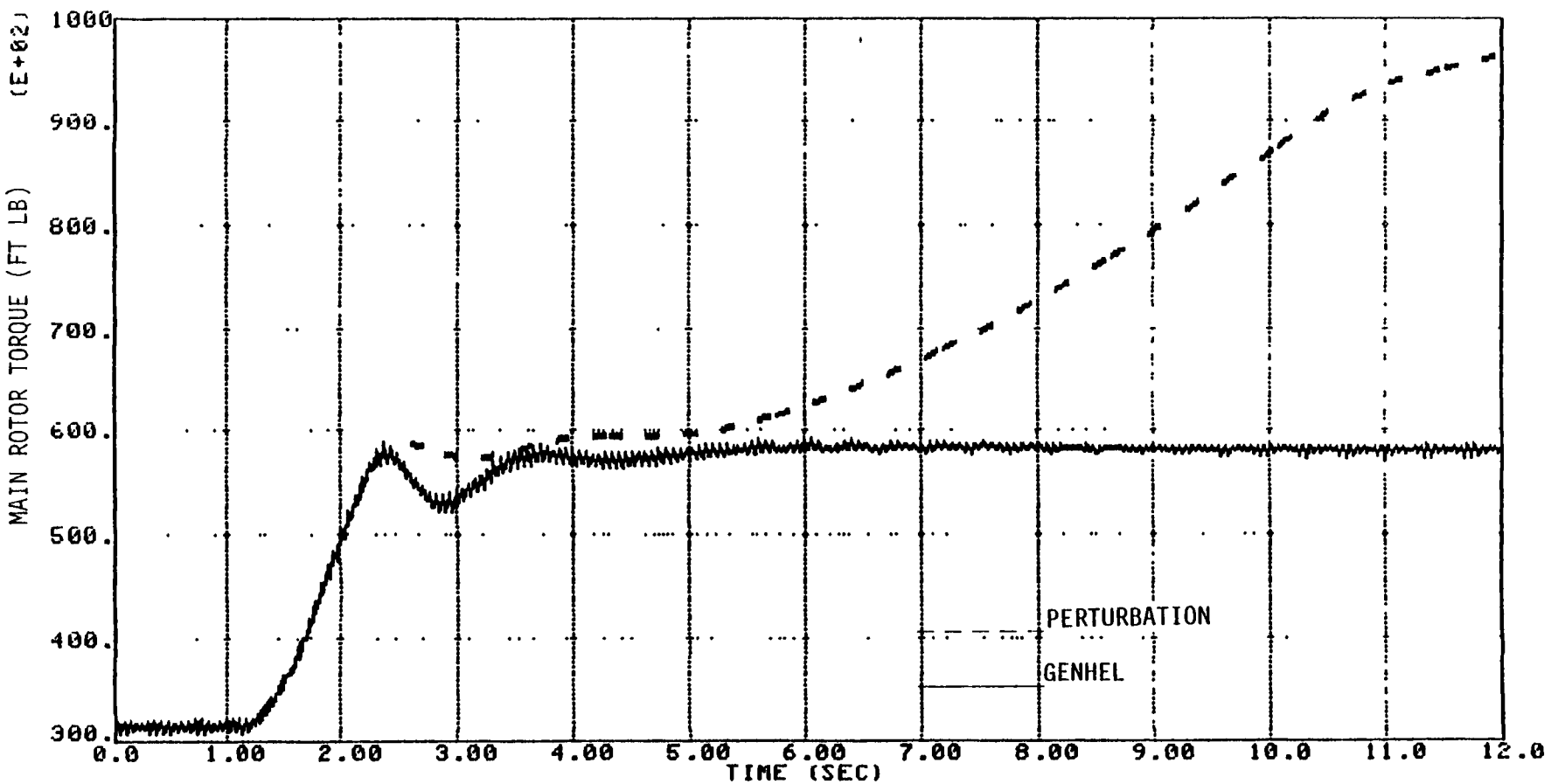

Figure 6.3d Rotor/Propulsion System, Main Rotor Speed

implements this model has a modular structure that provides flexibility to change, add or drop independent modules from consideration on any one run.

The perturbational model has been coupled with a nonlinear rotorcraft simulation. This coupling provides a means for checking out the model (other than with real test data) and provides a flight control system to "fly" the model.

The input-output software and plotting software developed for the nonlinear simulation are then also available to the perturbational model.

One rotor/propulsion interaction problem, rotor droop was demonstrated with the perturbational model. The model was also developed to look at other problems, such as hunting between engines, but this application was not tested.

The generic model formulation methodology checked out, but the model (consisting of the coefficients) did not. This was because of the difficulty encountered in identifying a rotor model. The periodic effects, as discussed in Appendix A, were not sufficiently understood before creating the data file for identifying the rotor model and performing the OSR runs. Since then, more has been learned about the periodic effects, most importantly their structure in multi-blade coordinates. The rotor model that was obtained was sufficient to test and check out the generic model methodology, but the coefficients did not match the response of the nonlinear rotor model.

VII. SUMMARY AND RECOMMENDATIONS

7.1 MODELS DEVELOPED

SCT has developed several models during the period of this contract. These models include:

(1) a nonlinear rotorcraft propulsion system model including two engine subroutines, two fuel control subroutines and a drive train subroutine.

(2) a mostly linear propulsion system model including two linear engine models, two nonlinear fuel control models and a linear drive train model,

(3) a mostly linear, perturbational rotor system model including a linear perturbational rotor model in multi-blade coordinates, a perturbational fuselage aerodynamics model in multi-blade coordinates, and a nonlinear lag damper model,

(4) an augmented version of the GENHEL simulation which consists of GENHEL [14] augmented to include the nonlinear propulsion system in (1) above,

(5) a perturbational rotor/propulsion model, which has been connected to the augmented GENHEL simulation in (4) so it can make use of the GENHEL flight control system, and which has been parameterized to model the RSRA.

The nonlinear and the mostly linear propulsion system models were developed as modules that could be connected into a rotorcraft system. The perturbational rotor and fuselage aerodynamics models were developed similarly as modules. The perturbational rotorcraft model was constructed by connecting the mostly linear propulsion system model and the perturbational rotor and fuselage aerodynamics models together.

Some of the models developed during this contract were checked out by comparing their responses with the responses of existing nonlinear simulations. No test data was analyzed. The drive train model, on the other hand, could not be checked out in

this manner because no previous drive train model was available with parameters for comparison. Further work is necessary to check out this model.

The perturbational fuselage aerodynamics model and the perturbational rotor model outputs were compared to outputs from the nonlinear GENHEL simulation for verification. The fit for this perturbational rotor model has been poor. The poor fit was attributed to coefficients in the model that were in error because the periodic effects in the rotor dynamics were not considered when the coefficients were identified from GENHEL response data. Analyses of the periodic effects in this and an associated study [17] have since determined a better form and approach for modeling these periodic effects in multi-blade coordinates. Further work should be performed to identify new rotor model coefficients making use of this new information.

7.2 RECOMMENDATIONS

Recommendations for further work with the perturbational rotorcraft models and generic methodology developed during this contract include the following:

- Develop parameters for a new perturbational rotor model. Include the effects of the periodic dynamics as described in Appendix A.
- Test the perturbational model in control system design.
- Analyze wind tunnel or flight test data by using the perturbational model as an equation structure for parameter identification and as a simulation for executing and testing the identified model.

REFERENCES

1. Frederickson, C., "Engine/Airframe Interface Dynamics Experience," Proceedings of specialists Meeting on Rotorcraft Dynamics," 13-15 February 1974.

2. Bell, Sikorsky, Vertol, et al., "Engine/Airframe/Drive Train Dynamic Interface Documentation," USARTL TR78-11 through TR78-15, 1978.

3. Gilmore, Daniel R., Jr., Jordon, Harold J., Pisano, Alan D., "Assessment of Augmented Electronic Fuel Controls For Modular Engine Diagnostics and Condition Monitoring," USARTL-Tr-78-32, prepared by General Electric Company, Aircraft Engine Group for Applied Technology Laboratory, USARTL (AVRADCOM), Fort Eustis, Va., December 1978.

4. "Tilt Rotor Research Aircraft Familiarization Document" NASA TM X-62 407, prepared by Tilt Rotor Project Office Staff, coordinated by Martin Maisel, January 1975.

5. Kuczynski, W.A., et. al., "The Influence of Engine/fuel Control Design on Helicopter Dynamics and Handling Qualities," presented at the National Forum of the American Helicopter Society, Washington D.C., May 1979.

6. Churchill, Gary B., "XV-15 Tilt Rotor Research Aircraft Flight Control Systems," Slide presentation at Meeting No. 46, SAE Aerospace Control and Guidance Systems Committee, Kahler Green Oaks Inn, Fort Worth, Texas, November 12-14, 1980.

7. Twomey, W.J., Ham, E.H. "Review of Engine/Airframe/Drive Train Dynamic Interface Development Problems," USARTL-TR-78-13, prepared by Sikorsky Aircraft for Applied Technology Laboratory, U.S. Army Research and Technology Laboratories (AVRADCOM), June 1978.

8. DeHoff, R.L., and Hall, W.E., "Systems Identification Principles Applied to Multivariable Control Synthesis of the F100 Turbofan Engine," presented at the 1977 JACL, San Francisco, CAlifornia, June 1977.

9. DeHoff, R.L., Hall, W.E., Adams, R.J., and Gupta, N.K. "Design of a Multivariable Controller Utilizing Linear Optimization Methods," AFAPL-TR-77-35, June 1977.

10. Rock, S.M., and DeHoff, R.L., "Variable Cycle Engine Multivariable Control Synthesis," AFAPL-Tr-79-2043, Feb. 1979.

11. DeHoff, R.L., "Identification of a STOL Propulsion Plant Model from Flight Data," Journal of Guidance and Control, Vol. 2 No. 3, May-June 1979.

12. Johnson, W., "The Influence of Engine/Transmission/Governor on Tilting Proprotor Aircraft Dynamics," NASA TMX-62455, June 1979.

13. Howlett, J.J., "RSRA Simulation Model," Volumes I and II, Sikorsky Aircraft SER 72009, NASA/Army Contract NAS1 - 13000, 1974.

14. Houck, J.A., Howlett, J.J., Browne, M.M., "Rotor Systems Research Aircraft Simulation Mathematical Model," NASA Technical Memorandum 78629, NASA Langley Research Center, November 1977.

15. Bailey, F.J., Jr., "A Simplified Theoretical Method of Determining the Characteristics of a Lifting Rotor in Forward Flight," NACA Rep. No. 716, 1941.

16. Fuller, James W., "Applications of Periodic Control In Rotorcraft and the Use of Multiblade Coordinates For Control Synthesis," SCT Tech Memo No. 5397-03, November, 1981.

17. Fuller, James W., Final Report to be submitted by SCT to NASA-Ames on contract NAS2-10976, Tech. Monitor Ronald W. Duval, 1982.

18. Biggers, J.C., "Some Approximations to the Flapping Stability of Helicopter Rotors," AHS Journal, October 1974.

19. Brockett, R.W., Finite Dimensional Linear Systems, John Wiley and Sons, Inc. 1970.

20. DuVal, Ronald W., Mackie, David B., "Identification of a Linear Model of Rotor-Fuselage Dynamics From Nonlinear Simulation Data," Paper No. 60 presented at the Sixth European Rotorcraft and Powered Lift Aircraft Forum, The University, Bristol, England, September 16-19, 1980.

21. Warmbrodt, W. and Hull, R., "Development of a Helicopter Rotor/Propulsion System Dynamics Analysis," Paper No. AIAA-82-1078, presented at the AIAA/SAE/ASME 18th Joint Propulsion Conference, Cleveland, Ohio, June 21-23, 1982.

This Page Intentionally Left Blank

APPENDIX A
TRANSFORMATION FROM ROTATING TO MULTI-BLADE COORDINATES

A.1 MULTI-BLADE TRANSFORMATION

The transformation from rotating to multi-blade coordinates is defined, for flapping of a five bladed rotor system, by

$$\overline{\beta} = \frac{2}{5} H^T \overline{\beta}_r \tag{A.1}$$

where $\overline{\beta} = \{\sqrt{2}\beta_0, \beta_{1c}, \beta_{1s}, \beta_{2c}, \beta_{2s}\}^T$

$=$ multi-blade flapping coordinates

$\overline{\beta}_r = \{\beta_1, \beta_2, \beta_3, \beta_4, \beta_5\}^T$

$=$ rotating frame blade flapping angles

$H^T =$ 5 x 5 transformation matrix

$\psi_i =$ azimuth angle of ith blade

and where

$$H^T = \begin{bmatrix} \frac{1}{\sqrt{2}} & \frac{1}{\sqrt{2}} & \frac{1}{\sqrt{2}} & \frac{1}{\sqrt{2}} & \frac{1}{\sqrt{2}} \\ -\cos\psi_1 & -\cos\psi_2 & . & . & -\cos\psi_5 \\ -\sin\psi_1 & . & . & . & -\sin\psi_5 \\ -\cos 2\psi_1 & . & . & . & -\cos 2\psi_5 \\ -\sin 2\psi_1 & . & . & . & -\sin 2\psi_5 \end{bmatrix} \tag{A.2}$$

Similarly,

$$\overline{\xi} = \frac{2}{5} H^T \overline{\xi}_r \tag{A.3}$$

where $\overline{\xi} = \{\sqrt{2}\xi_0, \xi_{1c}, \xi_{1s}, \xi_{2c}, \xi_{2S}\}^T$

$=$ multi-blade lagging coordinates

$$\bar{\xi}_r = \{\xi_1,\ \xi_2,\ \xi_3,\ \xi_4,\ \xi_5\}^T$$

$$= \text{rotating frame lagging angles}$$

$$H^T = \text{same as above}$$

The transformation, H, has the interesting properties

$$H^{-1} = \frac{2}{5} H^T \qquad (A.4)$$

$$\dot{H} = H J$$

$$\dot{H}^T = J^T H^T = -J H^T$$

$$\frac{d}{dt}(H^{-1}) = -\frac{2}{5} J H^T$$

where:

$$J = \begin{bmatrix} 0 & 0 & 0 & 0 & 0 \\ 0 & 0 & \Omega & 0 & 0 \\ 0 & -\Omega & 0 & 0 & 0 \\ 0 & 0 & 0 & 0 & 2\Omega \\ 0 & 0 & 0 & -2\Omega & 0 \end{bmatrix}$$

Ω = main rotor speed

Now, the equations of motion for the flapping and lagging of the blades are given in the rotating system by

$$\frac{d}{dt}\begin{Bmatrix} \bar{\beta} \\ \dot{\bar{\beta}} \\ \bar{\xi} \\ \dot{\bar{\xi}} \end{Bmatrix} = \begin{bmatrix} 0 & I & 0 & 0 \\ F_{(\psi)} & G_{(\psi)} & A_{(\psi)} & B_{(\psi)} \\ 0 & 0 & 0 & I \\ F'_{(\psi)} & G'_{(\psi)} & A'_{(\psi)} & B'_{(\psi)} \end{bmatrix} \begin{Bmatrix} \bar{\beta} \\ \dot{\bar{\beta}} \\ \bar{\xi} \\ \dot{\bar{\xi}} \end{Bmatrix} + \text{control inputs and fuselage inputs} \qquad (A.5)$$

where, assuming the blades are independent and identical, the coefficient matrices, $F_{(\psi)}$, $G_{(\psi)}, \ldots, B_{(\psi)}$, are diagonal. For example,

$$F_{(\psi)} = \begin{bmatrix} f_{(\psi_1)} & 0 & 0 & 0 & 0 \\ 0 & f_{(\psi_2)} & 0 & 0 & 0 \\ 0 & 0 & f_{(\psi_3)} & 0 & 0 \\ 0 & 0 & 0 & f_{(\psi_4)} & 0 \\ 0 & 0 & 0 & 0 & f_{(\psi_5)} \end{bmatrix}$$

But, the multi-blade coordinates ($\bar{\beta}$ and $\bar{\xi}$) are related to the individual blade angles ($\bar{\beta}_r$ and $\bar{\xi}_r$) in the rotating system via the transformation

$$\begin{Bmatrix} \bar{\beta} \\ \dot{\bar{\beta}} \\ \bar{\xi} \\ \dot{\bar{\xi}} \end{Bmatrix} = \frac{2}{5} \begin{bmatrix} H^T & 0 & 0 & 0 \\ -J\,H^T & H^T & 0 & 0 \\ 0 & 0 & H^T & 0 \\ 0 & 0 & -JH^T & H^T \end{bmatrix} \begin{Bmatrix} \bar{\beta}_r \\ \dot{\bar{\beta}}_r \\ \bar{\xi}_r \\ \dot{\bar{\xi}}_r \end{Bmatrix}$$

$$= \frac{2}{5} \mathcal{H}^T \begin{Bmatrix} \bar{\beta}_r \\ \dot{\bar{\beta}}_r \\ \bar{\xi}_r \\ \dot{\bar{\xi}}_r \end{Bmatrix} \qquad (A.6)$$

which follows from Eqs. (A.1) to (A.4). Thus, applying this transformation (Eq. A.6) to the blade equations in rotating coordinates (Eq. A.5) yields the blade equations in multi-blade coordinates.

$$\frac{2}{5}\mathcal{H}^T \frac{d}{dt} \begin{Bmatrix} \bar{\beta}_r \\ \dot{\bar{\beta}}_r \\ \bar{\xi}_r \\ \dot{\bar{\xi}}_r \end{Bmatrix} = \frac{2}{5}\mathcal{H}^T \begin{bmatrix} 0 & I & 0 & 0 \\ F_{(\psi)} & G_{(\psi)} & A_{(\psi)} & B_{(\psi)} \\ 0 & 0 & 0 & I \\ F'_{(\psi)} & G'_{(\psi)} & A'_{(\psi)} & B'_{(\psi)} \end{bmatrix} + \frac{2}{5}\mathcal{H} \begin{Bmatrix} \dot{\bar{\beta}}_r \\ \bar{\beta}_r \\ \dot{\bar{\xi}}_r \\ \bar{\xi}_r \end{Bmatrix} + \frac{2}{5}\mathcal{H}^T \text{ (control and fuselage inputs)} \qquad (A.7)$$

$$
H^T F(\psi) H = \begin{bmatrix}
f_0 & f_{1c} & f_{1s} & f_{2c} & f_{2s} \\
f_{1c} & f_0 + \frac{1}{2} f_{2c} & \frac{1}{2} f_{2s} & \frac{1}{2} f_{1c} & \frac{1}{2} f_{1s} \\
f_{1s} & \frac{1}{2} f_{2s} & f_0 - \frac{1}{2} f_{2c} & \frac{1}{2} f_{1s} & \frac{1}{2} f_{1c} \\
f_{2c} & \frac{1}{2} f_{1c} & -\frac{1}{2} f_{1s} & f_0 & 0 \\
f_{2s} & \frac{1}{2} f_{1s} & \frac{1}{2} f_{1c} & 0 & f_0
\end{bmatrix} +
$$

$$
\begin{bmatrix}
0 & 0 & 0 & 0 & 0 \\
0 & 0 & 0 & \frac{1}{2} f_{2c} & -\frac{1}{2} f_{2s} \\
0 & 0 & 0 & -\frac{1}{2} f_{2s} & -\frac{1}{2} f_{2c} \\
0 & \frac{1}{2} f_{2c} & -\frac{1}{2} f_{2s} & \frac{1}{2} f_{1c} & -\frac{1}{2} f_{1s} \\
0 & -\frac{1}{2} f_{2s} & -\frac{1}{2} f_{2c} & \frac{1}{2} f_{1s} & -\frac{1}{2} f_{1c}
\end{bmatrix} \cos 5\psi +
$$

$$
\begin{bmatrix}
0 & 0 & 0 & 0 & 0 \\
0 & 0 & 0 & \frac{1}{2} f_{2s} & +\frac{1}{2} f_{2c} \\
0 & 0 & 0 & +\frac{1}{2} f_{2c} & -\frac{1}{2} f_{2s} \\
0 & \frac{1}{2} f_{2s} & +\frac{1}{2} f_{2c} & \frac{1}{2} f_{1s} & +\frac{1}{2} f_{1c} \\
0 & +\frac{1}{2} f_{2c} & -\frac{1}{2} f_{2s} & \frac{1}{2} f_{1c} & -\frac{1}{2} f_{1s}
\end{bmatrix} \sin 5\psi
$$

Figure A.1 Example Dynamics Matrix Structure for Five-Bladed Rotor

for the generic model, the terms H^TFH, $H^TF'H$, etc. are diagonal and given by, for example;

$$H^TFH = f_0\ [I] \tag{A.10}$$

where [I] = 5 x 5 identity matrix

When periodic effects are not small, then there are additional coefficients on and off the diagonal of the "constant" matrix, as well as matrices of coefficients for periodic terms (e.g. the cos 5 term in Figure A.1).

A useful theorem about the solution of a periodically time varying equation at trim is found in [19]. This theorem states that the trim solution of a periodically time varying system at trim contains a constant part and a periodically time varying part.

$$x_{trim} = x_{const} + x_{(t)\ periodic} \tag{A.11}$$

The trim value is not constant but time varying.

A.2 IDENTIFICATION FORM

The terms in the equations of motion (Eq. A.8) for the rotor in multi-blade coordinates can be separated into several groups, as was done in Ref. 20. First, there is no need to include the portions of the blade accelerations containing the "J" terms in the OSR regression analysis, since they are already known. These "J" terms (i.e. $2J$, $\dot{J}$, J^2) can be subtracted off before the regression analysis. Second, as was found in the present study, the diagonal form of Eq. (A.10) can be assumed to simplify the regression for a constant coefficient model. In addition, Ref. 16 shows that if the diagonal structure of Eq. (5.10) is not imposed, the mode shapes cannot be correctly predicted by a constant coefficient model. Finally, the fuselage input portion of Eq. (A.8) can be studied to determine "known" terms such as inertial effects which can also be subtracted from a regression analysis.

Rearranging and multiplying out yields the useful form

$$\frac{d}{dt}\begin{Bmatrix}\bar{\beta}\\ \dot{\bar{\beta}}\\ \bar{\xi}\\ \dot{\bar{\xi}}\end{Bmatrix} = \left[\frac{2}{5}\begin{bmatrix} 0 & I & 0 & 0 \\ (H^TFH + H^TG\,H\,J) & (H^TG\,H) & (H^TA\,H + H^TBHJ) & (H^TB\,H) \\ 0 & 0 & 0 & I \\ (H^TF'H + H^TG'H\,J) & (H^TG'H) & (H^TA'H + H^TB'HJ) & (H^TB'H) \end{bmatrix}\right.$$

$$\left. - \begin{bmatrix} 0 & 0 & 0 & 0 \\ (J^2 + \dot{J}) & 2J & 0 & 0 \\ 0 & 0 & 0 & 0 \\ 0 & 0 & J^2 + \dot{J}) & 2J \end{bmatrix}\right] \begin{Bmatrix}\bar{\beta}\\ \dot{\bar{\beta}}\\ \bar{\xi}\\ \dot{\bar{\xi}}\end{Bmatrix}$$

$$+ \frac{2}{5}\begin{Bmatrix} 0 \\ H^T(\text{control and fuselage inputs to flapping}) \\ 0 \\ H^T(\text{control and fuselage inputs to lagging}) \end{Bmatrix} \quad (A.8)$$

The terms such as H^TFH (also H^TGH, $H^TG'H$, H^TAH, $H^TA'H$, etc.) have an interesting form, as shown in Refs. 16 and 17, and explained below. If the coefficient matrices $F_{(\psi)}$, $F'_{(\psi)}$, $G_{(\psi)}$, $G'_{(\psi)}$, etc. are expanded in series and truncated, for example, at second order,

$$F_{(\psi)} = F_0 + F_1\cos\psi + F_{2C}\cos 2\psi + F_{1s}\sin\psi + F_{2s}\sin 2\psi \quad (A.9)$$

then, after much trigonometric algebra, we get the form shown in Figure A.1.

The f_0 terms are the components that would appear in a constant coefficient model (i.e., one which neglects periodic rotor dynamics) [16,17]. The components f_{1c}, f_{2c}, etc. are associated with the periodic effects. For small advance ratios ($\mu < .3$) [18], the periodic effects, and thus these coefficients, are small.

The importance of these results to the present study is that, for a constant coefficient model such as is being developed

1 Report No.	2. Government Accession No	3 Recipient's Catalog No
CR 166380		

4 Title and Subtitle	5 Report Date
DEVELOPMENT OF A ROTORCRAFT/PROPULSION DYNAMICS INTERFACE ANALYSIS: VOLUME I	August 1982
	6 Performing Organization Code
7 Author(s)	8 Performing Organization Report No
Russell Hull	
9 Performing Organization Name and Address	10 Work Unit No
Systems Control Technology P.O. Box 10180 Palo Alto, CA 94303	T3753Y
	11 Contract or Grant No NAS2-10765
12 Sponsoring Agency Name and Address	13 Type of Report and Period Covered
National Aeronautics and Space Administration Washington, DC 20546	Final Report
	14 Sponsoring Agency Code 505-42-11

15 Supplementary Notes

Technical Monitor: William Warmbrodt (415) 965-5642
MS 247-1 FTS 448-5642
Ames Research Center, Moffett Field 94035

16 Abstract

A study was conducted to establish coupled rotor/propulsion analysis that would be applicable to a wide range of rotorcraft systems. The study included the following tasks: (1) development of a model structure suitable for simulating a wide range of rotorcraft configurations; (2) defined a methodology for parameterizing the model structure to represent a particular rotorcraft; (3) construction of a nonlinear coupled rotor/propulsion model as a test case to use in analyzing coupled system dynamics; and (4) an attempt to develop a mostly linear coupled model derived from the complete nonlinear simulations. Volume I contains the details of the modelling process and its implementation approach. Volume II contains documentation of the computer models developed under this investigation.

17 Key Words (Suggested by Author(s))	18 Distribution Statement
Rotor dynamics Propulsion systems Rotorcraft power train Engine dynamics	Unclassified - Unlimited STAR Category 07

19 Security Classif (of this report)	20 Security Classif (of this page)	21 No of Pages	22 Price*
Unclassified	Unclassified	132	

*For sale by the National Technical Information Service, Springfield, Virginia 22161

End of Document